GAIN SCHEDULED CONTROL USING THE DUAL YOULA PARAMETERIZATION

A Dissertation

by

YOUNG JOON CHANG

Submitted to the Office of Graduate Studies of
Texas A&M University
in partial fulfillment of the requirements for the degree of

DOCTOR OF PHILOSOPHY

May 2010

Major Subject: Mechanical Engineering

GAIN SCHEDULED CONTROL USING THE DUAL YOULA PARAMETERIZATION

A Dissertation

by

YOUNG JOON CHANG

Submitted to the Office of Graduate Studies of
Texas A&M University
in partial fulfillment of the requirements for the degree of

DOCTOR OF PHILOSOPHY

Approved by:

Chair of Committee,	Bryan Rasmussen
Committee Members,	Juergen Hahn
	Reza Langari
	Dennis O'Neal
Head of Department,	Dennis O'Neal

May 2010

Major Subject: Mechanical Engineering

ABSTRACT

Gain Scheduled Control Using the Dual Youla Parameterization. (May 2010)

Young Joon Chang, B.S., Inha University, Korea; M.S., Inha University, Korea

Chair of Advisory Committee: Dr. Bryan Rasmussen

Stability is a critical issue in gain-scheduled control problems in that the closed loop system may not be stable during the transitions between operating conditions despite guarantees that the gain-scheduled controller stabilizes the plant model at fixed values of the scheduling variable. For Linear Parameter Varying (LPV) model representations, a controller interpolation method using Youla parameterization that guarantees stability despite fast transitions in scheduling variables is proposed. By interconnecting an LPV plant model with a Local Controller Network (LCN), the proposed Youla parameterization based controller interpolation method allows the interpolation of controllers of different size and structure, and guarantees stability at fixed points over the entire operating region. Moreover, quadratic stability despite fast scheduling is also guaranteed by construction of a common Lyapunov function, while the characteristics of individual controllers designed *a priori* at fixed operating condition are recovered at the design points. The efficacy of the proposed approach is verified with both an illustrative simulation case study on variation of a classical MIMO control problem and an experimental implementation on a multi-evaporator vapor compression cycle system. The dynamics of vapor compression systems are highly nonlinear, thus the

gain-scheduled control is the potential to achieve the desired stability and performance of the system. The proposed controller interpolation/switching method guarantees the nonlinear stability of the closed loop system during the arbitrarily fast transition and achieves the desired performance to subsequently improve thermal efficiency of the vapor compression system.

DEDICATION

To my family and friends

ACKNOWLEDGEMENTS

I would like to thank my committee chair, Dr. Bryan Rasmussen, for his guidance and encouragement throughout this study. His knowledge and insight were essential in helping me through understanding and direction over research achievements. I would like to also thank my committee members, Dr. Dennis O'Neal, Dr. Reza Langari, and Dr. Juergen Hahn, for their guidance and support throughout the course of this research.

My gratitude is extended to Mr. Matt Elliott for his technical advice to experimental studies of vapor compression system, and to the research members in the Thermo-fluid Control Laboratory for sharing their knowledge for this study. Thanks to NSF (National Science Foundation) for their financial support throughout the duration of this study.

Finally, thanks to my parents and family for their continual support and encouragement, and to my lovely Yunhyung, for her endless love and patience.

TABLE OF CONTENTS

Page

Page

Page

LIST OF FIGURES

Page

Page

Page

Page

LIST OF TABLES

Page

1. INTRODUCTION

Many physical systems in nature exhibit complex dynamics. Researchers believe that nonlinear control system should be designed to regulate these systems within desired performance criteria and guarantee stability under any operating condition. With a system's nonlinearities and uncertainties, a single linear controller may not achieve acceptable performance throughout the entire set of operating conditions. Gain-scheduling is one of the most popular approaches for controlling nonlinear systems in practice and has been successfully applied to various fields both in academia and industry. Gain-scheduled control offers a means of constructing a nonlinear controller by interpolating a family of local controllers, thus dividing the nonlinear control design problem into several smaller problems where linear design tools are generally employed [1].

This "divide and conquer" approach enables various linear control design methods to be applied to nonlinear control problem and allows simplicity both in design and analysis. However, guaranteeing the stability of the nonlinear closed loop system is still a challenging task due to the presence of hidden coupling terms or unexpected additional dynamics during gain-scheduled controller interpolation [2].

Gain-scheduled control has also been applied to physical systems that include uncertainties. However, any modeling uncertainties or nonlinearities may result in a

---

This dissertation follows the style of *IEEE Transaction on Automatic Control.*

significant mismatch between plant model and the real system, thus a given model may not precisely reflect the nonlinear dynamics of the real system. In this case, conventional stability analyses may not be sufficient to evaluate the practical stability of nonlinear systems, thus stability with robustness consideration is a possible solution to improve the practicability assured in applications [3].

A vapor compression system might be a good example of implementation of gain-scheduled control since the dynamics of a vapor compression system meet the prescribed “highly nonlinear” condition and an advanced framework based on gain-scheduled control will have the potential to improve thermal efficiency and reduce the demanding load of those systems [4], [5].

In summary, this dissertation addresses a challenging problem in the control of nonlinear systems and proposes a solution to this problem by applying the theory and technique of gain-scheduled control. An advanced control design method which guarantees the nonlinear stability and desired performance of the system is developed to improve the efficiency of mechanical systems and guarantees of stability and performance will be shown both theoretically and experimentally.

1.1 Review of Gain-scheduled Control Literature

Gain-scheduling has been widely used to control nonlinear systems in a variety of industrial application, such as controls of vehicles [6], flights [7], [8], [9], power plants [10], [11], and hydraulic systems [12]. One significant advantage of gain-scheduling is its potential to incorporate linear control methods into a nonlinear control

design. Also, this paradigm does not require strict structural or analytic assumptions of the plant model. To ensure effective operation, scheduling variables should be selected to appropriately reflect the changes in plant dynamics as operating conditions change.

The design of a gain-scheduled controller for nonlinear systems can be described as a four-step process [13]: First, a linear model of the nonlinear system is determined from Jacobian linearization of the nonlinear plant about a family of equilibrium points or quasi-LPV plant modeling where nonlinear terms can be hidden by reformulating plant dynamics. Second, gain-scheduled controllers for the plant are designed with linear control design methods. Third, linear controllers are represented in terms of scheduling variables and interpolated by a specified interpolation method. Final step is evaluating stability and performance of the closed loop system on both the local and global level. Typically, stability can be only assured locally under the assumption of "slow-varying" and there are rarely global performance guarantees.

Many different design schemes have been proposed for gain-scheduling methodologies. However, if these designed plant models can't reflect the real system accurately, guaranteed global stability of the nonlinear system and desired performance may not be achieved [3], [13].

In classical gain-scheduling approaches, a nonlinear plant can be represented with a finite number of linearized models. Stabilizing controllers are designed for each local plant models then interpolated as a function of scheduling variables that may be exogenous or endogenous signals with respect to the plant. Controller interpolation methods that guarantee the stability for any fixed value of the scheduling parameter,

known as frozen parameter stability, have been proposed and recently focused on guaranteeing this level of stability by construction [14], [15], [16], [17]. The interpolation method used in common is called “Local Controller Network (LCN)” [18], [19], discussed extensively in the following section. Although it seems to be working properly in practice, this design procedure may not provide the stability and performance where scheduling variables are arbitrarily varying fast.

The LPV (or quasi-LPV) modeling method was recently introduced in nonlinear plant modeling techniques. In this framework, controller gains depend on the variation of plant dynamics and nonlinear terms of the plant model are hidden with newly-defined time-varying parameters that include scheduling variables, termed in “quasi-LPV modeling [20], [21], [22], [23].” LPV control theory has been useful to simplify the interpolation and realization associated with conventional gain-scheduling. Specifically, it enables the design of a single parameter-dependent gain-scheduled controller. However, controller synthesis may not be computationally feasible and stabilizing may not exist since gain-scheduled controllers cannot be designed at specific operating points [2].

Despite its successful applicability in many engineering problems, gain-scheduling remains an ad hoc approach. Stability analysis as well as performance assessment of a global gain-scheduled control system are not explicitly implemented in design procedure, mostly by extensive simulations [3], [24]. Furthermore, guaranteeing the stability of the nonlinear closed loop system is still a challenging problem. Simplicity in design, where linear controllers and ad hoc interpolation methods are used, is

contrasted with difficulties in analysis, thus guaranteeing that the stability of the resulting nonlinear closed loop system will be extremely challenging. Moreover, the presence of “hidden coupling” terms or “scheduling dynamics” due to the interpolation functions can create unanticipated stability problems.

Furthermore, no research has given an exact solution to guarantee stability when scheduling variables are varying rapidly. Conventional gain-scheduling approaches may not guarantee performance when the system includes modeling uncertainties. Thus introducing an advanced framework, improving system robustness, and guaranteeing global stability under arbitrary switching, satisfy the desired goal of nonlinear system control.

1.1.1 Scheduling Variables

Choice of scheduling variables in gain-scheduled plant models provides a design degree of freedom which can effectively reflect the dynamics of the system. Thus many different design schemes have been proposed for gain-scheduling methodologies, but there exist two rules-of-thumb – “scheduling variable should vary slowly” and “the scheduling variable should capture the plant’s nonlinearities” [2]. The “slowly varying” requirement is intended to extend local stability analysis to provide global results, and the “capturing the nonlinearities” assumption ensures nonlinear model accuracy. Scheduling variables may have exogenous or endogenous signals with respect to the system**.** Thus, in some cases, assumed rate limitations on the scheduling variables are not realistic, and advanced analysis techniques are required to guarantee stability.

1.1.2 LPV Plant Modeling

Clearly, gain-scheduled control design involves nonlinear plant modeling, controller interpolation, and stability/performance assessment - these three categories are closely related [19], [25]. In classical ways, the Local Model Network (LMN) approach has been proven to be effective for appropriately selected scheduling variables [18], [26]. Alternatively, the implication of LPV-way in gain scheduling is obvious since gain scheduling often involves a linear parameter varying system [20], [27]. Several LPV approaches such as off-equilibrium linearization (velocity-based linearization) and Lyapunov-based LPV methods are introduced in [28], [29], [30], [31]. In application, several works in quasi-LPV plant modeling techniques are incorporated in aerospace technologies [32], [33], [34].

1.1.3 Gain-scheduling via Linear Controller Interpolation

Many different approaches have also been proposed for controller interpolation [2], [35]. These include interpolation between controller transfer function, H_∞ controllers by linearly interpolating the solution of Ricatti equation [8], state-space matrices of balanced controller realizations, state feedback gains [7], and observer gains [16], [36], [37], [38], [39]. The interpolation method commonly used is called “Local Controller Network (LCN)”, [18], [19]. In essence, several controllers are implemented in parallel, and their respective outputs are blended to form the control signal. This approach is similar to fuzzy controllers [40], but instead of blending the values of state variables, the total output is a weighted average of the individual controller outputs. The

LCN is simple and intuitive, but may not stabilize the system at off-design points, and may require that the controllers be open-loop stable [24].

Controller interpolation methods that guarantee stability for any fixed value of the scheduling parameter, known as frozen parameter stability, have been proposed and have recently focused on guaranteeing the stability by construction [14], [17]. However, guaranteeing stability during transitions, particularly fast transitions, is challenging [41]. For a restricted case, Hespanha and Morse considered this interpolation "switching between stabilizing controllers" and proposed the suitable interpolation method via the realization of controller transfer matrices and stability with impulse effect [15].

1.1.4 Gain-scheduling via LPV Control Synthesis

The LPV (or quasi-LPV) gain-scheduling method assumes an LPV plant representation, where the parameter variations capture the system nonlinearities. Nonlinear controller is synthesized based on the LPV plant model, and guarantees nonlinear stability by construction [13], [20], [21]. While the problem of guaranteeing stability is solved, the resulting LPV controller does not allow the user to design specific controllers under key operating conditions [42], [43], [44]. Moreover, the control synthesis procedure may prove infeasible.

1.1.5 Stability Analysis

For the local and global-level stability analysis, a Lyapunov-based nonlinear stability criterion is exploited in this work. Using the Lyapunov-based stability analysis,

many works have introduced the LMI-based algebraic conditions to provide a common Lyapunov function to guarantee stability over operating envelopes using parameter-dependent functions under discrete output feedback [45], [46], [47], continuous output feedback LPV control [48], and state-feedback control [49]. Liberzon proposed the commutativity of nonlinear system based on Lie-algebra as a preliminary condition for the existence of a common Lyapunov function [50], [51], [52], [53]. Other works have derived specific algebraic conditions as a necessity of existence in similar ways [54], [55]. Comparatively, Blondel explained it using "simultaneous stabilization" concepts based on Nyquist and Popov criterion in frequency domain [56], [57].

1.2 Youla Parameterization-based Gain-Scheduling

Gain-scheduling based on the Youla parameterization is a recently proposed approach [58], [59], [60], [61], utilizing the idea proposed by Youla, Bongiorno, and Jabr in 1976 [62]. The crux of the Youla parameterization is the ability to explain how all stabilizing controllers can be parameterized in terms of a single variable, called "Youla parameter" Q; all plant models can be parameterized in terms of dual Youla parameter S. Under this framework, the closed loop system is affine in the Youla parameters and allows the problem of the search for an optimal stabilizing controller to be posed as a convex optimization problem [63].

The dual Youla parameter is the open-loop transfer function between input and output vectors for the connection of the Q parameter in the standard Youla parameterization. Thus stability of the closed-loop system requires stability of the

nominal closed-loop system and the real system. The magnitude of the dual Youla parameter is a measure of the difference between the nominal and real system. These two important points make the Youla parameterization useful in both design of different types of controller and the validation of closed-loop performance. By virtue of Youla-based gain-scheduling, interpolation between controllers of different sizes and structures or open-loop unstable is allowable [24].

1.3 Stability Analysis with Robustness Consideration

One of the significant impacts of gain-scheduling strategy on nonlinear system controls is its applicability to physical systems whose dynamics are highly nonlinear or have a high uncertainty level [64], [65]. When an LPV plant model includes unstructured uncertainties or modeling error and these factors significantly affect the system dynamics, plant model may not precisely reflect the nonlinear system and conventional stability analyses may not be sufficient to guarantee the stability of the nonlinear system [66], [67]. Any plant model could possibly contain the unstructured modeling error, thus unmodelled dynamics uncertainty could be addressed with a simple nominal model [3] and investigated here to improve robustness of the perturbed nonlinear system.

Thus an LPV closed loop system with uncertainty is prepared and its state matrix is forced to form in a block-diagonal structure by construction. The resulting system is then guaranteed to be robustly stable where the preliminary condition, $\|\Delta\|_\infty < 1$, is satisfied. The proposed framework, utilizing L_2 gain of the modified LPV/LQN system via optimizing feedback gains of the closed system, guarantees the global level of robust

stability by minimizing the L_2 gain that remains within desired bounds over the operating envelop [68], [69].

1.4 Control of Vapor Compression Systems

Vapor compression systems have been widely used for residential and industrial purposes and consume a huge amount of energy [70]. Thermal efficiency of the system has been considered a key aspect in energy saving since energy demand in air conditioning systems will be reduced by achieving the desired energy efficiency via developing an accurate system model and advanced control strategy [71], [72].

Unfortunately, the dynamics of these systems are well known to be highly nonlinear, and vary significantly over operating conditions. Although a very strictly designed controller could possibly stabilize the system, significant performance would be sacrificed to guarantee the desired global stability, thus an advanced gain-scheduled control approach can be an intuitive solution for these systems [5].

For these purposes, an advanced gain-scheduling framework based on previously obtained results is applied to the vapor compression system. This experimental case study illustrates the effectiveness of the proposed Youla-based gain-scheduling framework in practice while achieving desired stability and performance.

1.5 Research Objectives

The main goal of this research is to create an advanced gain-scheduling method for the nonlinear system that guarantees stability and an acceptable level of performance. This research will utilize the Youla parameter-based framework for gain scheduling, under the assumption that local controllers have been designed *a priori*. Thus, the selected problem is to ensure local controller recovery at specified design points while utilizing an interpolation scheme that guarantees stability at off-design conditions and during scheduling transitions. The local controllers may be of different state dimensions and possibly open-loop unstable. Research achievements include:

- Examining the general case of Youla parameter-based gain-scheduling, and identify elements of design freedom
- Develop a Youla parameter based framework for LPV systems that guarantees stability of the nonlinear closed loop system while scheduling variables arbitrarily vary fast
- Eliminate the need to run multiple local controllers in parallel by developing an LPV controller synthesis procedure that ensures local controller recovery and closed loop stability
- Extend stability analysis to include robustness and performance considerations
- Experimental case study demonstrating the above techniques

1.6 Dissertation Organization

The remainder of this dissertation is organized as follows. Section 2 describes fundamentals and background on gain scheduled control and Youla parameterization. Section 3 examines general case of Youla-based gain scheduling and develops a specific Youla based framework for an LPV system that guarantees stability of the nonlinear closed loop system while scheduling variables vary arbitrarily fast. Based on the results obtained in Section 3, extended stability analysis to include robustness and performance considerations is presented in Section 4. Section 5 discusses the experimental case study that demonstrates the above techniques by applying to vapor compression system. Conclusions and recommendations for future work are given in Section 6.

2. INTRODUCTION TO GAIN SCHEDULED CONTROL

Many physical systems have been observed to be highly nonlinear and vary arbitrarily fast in a wide range of operating envelopes. To achieve the desired control of nonlinear systems, the nonlinear control strategy should guarantee acceptable performance as well as nonlinear stability throughout the operating conditions [1]. Gain-scheduled control paradigm has successfully been proved to be an efficient way to satisfy the stability and performance criteria required in nonlinear system analyses. This section presents fundamentals of gain-scheduled control and the Youla parameterization, an advanced controller interpolation method used in gain-scheduled control design and implementation.

2.1 Introduction

As discussed in the introduction, gain-scheduling has shown good potential to incorporate linear control methods into nonlinear control design and has been widely used to control nonlinear systems in a variety of industrial applications [1]. In general, when a plant is modeled with the gain-scheduled control paradigm implemented by the collection of linear time-invariant approximations to a nonlinear plant at a fixed operating condition where scheduling variables are assumed to be varying slowly, then individual controllers are designed explicitly at fixed operating points. Plant model is also assumed to capture the nonlinearities that exist in real systems.

Plant models of a nonlinear system are determined from first principles or by interpolating identified models. Then local controllers for the plant are designed by linear control design methods and linear controllers are represented in terms of scheduling variables and interpolated by a specified interpolation method. Stability and performance of the closed loop system should be evaluated both locally and globally.

Despite overwhelming successes in gain scheduling, few approaches guarantee stability while scheduling variables are varying rapidly or where the system is highly nonlinear and includes modeling uncertainties. Thus improving system robustness and guaranteeing global stability under arbitrary switching will be the motivation for this dissertation.

The remainder of this section is organized as follows. Section 2.2 describes nonlinear plant modeling, including LPV and LMN frameworks. Section 2.3 examines controller interpolation methods in gain-scheduling such as LPV synthesis and LCN interpolation. Stability analysis to include nonlinear stability, linear stability with Linear Matrix Inequalities (LMIs), and LMI-based stability with performance is presented in Section 2.4. Finally, Youla parameterization-based gain-scheduling with mathematical backgrounds is discussed in Section 2.5. This section is described with details in reference [5].

2.2 Nonlinear Plant Modeling

This section discusses nonlinear plant modeling and local control design in gain-scheduling. Considering the standard feedback loop of the nonlinear control system

depicted in Figure 2.1, the plant and controller in Figure 2.1 are assumed to be nonlinear where d is disturbance inputs, u is control outputs, z is performance outputs, and y is control inputs.

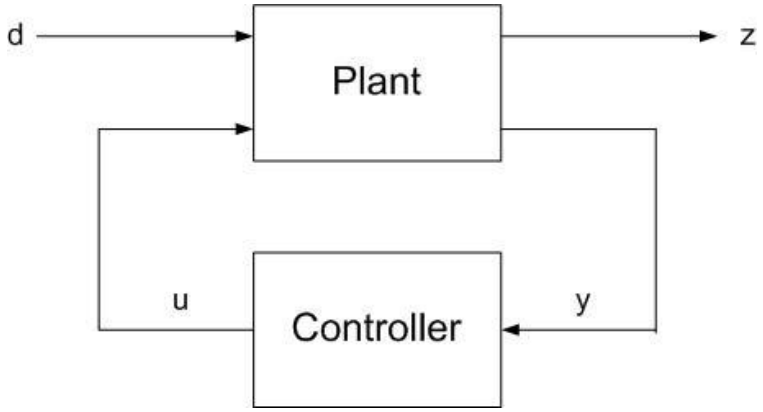

Fig. 2.1. General closed loop of nonlinear system.

2.2.1 Nonlinear Plant Model

A general representation of nonlinear control system in Figure 2.1 is given by

$$\begin{aligned} \dot{x} &= f(x,u,d) \\ y &= g(x,u,d) \\ z &= h(x,u,d) \end{aligned} \tag{2.1}$$

where x is the state of the system, y is system outputs (control inputs), and z is performance outputs. Note that the functions $f, g,$ and h are assumed to be continuously differentiable in real space.

2.2.2 Linearization-based Plant Modeling

The nonlinear plant representation in Equation 2.1 can be linearized around the equilibrium point (x_0, u_0, d_0) using Jacobian linearization. The resulting state space representation of the nonlinear system is derived by a low-order Taylor series expansion as given by

$$\begin{aligned}
\delta x &= \left(\left.\frac{\partial f}{\partial x}\right|_{x_0,u_0,d_0} \right)\delta x + \left(\left.\frac{\partial f}{\partial u}\right|_{x_0,u_0,d_0} \right)\delta u + \left(\left.\frac{\partial f}{\partial d}\right|_{x_0,u_0,d_0} \right)\delta d \\
\delta y &= \left(\left.\frac{\partial g}{\partial x}\right|_{x_0,u_0,d_0} \right)\delta x + \left(\left.\frac{\partial g}{\partial u}\right|_{x_0,u_0,d_0} \right)\delta u + \left(\left.\frac{\partial g}{\partial d}\right|_{x_0,u_0,d_0} \right)\delta d \\
\delta z &= \left(\left.\frac{\partial h}{\partial x}\right|_{x_0,u_0,d_0} \right)\delta x + \left(\left.\frac{\partial h}{\partial u}\right|_{x_0,u_0,d_0} \right)\delta u + \left(\left.\frac{\partial h}{\partial d}\right|_{x_0,u_0,d_0} \right)\delta d
\end{aligned} \tag{2.2}$$

where $\delta x = x - x_0$, $\delta u = u - u_0$, $\delta d = d - d_0$, $\delta y = y - y_0$, and $\delta z = z - z_0$.

The Jacobian matrices of states, control inputs, and performance outputs in Equation 2.2 can be a function of the system variables (x, u, d). The subset of the variables that parameterize the Jacobian matrices can be denoted as a scheduling variable $\theta \subset (x, u, d)$. Thus a linear approximation of a nonlinear plant model around the equilibrium point, $\theta_0 \subset (x_0, u_0, d_0)$, is given by a Linear Time Invariant (LTI) model as follows:

$$\begin{bmatrix} \delta \dot{x} \\ \delta y \\ \delta z \end{bmatrix} = \begin{bmatrix} A_p(\theta_0) & B_{up}(\theta_0) & B_{dp}(\theta_0) \\ C_{py}(\theta_0) & D_{uy}(\theta_0) & D_{dy}(\theta_0) \\ C_{pz}(\theta_0) & D_{uz}(\theta_0) & D_{dz}(\theta_0) \end{bmatrix} \begin{bmatrix} \delta x \\ \delta u \\ \delta d \end{bmatrix} \tag{2.3}$$

where $\begin{bmatrix} A_p(\theta_0) & B_{up}(\theta_0) & B_{dp}(\theta_0) \\ C_{py}(\theta_0) & D_{uy}(\theta_0) & D_{dy}(\theta_0) \\ C_{pz}(\theta_0) & D_{uz}(\theta_0) & D_{dz}(\theta_0) \end{bmatrix} = \begin{bmatrix} \left(\frac{\partial f}{\partial x}\Big|_{x_0,u_0,d_0}\right) & \left(\frac{\partial f}{\partial u}\Big|_{x_0,u_0,d_0}\right) & \left(\frac{\partial f}{\partial d}\Big|_{x_0,u_0,d_0}\right) \\ \left(\frac{\partial g}{\partial x}\Big|_{x_0,u_0,d_0}\right) & \left(\frac{\partial g}{\partial u}\Big|_{x_0,u_0,d_0}\right) & \left(\frac{\partial g}{\partial d}\Big|_{x_0,u_0,d_0}\right) \\ \left(\frac{\partial h}{\partial x}\Big|_{x_0,u_0,d_0}\right) & \left(\frac{\partial h}{\partial u}\Big|_{x_0,u_0,d_0}\right) & \left(\frac{\partial h}{\partial d}\Big|_{x_0,u_0,d_0}\right) \end{bmatrix}$

Under linearization-based modeling methods, the nonlinear plant can be decomposed into several linear approximations around specific operating conditions. Similarly in the gain-scheduling paradigm, a nonlinear plant model can be represented in terms of several LTI plant models obtained at specific operating points that are suitable for utilizing linear control design tools; those plant models are parameterized by a set of scheduling variables that indicate the current states of the nonlinear system. Note that a local LTI approximation of the nonlinear plant at equilibrium point is not identical to a Linear Parameter Varying (LPV) representation at specific operating point; this will be described in the following section.

2.2.3 Linear Parameter Varying (LPV) Plant Modeling

A Linear Parameter Varying (LPV) representation of the nonlinear system is a special case of a system modeling method defined as “A linear system whose dynamics depend on exogenous parameters with values that are unknown *a priori* but can be measured on-line” [13]. A state space representation of LPV system is given in Equation 2.4

$$\begin{bmatrix} \dot{x} \\ y \\ z \end{bmatrix} = \begin{bmatrix} A_p(\theta(t)) & B_{up}(\theta(t)) & B_{dp}(\theta(t)) \\ C_{py}(\theta(t)) & D_{uy}(\theta(t)) & D_{dy}(\theta(t)) \\ C_{pz}(\theta(t)) & D_{uz}(\theta(t)) & D_{dz}(\theta(t)) \end{bmatrix} \begin{bmatrix} x \\ u \\ d \end{bmatrix} \tag{2.4}$$

If there does not exist an LPV representation of the nonlinear system in nature, an alternative plant representation approach called “quasi-LPV representation” can be potentially used to parameterize a family of linear models. In the quasi-LPV method, nonlinear terms are hidden with newly defined time-varying parameters that are then included in the scheduling variable [73]. Note that quasi-LPV representations are not unique and a suitable representation may not be well suited for controller design.

2.3 Controller Interpolation

A rough categorization of controller design methods on gain scheduled control would include two classes: 1) local linear control designs and 2) LPV control design methods [13]. The former approach is extensively used in practice and allows a sufficiently large degree of freedom in the design process. However it may suffer from a general lack of suitable tools for stability analysis. The latter has the advantage that some level of stability is guaranteed by construction of the controller but the controllers are designed as a whole and synthesized with common dimension and structure and no guarantee of existence. Thus some freedom in the design process may be lost and result in difficulties during the computation.

2.3.1 Local Controller Network (LCN)

2.3.1.1 Local Controller Design

In this framework, a nonlinear control design problem can be decomposed into several linear control problems by employing many linear design tools, often called the "divide-and-conquer" method. The local linear controllers can be designed at each design point which is suitable for implementing linear control design, denoted as follows

$$\begin{bmatrix} \delta\dot{x}_k \\ \delta u \end{bmatrix} = \begin{bmatrix} A_k(\theta_0) & B_k(\theta_0) \\ C_k(\theta_0) & D_k(\theta_0) \end{bmatrix} \begin{bmatrix} \delta x_k \\ \delta u \end{bmatrix} \tag{2.5}$$

Design methods of local linear controllers have been reported from PID control to LQG and H_∞ control [2], [5]. Controller interpolation between these locally designed controllers is implemented by parameterizing them in scheduling variables, a key idea of gain-scheduled control which will be intensively discussed in the next section.

2.3.1.2 Local Controller Network (LCN)

Controller interpolation is the crux of gain-scheduling approaches and many different controller interpolation methods have been proposed. These include the interpolation of poles, zeros, and gains, interpolation of H_∞ controllers by interpolating Riccati equations, interpolations of balanced state space matrix coefficients, interpolation of state feedback gains and observer gains, and the interpolation of pole placement of state feedback gains [13]. Alternatively, several approaches have been proposed that implement controller blending as a function of operating condition then forming a global nonlinear controller [2].

The latter type of gain-scheduled control is often called "output-blending," similar to the Tagaki-Sugeno model that is widely used in the derivation of fuzzy membership function [40]. By virtue of output-blending, interpolation between controllers with different dimension and structure is allowable without any restriction on the design of local controllers.

Under this type of controller interpolation, a nonlinear controller can be formed by blending the weighted outputs of several linear controllers. These weighting functions can be presented in terms of scheduling variables ρ, as $\alpha(t) = f(\rho(t))$ and the weighted sum of those functions is commonly assumed to be $\alpha_i(t) \in [0,1]$ and $\sum \alpha_i(t) = 1$, but this assumption is situation-dependent and may not be necessary in some cases.

This output-blending approach results in a Local Controller Network (LCN), widely used in practice due to its simplicity during controller interpolation. A controller is constructed using a linear approximation of the nonlinear model, either first principle model or empirical identification model, by employing linear control design tools. The weighted sum of outputs from a family of local controllers is then applied to the nonlinear plant.

Similarly, a Local Model Network (LMN) is constructed by computing local plant models in parallel. This is assumed to adequately represent the dynamics of nonlinear system where the local linear representations of the plant are obtained from linearization of nonlinear plant or empirically through system identification techniques. This LMN can be simply denoted as $P_\alpha(s) = \sum \alpha_i P_i(s)$, and similarly the LCN as

$K_\alpha(s) = \sum \alpha_i K_i(s)$. The interconnected LCN/LMN system is depicted in Figure 2.2, and the simplified diagram in Figure 2.3.

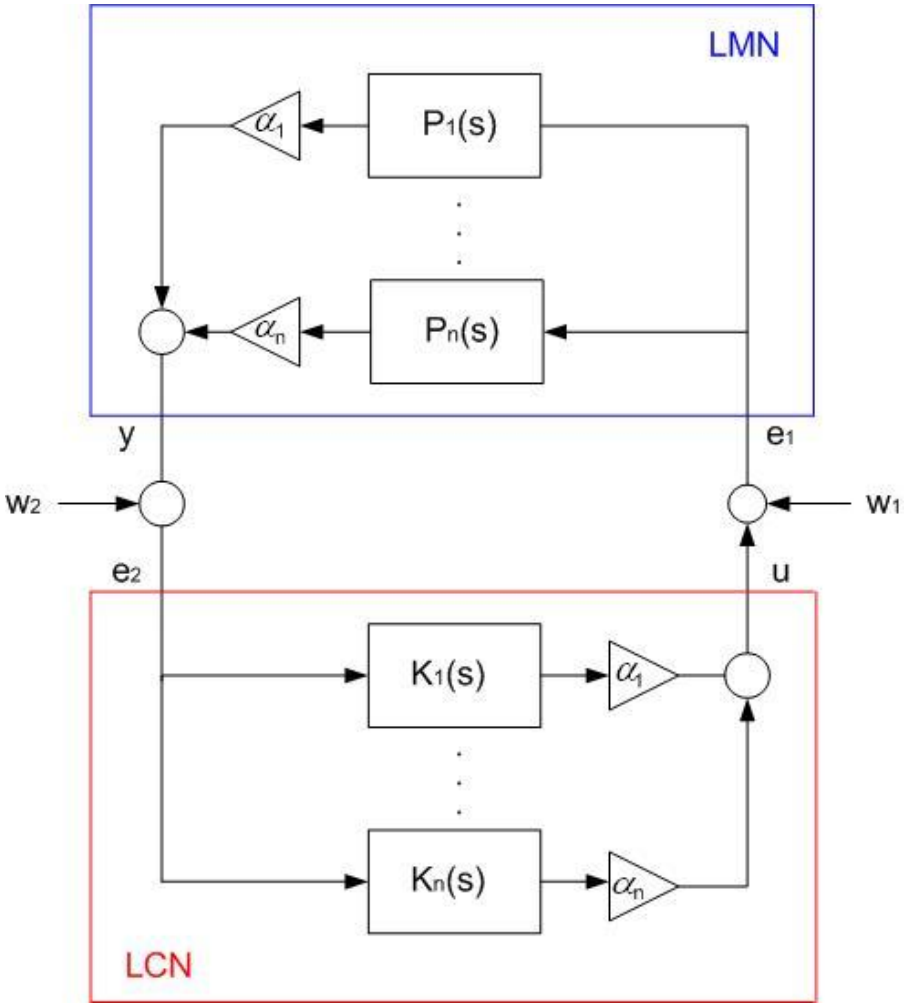

Fig. 2.2. Interconnected system of LMN/LCN.

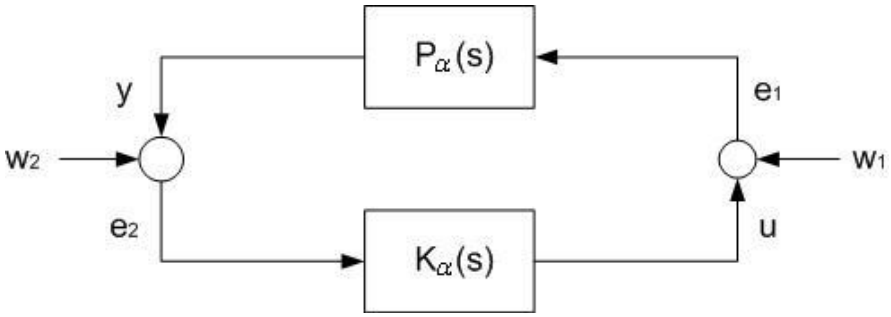

Fig. 2.3. Simple diagram of LMN/LCN interconnected system.

2.3.1.3 LCN/LMN Closed Loop System

Consider the interconnected LCN/LMN system derived in Figure 2.2. Under this framework, a set of local linear models of plant $P_i(s)$ is given by

$$\begin{bmatrix} \dot{x}_{pi} \\ y_{pi} \end{bmatrix} = \begin{bmatrix} A_{pi} & B_{pi} \\ C_{pi} & D_{pi} \end{bmatrix} \begin{bmatrix} x_{pi} \\ e_1 \end{bmatrix} \tag{2.6}$$

and a set of local linear controllers $K_i(s)$ is given by

$$\begin{bmatrix} \dot{x}_{ki} \\ u_{ki} \end{bmatrix} = \begin{bmatrix} A_{ki} & B_{ki} \\ C_{ki} & 0 \end{bmatrix} \begin{bmatrix} x_{ki} \\ e_2 \end{bmatrix} \tag{2.7}$$

The state space representation of the closed loop from $\begin{bmatrix} w_1 & w_2 \end{bmatrix}^T$ to $\begin{bmatrix} u & y \end{bmatrix}^T$ is given in Equation 2.8, denoted $G_\alpha(s)$. Note that this closed loop can be represented as a system affinely parameterized in α with the constraint $\sum \alpha_i(t) = 1$. Alternatively, the plant and controller representations can be formed in a polytopic system of individual plant models and controllers respectively as given by Equations 2.9-10.

$$\begin{bmatrix}\dot{x}_p\\ \dot{x}_k\end{bmatrix}=\underbrace{\begin{bmatrix}A_p & B_pC_k\\ B_kC_p & A_k\end{bmatrix}}_{A_G(\alpha)}\begin{bmatrix}x_p\\ x_k\end{bmatrix}+\underbrace{\begin{bmatrix}B_p & 0\\ 0 & B_k\end{bmatrix}}_{B_G}\begin{bmatrix}w_1\\ w_2\end{bmatrix}$$
$$\begin{bmatrix}u\\ y\end{bmatrix}=\underbrace{\begin{bmatrix}0 & C_p\\ C_k & 0\end{bmatrix}}_{C_G(\alpha)}\begin{bmatrix}x_p\\ x_k\end{bmatrix} \tag{2.8}$$

$$\begin{bmatrix}\dot{x}_{p1}\\ \vdots\\ \dot{x}_{pn}\end{bmatrix}=\begin{bmatrix}A_{p1} & & 0\\ & \ddots & \\ 0 & & A_{pn}\end{bmatrix}\begin{bmatrix}x_{p1}\\ \vdots\\ x_{pn}\end{bmatrix}+\begin{bmatrix}B_{p1}\\ \vdots\\ B_{pn}\end{bmatrix}e_1$$
$$y=\begin{bmatrix}\alpha_1C_{p1} & \cdots & \alpha_nC_{n1}\end{bmatrix}\begin{bmatrix}x_{p1}\\ \vdots\\ x_{pn}\end{bmatrix} \tag{2.9}$$

$$\begin{bmatrix}\dot{x}_{k1}\\ \vdots\\ \dot{x}_{kn}\end{bmatrix}=\begin{bmatrix}A_{k1} & & 0\\ & \ddots & \\ 0 & & A_{kn}\end{bmatrix}\begin{bmatrix}x_{k1}\\ \vdots\\ x_{kn}\end{bmatrix}+\begin{bmatrix}B_{k1}\\ \vdots\\ B_{kn}\end{bmatrix}e_2$$
$$u=\begin{bmatrix}\alpha_1C_{k1} & \cdots & \alpha_nC_{kn}\end{bmatrix}\begin{bmatrix}x_{k1}\\ \vdots\\ x_{kn}\end{bmatrix} \tag{2.10}$$

2.3.2 LPV Control Synthesis

One recently used control design method in gain-scheduling is the LPV control design. Under this framework, an LPV representation of the nonlinear plant is assumed to exist and the associating controllers are designed as a whole with common size and structure where each controller shares the state variables. Thus, if this representation exists, stability of the nonlinear closed loop system is guaranteed when prescribed conditions restricted to the scheduling variable are satisfied. Specifically, these conditions advocate that scheduling variables are measurable, bounded, and that the time

derivative of scheduling variables is bounded. These pre-conditions may be very conservative in practice and thus current research attempts to reduce them [5].

Although the LPV control cannot allow a sufficiently large design degree of freedom in design and implementation of gain-scheduling, e.g., design local controllers at key operating point *a priori* are not available, it guarantees a certain level of stability of the system by construction. First, we assume parameter variations in the LPV plant model as modeling uncertainty where a single LTI controller is sought so that a small gain condition is met [24]. If there exists an LTI controller that satisfies the condition, stability can be guaranteed for arbitrarily fast variations in the scheduling parameter, but this generally results in a poorly performing controller due to extremely conservative assumptions of control design.

Alternatively, an LPV controller can be sought so that stability of the closed loop system is guaranteed by existence of a common or parameter-dependent Lyapunov function. Under this framework, an interpolated controller can be sought by solving a set of Linear Matrix Inequalities (LMIs) which allows enhanced efficiency in analysis [24] [74]. However, guaranteeing stability in this way may potentially be very conservative in that the common Lyapunov function should be found over the entire operating envelope where scheduling variables may change arbitrarily fast. Thus recent researches have employed parameter dependent Lyapunov functions that can reduce some of the severe restrictions if the time derivative of the scheduling variable can be bounded [51].

LPV gain scheduling has been proved to be successful for guaranteeing a certain level of stability by construction, but lack of existence and conservatism of the design process cause computational difficulties and limit wide application in practice.

2.4 Stability Analysis

As mentioned in Section 1, guaranteeing the closed loop stability of nonlinear system has been a challenging problem. Some research has successfully shown the stability of the nonlinear system at local operation conditions, but little research has shown global stability. Furthermore, the endogenous scheduling system requires more careful evaluation in order to guarantee the stability over operating regions since endogenously scheduling variables or their bounds cannot be known *a priori*. Thus guaranteeing the desired level of performance and stability of the gain-scheduled closed loop system under any operating conditions is he primary research objective of this dissertation.

2.4.1 Stability Classification

Stability analyses of gain-scheduled closed loop systems can be roughly categorized into linear and nonlinear stability criteria [13], [64]. The simplest criteria in linear stability analyses, i.e., stability evaluated for linearized system, is frozen parameter stability where closed loop stability is evaluated and the standard feedback loop of linearized plant model and linear controller is examined to be Hurwitz. Note that frozen parameter stability is a merely guarantee of stability at fixed scheduling

parameters. Although this stability criterion is commonly used in practice, it may not be sufficient for the nonlinear stability of real systems when significant nonlinear dynamics are neglected during the linearization.

In contrast, nonlinear stability ensures the practical stability of nonlinear system in that stability is evaluated for closed loop systems without neglecting any aspects of the system techniques. There exist several nonlinear stability analyses in literature [46], but Lyapunov stability is one of most commonly used solutions to achieve nonlinear stability. Under this criterion, the existence of the common or parameter-dependent Lyapunov function with respect to the trajectories of the nonlinear system will guarantee the asymptotic stability of the nonlinear system globally or for reasonably large region around the equilibrium point [36].

2.4.1.1 Linear Stability Analysis

One of the common methods used in linear stability analysis can be examined simply by evaluating the closed loop stability of the linearized plant model. In nonlinear system approaches, this level of stability can be guaranteed for any fixed value of the scheduling variables without considering scheduling dynamics. However, the global controller, which is formed by interpolation between local stabilizing controllers, may not stabilize the system at the intermediate operating points, i.e., off-design points, even if local controllers may stabilize at design points.

The simple example given below efficiently illustrates the possibility that a global control system violates stability. Using the linear control design under the Local

Controller Network (LCN) approach, an interpolated controller could be defined as a convex set of two local controllers where weighting factor $\alpha_i \in [0,1]$ (Equation 2.12). Note that individual controllers K_1 and K_2 successfully stabilize the plant but the interpolated controller K_I, denoted in Equation 2.12, fails to stabilize the plant for $\alpha \in [0.25, 1]$

$$P(s) = \frac{1}{s+1}, K_1(s) = \frac{-1}{s+0.5}, K_2(s) = \frac{-1}{s-0.5} \tag{2.11}$$

$$K_I(s) = \alpha K_1 + (1-\alpha)K_2 \tag{2.12}$$

Several studies have proposed controller interpolation methods that guarantee frozen parameter stability under the preliminary condition that scheduling variables are changed sufficiently slowly, then the stability of nonlinear system will be guaranteed when the condition is valid over the operating regions.

Alternatively, other approaches define the acceptable rate of change on scheduling variables, but the "slowly varying" assumptions are still essential to guarantee the global stability of a given system. Thus, these types of approaches may be valid for exogenously-scheduling systems where the rate of change of the scheduling variable is usually known *a priori* and nonlinear behavior of many systems is more appropriately captured by scheduling parameters that are functions of system outputs. However, guaranteeing the stability of endogenously scheduled systems is much harder to achieve since a bound on the rate of change may not be known *a priori*.

2.4.1.2 General Nonlinear Stability Analysis

Any linear stability technique merely evaluates whether the system is asymptotically stable for infinitesimal deviations around the equilibrium point [46]. It may not be sufficient to guarantee the stability of the nonlinear system particularly when scheduling variable changes in a wide range of operating conditions. To guarantee the desired global stability under arbitrary variations, the nonlinear stability of the closed loop system should be evaluated.

A well-known method for guaranteeing this level of stability of a nonlinear system is to use Lyapunov stability criterion, defined in Theorem 2.1 [25]. Before explaining the Lyapunov stability, some key definitions related to this criterion are addressed for better understanding of the stability analysis in this dissertation.

Definition 2.1) Stability of an equilibrium point [25]

The equilibrium point $x = 0$ of the autonomous system $\dot{x} = f(x)$ is

- stable if, for each $\varepsilon > 0$, there is $\delta = \delta(\varepsilon) > 0$ such that

$$\|x(0)\| < \delta \Rightarrow \|x(t)\| < \varepsilon \ , \ \forall t \geq 0 \tag{2.13}$$

- unstable if it is not stable
- asymptotically stable if it is stable and there exists δ such that

$$\|x(0)\| < \delta \Rightarrow \lim_{t \to \infty} x(t) = 0 \tag{2.14}$$

Definition 2.2) Global asymptotic stability [25]

The equilibrium point $x = 0$ of the autonomous system $\dot{x} = f(x)$ is globally asymptotically stable if

- $x = 0$ is asymptotically stable and
- $\lim_{t \to \infty} x(t) = 0$ for all $x_0 \in R^n$ (2.15)

Definition 2.3) Class K functions [25]

The continuous function ψ is called a *class K* function if

- $\psi(0) = 0$ (2.16)
- $\psi(\|x\|) > 0, \quad \forall \|x\| > 0$ (2.17)
- $\psi(\|x\|)$ is strictly monotonically increasing with $\|x\|$ (2.18)

Definition 2.4) Positive-definite functions [25]

The continuous function $V(x,t)$ is positive definite on $G \in R^n$ if

- $V(x,t) \geq \psi(\|x\|), \quad \forall x \in G$ and $\forall t \geq 0$ (2.19)

Definition 2.5) Decrescent functions [25]

The continuous function $V(x,t)$ is called a decrescent function on $G \in R^n$ if there exists a *class K* function β such that

- $V(x,t) \leq \beta(\|x\|), \quad \forall x \in G$ and $\forall t \geq 0$ (2.20)

Theorem 2.1) Lyapunov stability [25]

Let $x = 0$ be an equilibrium point for the nonlinear autonomous system $\dot{x} = f(x)$. Let $V : R^n \to R$ be a continuously differentiable function such that

$$V(0) = 0 \text{ and } V(x) > 0 \quad \forall x \neq 0 \tag{2.21}$$

$$\text{c} \Rightarrow V(x) \to \infty \tag{2.22}$$

$$\dot{V}(x) < 0 \quad \forall x \neq 0 \tag{2.23}$$

Then the equilibrium point $x = 0$ is a globally asymptotically stable.

Proof:

Assume there exists $\exists \varphi$ in class k function such that $V(x,t) \geq \varphi(\|x\|)$ where $\forall x \in B(0,h)$, $t \geq t_0$. Also, when $\dot{V}(x,t) \leq 0$ is satisfied along the trajectories of system $\dot{x} = f(x)$ then we know that

$$V(x,t) \leq V(x_0, t_0) \tag{2.24}$$

Next, let δ be the smallest $\|x_0\|$ such that $V(x_0, t_0) = \varphi(\varepsilon)$. Given $\varepsilon > 0$, for all δ,

$$\|x_0 - \theta\| < \delta \Rightarrow \|x(t) - \theta\| < \varepsilon \tag{2.25}$$

Then we know that:

$$\|x_0\| < \delta \Rightarrow V(x_0, t_0) < \varphi(\varepsilon) \tag{2.26}$$

$$\|x_0\| < \delta \Rightarrow V(x,t) \leq \varphi(\varepsilon) \tag{2.27}$$

Finally, we can conclude that the solution to the nonlinear autonomous system $\dot{x} = f(x)$ is globally asymptotically stable using the final form in Equation 2.28

$$\varphi(\|x(t)\|) \leq \varphi(\varepsilon) \Rightarrow \|x(t)\| < \varepsilon \tag{2.28}$$

A function $V(x)$ that satisfies the conditions in Equation 2.21-23 is called a Lyapunov function; thus a Lyapunov function should be a positive-definite decrescent function and the negative form of Lie-derivative $-\dot{V}(x)$ is positive-definite. The quadratic form of Lyapunov function $V(x) = x^T Px, P > 0$ has been widely used for linear, LPV, and polytopic systems where x is system states and P is Lyapunov matrix. For linear autonomous systems $\dot{x} = Ax$ the choice of quadratic function leads to the condition in Equation 2.23 as $\dot{V}(x) = x^T (A^T P + PA)x < 0$ such that the condition for stability is equivalent to finding a solution to the well-known Lyapunov Equation $A^T P + PA = -Q$ where Q is a positive-definite matrix [74].

2.4.1.3 Nonlinear Stability with Guarantee of Worst Performance

Despite the fact that the nonlinear stability guarantees closed loop stability of the nonlinear system, it may not be sufficient for assuming the practical stability required in gain-scheduled control. Under the gain-scheduling framework, the LMN or LPV representation of the nonlinear system may perform reasonably well - merely within a specified operating range. Thus, any stability guarantees will be valid only when the system does not leave the operating range during the entire operation [65].

Furthermore, guarantees of the worst case performance will be useful in improving practical aspects of the stability analysis for nonlinear systems and extending the Lyapunov stability to performance consideration through examining worst performance bounds from system inputs to outputs or disturbance. To implement the

performance efficiently, Linear Matrix Inequalities (LMIs) techniques are commonly used to permit simplicity in analysis [39], [75], described in the following section.

2.4.2 Stability Analysis with Performance Bounds via LMIs

Linear matrix inequalities (LMI) have the form $F(x) = F_0 + \sum_{i=1}^{m} x_i F > 0$ where $x \in R^m$ is the variable and $F_i = F_i^T \in R^{n \times n}$, $i = 1,...,m$ are given. This inequality means that $F(x)$ is positive-definite, i.e., $u^T F(x) u > 0$ for all nonzero $u \in R^n$. Also, this LMI is a convex constraint on x, i.e., the set $\{x \mid F(x) > 0\}$ is convex. Although the LMI may have a specialized form, it can represent a wide variety of convex constraints on x. In particular, linear inequalities, quadratic inequalities, and constraints that arise in control theory, such as Lyapunov and convex quadratic matrix inequalities, can be cast in the form of LMI [74].

This vector gives more flexibility as well as simplicity to the analyses in practice, thus many complex problems in analytic or computational studies can be easily solved by formulating them into LMIs. For example, multiple LMIs $F^{(1)}(x) > 0, \ldots, F^{(p)}(x) > 0$ can be expressed as a single LMI $diag(F^{(1)}(x) > 0, \ldots, F^{(p)}(x)) > 0$, therefore a set of LMIs can simply be converted into a single LMI [74].

When the matrix F_i is diagonal, the LMI $F(x) > 0$ is just a set of linear inequalities. The LMI formula described above can be converted into a simple LMI

formula called "Schur complement." Note that these two formulae are completely identical and Q and R are symmetric and positive-definite matrices [49]:

$$R(x) > 0, \text{ and } Q(x) - S(x)R(x)^{-1}S(x)^T > 0 \tag{2.29}$$

$$\begin{bmatrix} Q(x) & S(x) \\ S(x)^T & R(x) \end{bmatrix} > 0 \tag{2.30}$$

Also, LMI-based analyses have best-fit for the polytopic system representation showing that overall system is composed of a convex hull of several linear systems, described as follows.

Definition 2.6) Convex hull and polytopic systems [74]

The convex hull of a given set of points $x_1, \cdots, x_n$ is defined as:

$$Co(\{x_1, \cdots, x_n\}) = \left\{ x \in R \,\middle|\, x = \sum_{j=1}^{n} \alpha_i x_i, \alpha_i \in [0,1], \sum_{i=1}^{n} \alpha_i = 1 \right\} \tag{2.31}$$

Then, a state space representation of the polytopic system is given by

$$\begin{bmatrix} \dot{x} \\ z \end{bmatrix} = \begin{bmatrix} A(t) & B(t) \\ C(t) & 0 \end{bmatrix} \begin{bmatrix} x \\ w \end{bmatrix} \tag{2.32}$$

where $A(t) = Co(\{A_1, \cdots, A_n\})$, $B(t) = Co(\{B_1, \cdots, B_n\})$, and $C(t) = Co(\{C_1, \cdots, C_n\})$.

Note that $Co(\{A_1, \cdots, A_n\})$ is formed by the combination of system matrices and its weighting function, $\alpha_1 A_1 + \alpha_2 A_2 + \ldots + \alpha_n A_n$, and the sum of weighting function $\sum \alpha_i$ needs not be one. Under these conditions, the closed loop of the LMN/LCN has a

polytopic relationship, affine in weighting function α , that allows the convex optimization in controller interpolation. This will be discussed later in this dissertation.

Let a quadratic Lyapunov function be $V(x) = x^T Px, P > 0$, then a necessary and sufficient condition for asymptotic stability of the linearized system is determined by the existence of a solution to the LMI $A^T P + PA < 0$. For polytopic systems, asymptotic stability can be guaranteed by the solution of a set of LMIs $A_i^T P + PA_i < 0$, $i = 1, \cdots, m$ for the common Lyapunov matrix $P > 0$.

2.4.2.1 H_∞ performance

Among various norm-based performance definitions, the most commonly used one in stability is H_∞ performance, denoted as [44]:

$$\|G\|_\infty \equiv \max_w \bar{\sigma}(G(jw)) = \sup_{\substack{w \in L_2 \\ w \neq 0}} \frac{\|z\|_2}{\|w\|_2} \tag{2.33}$$

H_∞ performance is known as a power norm, defined by finite energy to finite energy, and also an induced norm in terms of expected values of stochastic signals. The H_∞ norm is usually computed numerically fom a state space realization as the smallest value of γ such that the Hamiltonian matrix H has eigenvalues on the imaginary axis. In robust control, the H_∞ norm is commonly used because it is convenient for representing unstructured modeling uncertainty [69], [75] and satisfies the multiplicative property that is useful in analysis.

$$\|A(s)B(s)\|_\infty \le \|A(s)\|_\infty \|B(s)\|_\infty \tag{2.34}$$

Using this definition, LMI conditions for an upper bound on the H_∞ gain can be prepared and the resulting asymptotic stability criterion is given as follows

Theorem 2.2) Stability using H_∞ performance

The standard LTI system is given as

$$\begin{bmatrix} \dot{x} \\ z \end{bmatrix} = \begin{bmatrix} A & B \\ C & 0 \end{bmatrix} \begin{bmatrix} x \\ w \end{bmatrix} \tag{2.35}$$

Then the system in Equation 2.32 is asymptotically stable and has an H_∞ norm less than γ if and only if there exists $P > 0$ such that

$$\begin{pmatrix} A^T P + PA + C^T C & PB \\ B^T P & -\gamma^2 I \end{pmatrix} < 0 \tag{2.36}$$

Proof: See [74]

For the polytopic system, this LMI formulation can be easily extended as the set of LMIs:

$$\begin{pmatrix} A_i^T P + PA_i + C_i^T C_i & PB_i \\ B_i^T P & -\gamma^2 I \end{pmatrix} < 0, \text{ for } i = 1, \cdots, m. \tag{2.37}$$

2.4.2.2 H_2 performance

Another norm-based performance used widely in practice is H_2 performance, denoted by [49].

$$\|G\|_2 \equiv \sqrt{\frac{1}{2\pi}\int_{-\infty}^{\infty} tr(G(jw)^H G(jw))dw} = \sqrt{\frac{1}{2\pi}\int_{-\infty}^{\infty} \sum_i \sigma_i^2(G(jw))dw} \qquad (2.38)$$

The H_2 norm can be interpreted as a 2-norm output resulting from applying unit impulses $\delta_i(t)$ to each output. In general, the H_2 norm has a number of outstanding mathematical as well as numerous properties and its minimization has important engineering implications. In stochastic process, this interpretation allows the implementation of optimal control in terms of Linear Quadratic Gaussian (LQG) where we measure the expected root mean square (rms) value of the output in response to white noise excitation.

However, the H_2 norm is not an induced norm and does not satisfy the multiplicative property. Note that the inducing norm is defined as a maximum gain for all possible input directions, $\|G\|_{ip} \equiv \max_{w\neq 0} \frac{\|Gw\|_p}{\|w\|_p}$ where $\|w\|_p = (\sum_i |w_i|^p)^{\frac{1}{p}}$. Thus looking for the direction of vector w so that the ratio $\frac{\|z\|_p}{\|w\|_p}$ is maximized then the induced norm gives the largest possible amplifying power of the matrix.

Theorem 2.3) Lyapunov stability [74]

The system in Equation 2.29 is asymptotically stable and has the H_2 norm less than γ if and only if there exists $P > 0$ such that

$$\begin{pmatrix} A^T P + PA & PB \\ B^T P & -\gamma I \end{pmatrix} < 0 \text{ and } \begin{pmatrix} P & C^T \\ C & \gamma I \end{pmatrix} > 0 \tag{2.39}$$

Equivalently,

$$\begin{pmatrix} A^T P + PA & PC^T \\ CP & -\gamma I \end{pmatrix} < 0 \text{ and } \begin{pmatrix} P & B_i \\ B_i{}^T & \gamma I \end{pmatrix} > 0 \tag{2.40}$$

Proof: See [74]

Also, these LMIs can be extended to polytopic systems as the set of LMIs

$$\begin{pmatrix} A_i{}^T P + PA_i & PB_i \\ B_i{}^T P & -\gamma I \end{pmatrix} < 0 \text{ and } \begin{pmatrix} P & C_i{}^T \\ C_i & \gamma I \end{pmatrix} > 0, \text{ for } i = 1, \cdots, m. \tag{2.41}$$

Equivalently,

$$\begin{pmatrix} A_i{}^T P + PA_i & PC_i{}^T \\ C_i P & -\gamma I \end{pmatrix} < 0 \text{ and } \begin{pmatrix} P & B_i \\ B_i{}^T & \gamma I \end{pmatrix} > 0, \text{ for } i = 1, \cdots, m. \tag{2.42}$$

Note that the difference between the interpretation of the H_2 and H_∞ norms may help the readers to understand the applications in practice. Minimizing H_∞ norm corresponds to minimizing the peak of the largest singular value, i.e., "worst direction and worst frequency," while minimizing the H_2 norm results in minimizing the sum of the square root of all singular values over all frequencies, i.e., "average direction and average frequency" [3].

2.4.3 Conclusion: Stability of Gain-scheduled Control System

In gain-scheduled control, the closed loop of the nonlinear system is represented as a polytopic model and the associated stability can be determined using an LMI-based Lyapunov stability analysis. Using Lyapunov stability, the interconnected LMN/LCN system can be guaranteed to be stable for arbitrarily fast variations of the scheduling variable where a common Lyapunov function can be found for each local plant model in the polytopic system. For exogenous gain scheduled systems, this condition would be sufficient for guaranteeing the stability globally throughout the operating envelope since the change in scheduling variables is known a priori.

However, for endogenously-scheduled systems, the above conditions may not be sufficient to guarantee global stability because a bound of change of scheduling variables may not be known *a priori*. For practical stability, it is necessary to ensure the scheduling variable remains within acceptable bounds for an assumed class of disturbances. Although the existence of a common Lyapunov function guarantees stability through bounded inputs and outputs, if sudden changes in inputs or outputs drive the system outside of the region then the instability occurs.

Thus, guarantees of the worst case performance from disturbances to system inputs and outputs could be very useful to ensure the practical stability of the physical systems. In essence, Lyapunov stability can be extended to generate the worst case of norm-based performance bounds on system outputs, controller outputs or scheduling variables, thus the LMI-based method is used efficiently in the stability of a gain scheduled closed loop system.

2.5 Youla-based Gain-scheduled Control

2.5.1 General Youla Parameterization

Youla parameterization is one of the more recent approaches in gain scheduling and is based on the work by Youla et al, in the 1970's [62]. The crux of Youla parameterization can be described as "all stabilizing controllers can be parameterized in terms of a single parameter," often called "Youla parameter," denoted by Q. Under this framework, the closed loop system can be represented as an affine system in the Youla parameter Q that allows the optimal design of the stabilizing controller to be a convex optimization problem.

In general, Youla parameterization is implemented through coprime factorization. For plant models and controllers, factorization leads to the models and controllers being represented as the ratio of two stable transfer functions. This factorization is termed coprime when two transfer functions have no common zeros in RHP. Thus coprime factorization excludes any pole-zero cancellations in the fractional representation.

In multivariable cases, the plant model and nominal controller transfer functions are factored into the product of a stable transfer function and a transfer function with a stable inverse. In the mathematical view, a dynamic system (plant model and controller) can be decomposed into right and left coprime factors $P(s) = NM^{-1} = \tilde{M}^{-1}\tilde{N}$.

Using this coprime factorization, the controller can be decomposed into left and right coprime factors, $K(s) = UV^{-1} = \tilde{V}^{-1}\tilde{U}$ and a plant model into

$P(s) = NM^{-1} = \tilde{M}^{-1}\tilde{N}$ such that $U, \tilde{U}, V, \tilde{V} \in RH_\infty$ and $N, \tilde{N}, M, \tilde{M} \in RH_\infty$. If a nominal plant model P_0 is stabilized by a nominal controller K_0 and its coprime factors satisfy the double Bezout identities (Equation 2.43), then all stabilizing controllers can be parametrized in terms of coprime factors of the nominal controller/plant and Youla parameter, denoted by Q (Equation 2.44). Similarly, all plants that can be stabilized by the nominal controller K_0 are parameterized in terms of the dual Youla parameter S (Equation 2.45)

$$\begin{bmatrix} M & U \\ N & V \end{bmatrix} \begin{bmatrix} \tilde{V} & -\tilde{U} \\ -\tilde{N} & \tilde{M} \end{bmatrix} = \begin{bmatrix} I & 0 \\ 0 & I \end{bmatrix} \tag{2.43}$$

$$\begin{aligned} K(Q) &= (U_0 + M_0 Q)(V_0 + N_0 Q)^{-1} \\ &= (\tilde{V}_0 + Q\tilde{N}_0)^{-1}(\tilde{U}_0 + Q\tilde{M}_0) \end{aligned} \tag{2.44}$$

$$\begin{aligned} P(S) &= (N_0 + V_0 S)(M_0 + U_0 S)^{-1} \\ &= (\tilde{M}_0 + S\tilde{U}_0)^{-1}(\tilde{N}_0 + S\tilde{V}_0) \end{aligned} \tag{2.45}$$

Dual Youla parameterization allows us to represent all stabilizing controllers and stabilizable plants as a Linear Fractional Transformation (LFT) [76]. Under this framework, a standard feedback control loop with stabilizing controller K_0 (Figure 2.4) can be equivalent to the decomposed system showing that all stabilizing controllers can be represented as a lower LFT of interconnection matrix J_k and Youla parameter Q, denoted by $F_l(J_k, Q)$. Also, the class of all stabilizable plants can be represented as an upper LFT of interconnection matrix J_p and dual Youla parameter S, denoted by $F_u(J_p, S)$. The associating closed loop system can be interconnected with those two

systems, $F_l(J_k, Q)$ and $F_u(J_p, S)$, as shown in Figure 2.5. Note that the interconnected LQN/LSN system is equivalent to the standard feedback control system in Figure 2.5.

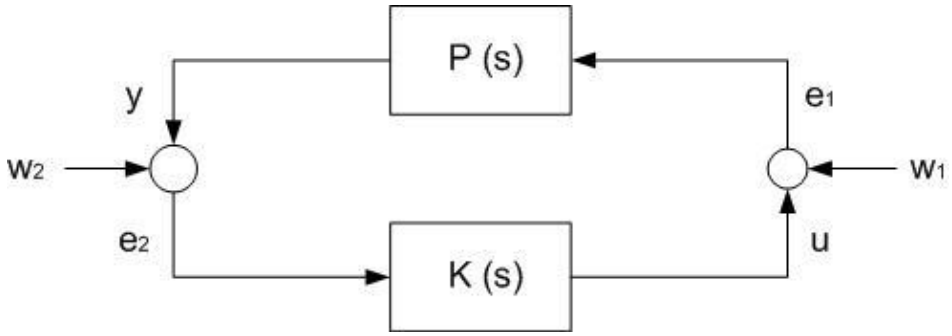

Fig. 2.4. Feedback control loop.

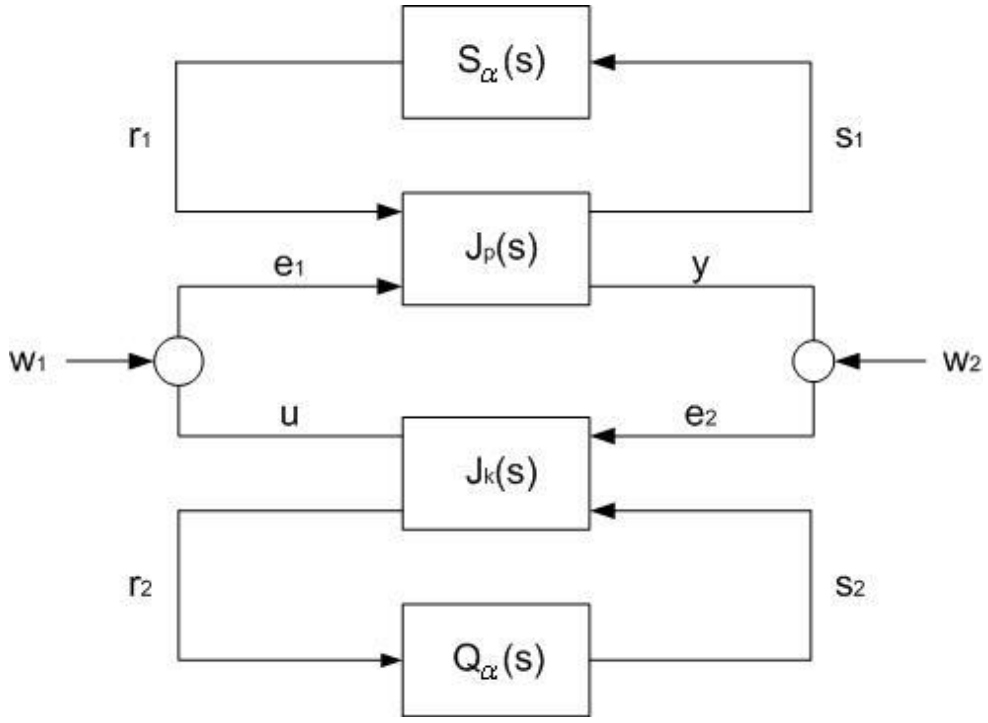

Fig. 2.5. Feedback control loop with dual Youla parameterization.

$$J_K(s)=\begin{bmatrix} U_0V_0^{-1} & \tilde{V}_0^{-1} \\ V_0^{-1} & -V_0^{-1}N_0 \end{bmatrix} \tag{2.46}$$

$$J_p(s)=\begin{bmatrix} N_0M_0^{-1} & \tilde{M}_0^{-1} \\ M_0^{-1} & -M_0^{-1}U_0 \end{bmatrix} \tag{2.47}$$

The closed loop system of standard feedback loop in Figure 2.4 can be represented by

$$\begin{aligned} \begin{bmatrix} e_1 \\ e_2 \end{bmatrix} &= \begin{bmatrix} (I-KP)^{-1} & K(I-PK)^{-1} \\ P(I-KP)^{-1} & (I-PK)^{-1} \end{bmatrix}^{-1} \begin{bmatrix} w_1 \\ w_2 \end{bmatrix} \\ &= \begin{bmatrix} M & 0 \\ 0 & V \end{bmatrix} \begin{bmatrix} M & U \\ N & V \end{bmatrix}^{1} \begin{bmatrix} w_1 \\ w_2 \end{bmatrix} \end{aligned} \tag{2.48}$$

Thus the stability of the closed loop system is guaranteed when the system $\begin{bmatrix} (I-KP)^{-1} & K(I-PK)^{-1} \\ P(I-KP)^{-1} & (I-PK)^{-1} \end{bmatrix}^{-1}$ or $\begin{bmatrix} M & 0 \\ 0 & V \end{bmatrix} \begin{bmatrix} M & U \\ N & V \end{bmatrix}^{-1}$ is Hurwitz. To show the ability of convex optimization of the closed loop system in terms of (dual) Youla parameters, the above system representation can be written as follows [63]

$$\begin{bmatrix} I & -K(Q) \\ -P(S) & I \end{bmatrix}^{-1} = \begin{bmatrix} I & -K_0 \\ -P_0 & I \end{bmatrix}^{-1} + \begin{bmatrix} M_0 & U_0 \\ N_0 & V_0 \end{bmatrix} \left\{ \begin{bmatrix} I & -Q \\ -S & I \end{bmatrix}^{-1} - I \right\} \begin{bmatrix} \tilde{V}_0 & \tilde{U}_0 \\ \tilde{N}_0 & \tilde{M}_0 \end{bmatrix} \tag{2.49}$$

Note that the closed loop system is affine in Youla parameter Q and dual Youla parameter S which allow the design of the optimal stabilizing controller to be a controller design through the convex optimization that is computationally feasible. Also, the closed loop system is stable when systems $\begin{bmatrix} I & -K_0 \\ -P_0 & I \end{bmatrix}^{-1}$ and $\begin{bmatrix} I & -Q \\ -S & I \end{bmatrix}^{-1}$ are

Hurwitz. This is confirmed by the examination of the interconnection of matrices J_k and J_p (Equation 2.50) using the double Bezout identities. The closed loop system in Figure 2.5 is internally stable if and only if the system in Figure 2.6 is stable [5], [63].

$$F_l(J_p, J_k) = \begin{bmatrix} 0 & I \\ I & 0 \end{bmatrix} \tag{2.50}$$

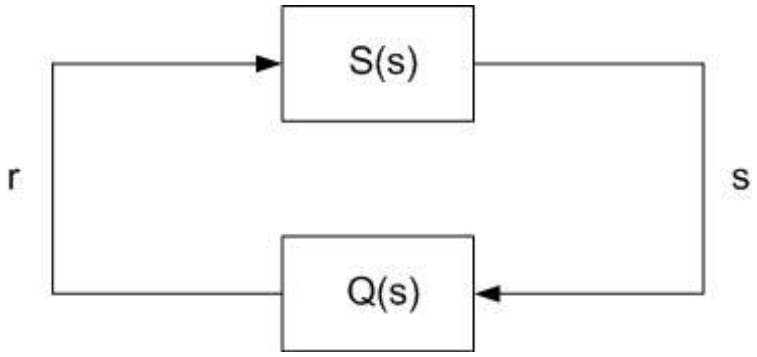

Fig. 2.6. Simple diagram of feedback loop using Dual Youla parameterization.

2.5.2 Interpolation of Dual Youla Parameters

Although the LCN/LMN approach has been successfully applied in practice, there exist several shortcomings in the aspect of stability. For example, even when all stabilizing controllers can stabilize the plant at every fixed operating points, the blended controller may not stabilize the plant at the intermediate points over the operating envelopes. Furthermore, classical gain scheduling approaches require that locally defined plant models and controllers should be open loop stable for guaranteeing the internal stability of the closed loop system.

The Youla-based gain-scheduling framework allows the parameterization of plant models and stabilizing controllers designed at local operating points and guarantees recovery of the original local controllers at the design point and increases the stability of gain-scheduled systems by guaranteeing frozen parameter stability at intermediate design points while recovering the original local controllers at the design points.

Variations of this approach have been termed $J-Q$ interpolation [14], or blending of the Youla parameters [77]. By virtue of the Youla parameterization, this framework permits the scheduling of unstable controllers [78]. Moreover, this framework has the intuitive appeal of isolating common controller elements in function J_k and blending only the differences between the individual controllers. When implementing a blended controller for a plant P_0, the blended controller may be constructed as in Equation 2.44 where $K_0 = U_0 V_0^{-1}$ is any controller that stabilizes the plant. Note that the original local controller K_i is recovered at $\alpha_i = 1$.

Moreover, when $K(Q)$ stabilizes P_0 for any $Q \in RH_\infty$, then $K(Q_\alpha)$ also stabilizes P_0 for every frozen value of α, since each $Q_i \in RH_\infty$ and thus $\sum \alpha_i Q_i \in RH_\infty$, something not necessarily guaranteed with the LCN framework. The systematic differences between the conventional LCN framework and Youla-based $J-Q$ interpolation method can be easily depicted in Figure 2.7-2.8.

$$K(Q_\alpha) = \left[U_0 + M_0\left(\sum \alpha_i Q_i\right)\right]\left[V_0 + N_0\left(\sum \alpha_i Q_i\right)\right]^{-1} \tag{2.51}$$

Similarly, the nonlinear plant can be characterized by a group of dual Youla parameters, S_i [58], [63]. In this case, the coprime factors are selected as to satisfy another Bezout identity (Equation 2.52). The nonlinear model is formed as shown in Equation 2.53 with the dual Youla parameters constructed as $S_i = \tilde{N}_i M_0 - \tilde{M}_i N_0$.

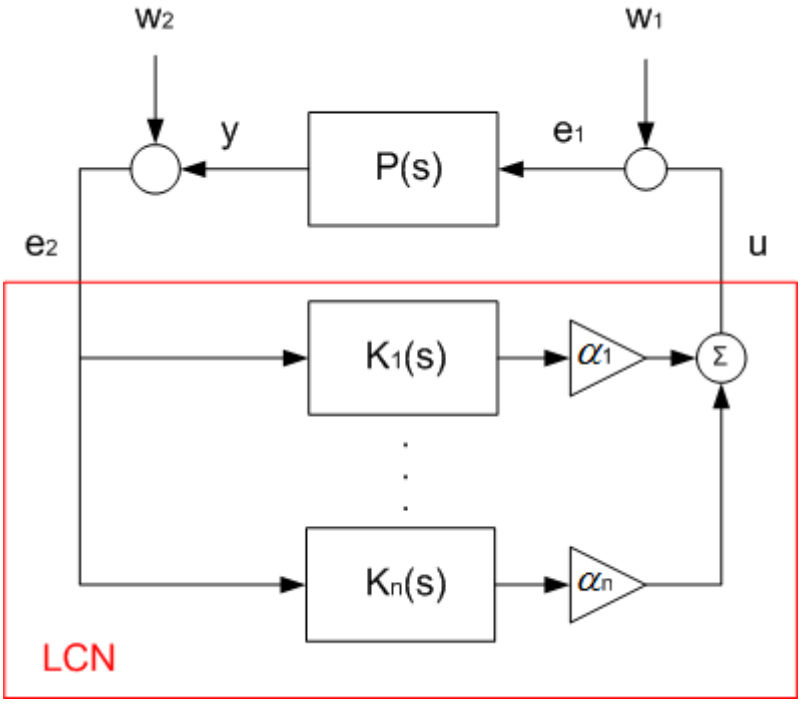

Fig. 2.7. Output blending of local controller network (LCN).

$$\begin{bmatrix} M_i & U_0 \\ N_i & V_0 \end{bmatrix} \begin{bmatrix} \tilde{V}_0 & -\tilde{U}_0 \\ -\tilde{N}_i & \tilde{M}_i \end{bmatrix} = \begin{bmatrix} I & 0 \\ 0 & I \end{bmatrix} \tag{2.52}$$

$$P(S_\alpha) = \left[N_0 + V_0\left(\sum \alpha_i S_i\right)\right]\left[M_0 + U_0\left(\sum \alpha_i S_i\right)\right] \tag{2.53}$$

$$J_P(s) = \begin{bmatrix} N_0 M_0^{-1} & \tilde{M}_0^{-1} \\ M_0^{-1} & -M_0^{-1} U_0 \end{bmatrix} \tag{2.54}$$

$$F_l(J_P, J_K) = \begin{bmatrix} 0 & I \\ I & 0 \end{bmatrix} \tag{2.55}$$

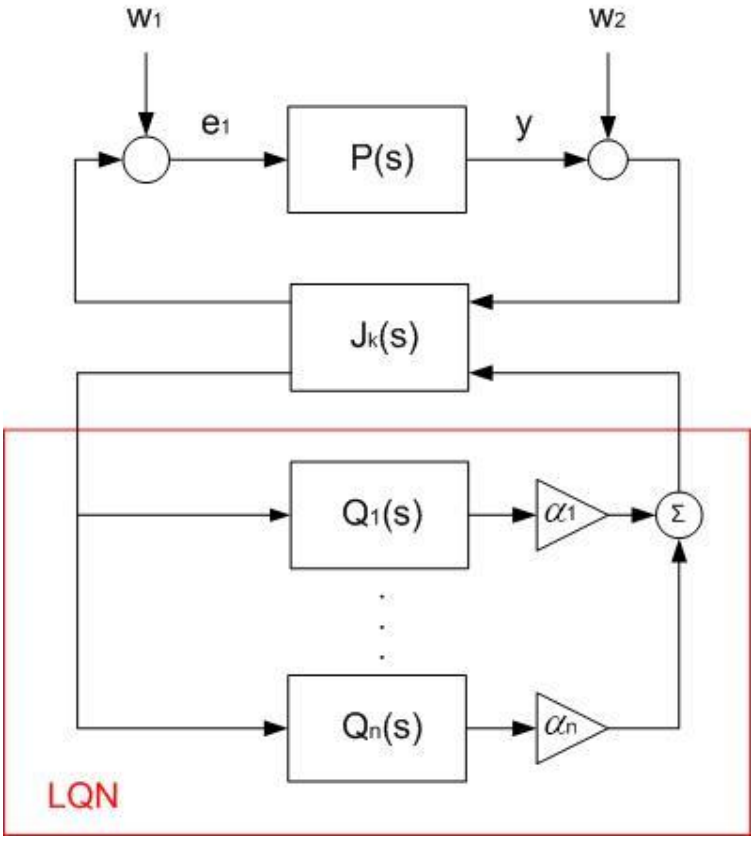

Fig. 2.8. Output blending of local Q-network (LQN).

The interpolated plant model in terms of dual Youla parameter is called Local S-Network (LSN) and the resulting interconnected LQN/LSN system is depicted in Figure 2.9. The interconnection of matrices J_k and J_p can be determined by Equation 2.55. Clearly, the interconnected system can be described as a simplified representation on the

left hand side thus the condition for stability of the overall system is equivalent to the stability of the simplified system also shown in Figure 2.10.

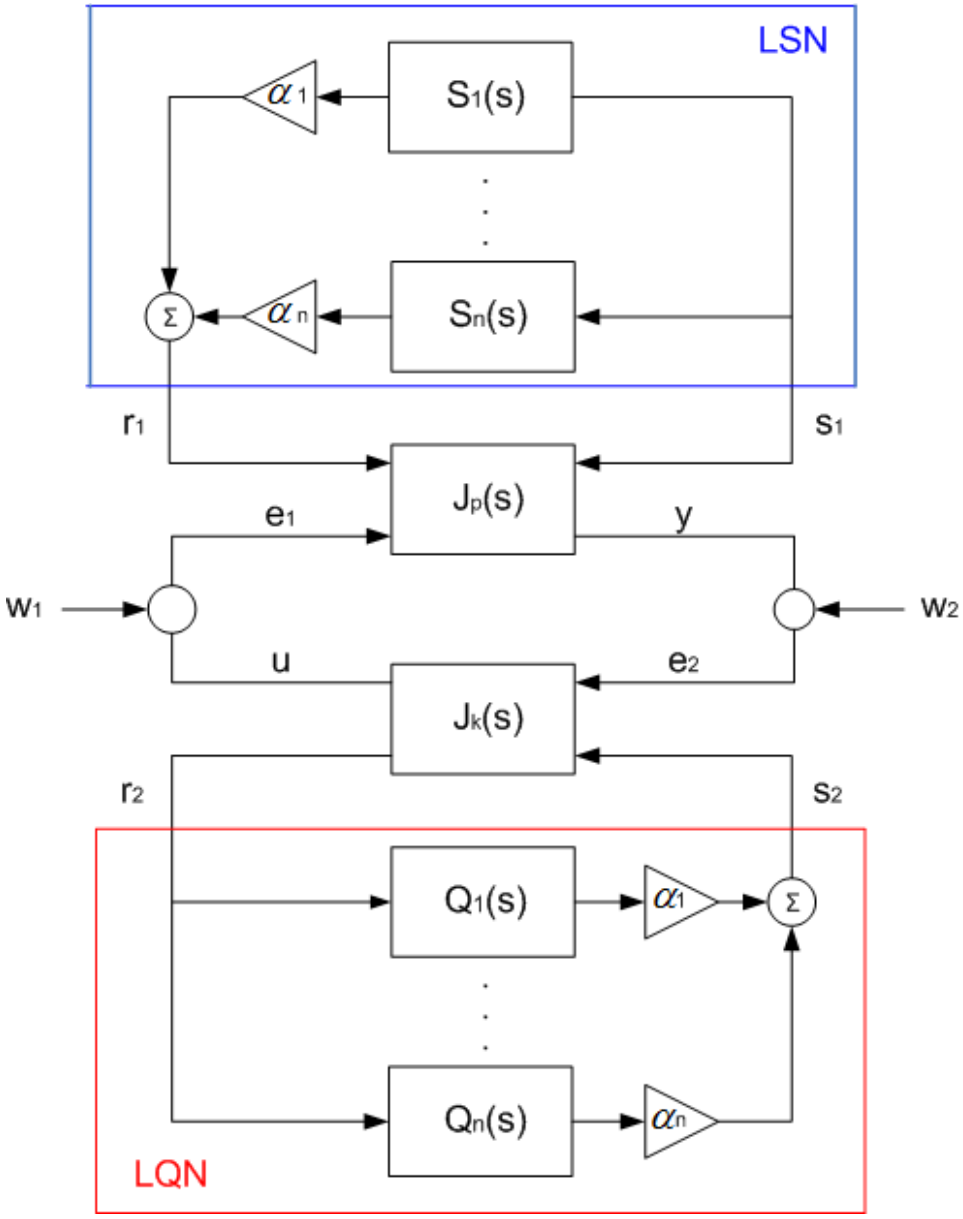

Fig. 2.9. Closed loop system with LQN/LSN.

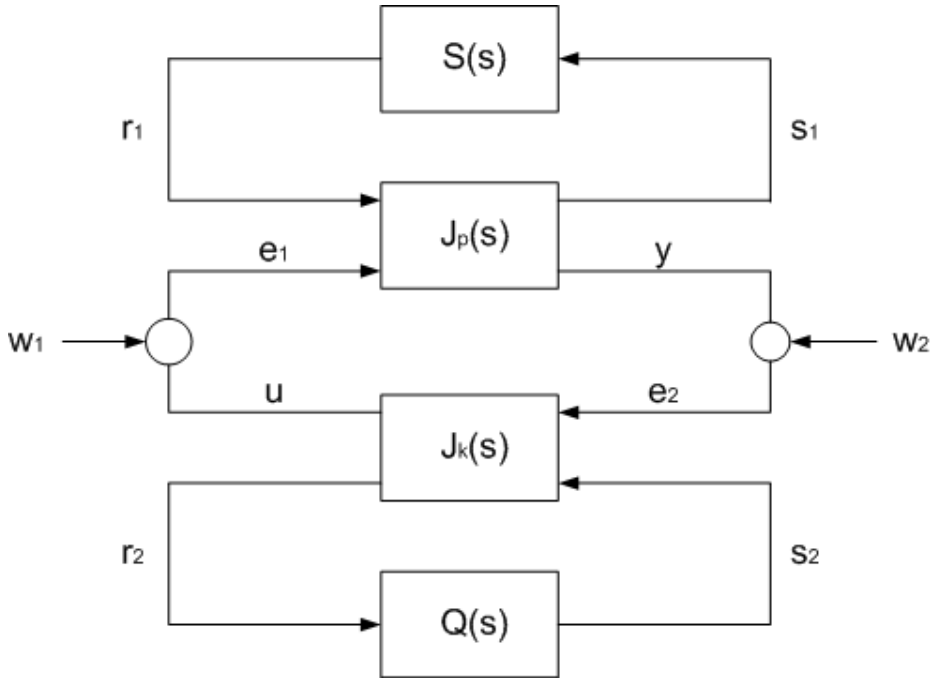

Fig. 2.10. Feedback loop of LQN/LSN interconnected system.

One of the important aspects in Youla-based gain scheduling is the local controller recovery procedure. To demonstrate local controller recovery, a standard mathematical expression of Youla parameter is considered

$$\begin{aligned} Q_i &= \tilde{U}_i V_0 - \tilde{V}_i U_0 \\ &= \left(\tilde{V}_i \tilde{V}_i^{-1}\right)\left(\tilde{U}_i V_0 - \tilde{V}_i U_0\right)\left(V_0^{-1} V_0\right) \\ &= \tilde{V}_i \left(\tilde{V}_i^{-1}\tilde{U}_i V_0 V_0^{-1} - \tilde{V}_i^{-1}\tilde{V}_i U_0 V_0^{-1}\right) V_0 \\ &= \tilde{V}_i \left(\tilde{V}_i^{-1}\tilde{U}_i - U_0 V_0^{-1}\right) V_0 \\ &= \tilde{V}_i \left(K_i - K_0\right) V_0 \end{aligned} \tag{2.56}$$

Also, a nominal controller can be derived using coprime factorization and the Bezout identity as follows:

$$
\begin{aligned}
K_0(Q) &= (U_0 + M_0 Q)(V_0 + N_0 Q)^{-1} \\
&= \left(U_0 \left(V_0^{-1} V_0\right) + \left(\tilde{V}_0^{-1} \tilde{V}_0\right) M_0 Q\right)(V_0 + N_0 Q)^{-1} \\
&= \left(\left(U_0 V_0^{-1}\right) V_0 + \tilde{V}_0^{-1}\left(\tilde{V}_0 M_0\right) Q\right)(V_0 + N_0 Q)^{-1} \\
&= \left(K_0 V_0 + \tilde{V}_0^{-1}\left(I + \tilde{U}_0 N_0\right) Q\right)(V_0 + N_0 Q)^{-1} \\
&= \left(K_0 V_0 + \left(\tilde{V}_0^{-1} + \tilde{V}_0^{-1} \tilde{U}_0 N_0\right) Q\right)(V_0 + N_0 Q)^{-1} \\
&= \left(K_0 V_0 + \left(\tilde{V}_0^{-1} + K_0 N_0\right) Q\right)(V_0 + N_0 Q)^{-1} \\
&= \left(K_0 (V_0 + N_0 Q) + \tilde{V}_0^{-1} Q\right)(V_0 + N_0 Q)^{-1} \\
&= K_0 + \tilde{V}_0^{-1} Q (V_0 + N_0 Q)^{-1}
\end{aligned}
\tag{2.57}
$$

Using the results obtained above, local controller recovery can be shown by

$$
\begin{aligned}
K_0(Q_i) &= (U_0 + M_0 Q_i)(V_0 + N_0 Q_i)^{-1} \\
&= \left(U_0 + M_0 \left(\tilde{U}_i V_0 - \tilde{V}_i U_0\right)\right)\left(V_0 + N_0 \left(\tilde{U}_i V_0 - \tilde{V}_i U_0\right)\right)^{-1} \\
&= \left(U_0 + M_0 \tilde{U}_i V_0 - M_0 \tilde{V}_i U_0\right)\left(V_0 + N_0 \tilde{U}_i V_0 - N_0 \tilde{V}_i U_0\right)^{-1} \\
&= \left(U_0 + \left(U_i \tilde{M}_0\right) V_0 - \left(I + U_i \tilde{N}_0\right) U_0\right)\left(V_0 + \left(V_i \tilde{M}_0 - I\right) V_0 - \left(V_i \tilde{N}_0\right) U_0\right)^{-1} \\
&= \left(U_0 + U_i \tilde{M}_0 V_0 - U_0 - U_i \tilde{N}_0 U_0\right)\left(V_0 + V_i \tilde{M}_0 V_0 - V_0 - V_i \tilde{N}_0 U_0\right)^{-1} \\
&= \left(U_i \tilde{M}_0 V_0 - U_i \tilde{N}_0 U_0\right)\left(V_i \tilde{M}_0 V_0 - V_i \tilde{N}_0 U_0\right)^{-1} \\
&= \left(U_i \left(\tilde{M}_0 V_0 - \tilde{N}_0 U_0\right)\right)\left(V_i \left(\tilde{M}_0 V_0 - \tilde{N}_0 U_0\right)\right)^{-1} \\
&= U_i V_i^{-1}
\end{aligned}
\tag{2.58}
$$

Equivalently,

$$
\begin{aligned}
K_0(Q_i) &= K_0 + \tilde{V}_0^{-1} Q_i \left(I + V_0^{-1} N_0 Q_i \right)^{-1} V_0^{-1} \\
&= K_0 + \tilde{V}_0^{-1} \left(\tilde{V}_i \left(K_i - K_0 \right) V_0 \right) \left(I + V_0^{-1} N_0 \left(\tilde{V}_i \left(K_i - K_0 \right) V_0 \right) \right)^{-1} V_0^{-1} \\
&= K_0 + \tilde{V}_0^{-1} \tilde{V}_i \left(K_i - K_0 \right) V_0 \left(I + V_0^{-1} N_0 \tilde{V}_i \left(K_i - K_0 \right) V_0 \right)^{-1} V_0^{-1} \\
&= K_0 + \tilde{V}_0^{-1} \tilde{V}_i \left(K_i - K_0 \right) \left(I + N_0 \tilde{V}_i \left(K_i - K_0 \right) \right)^{-1} \\
&= K_0 + \tilde{V}_0^{-1} \tilde{V}_i \left(I + \left(K_i - K_0 \right) N_0 \tilde{V}_i \right)^{-1} \left(K_i - K_0 \right) \\
&= K_0 + \tilde{V}_0^{-1} \left(\tilde{V}_i^{-1} + \left(K_i - K_0 \right) N_0 \right)^{-1} \left(K_i - K_0 \right) \\
&= K_0 + \tilde{V}_0^{-1} \left(\tilde{V}_i^{-1} + \left(\tilde{V}_i^{-1} \tilde{U}_i - \tilde{V}_0^{-1} \tilde{U}_0 \right) N_0 \right)^{-1} \left(K_i - K_0 \right) \\
&= K_0 + \tilde{V}_0^{-1} \left(\tilde{V}_i^{-1} \left(I + \tilde{U}_i N_0 \right) - \tilde{V}_0^{-1} \tilde{U}_0 N_0 \right)^{-1} \left(K_i - K_0 \right) \\
&= K_0 + \tilde{V}_0^{-1} \left(\tilde{V}_i^{-1} \left(\tilde{V}_i M_0 \right) - \tilde{V}_0^{-1} \tilde{U}_0 N_0 \right)^{-1} \left(K_i - K_0 \right) \\
&= K_0 + \tilde{V}_0^{-1} \left(M_0 - \tilde{V}_0^{-1} \tilde{U}_0 N_0 \right)^{-1} \left(K_i - K_0 \right) \\
&= K_0 + \tilde{V}_0^{-1} \left(\tilde{V}_0^{-1} \left(\tilde{V}_0 M_0 - \tilde{U}_0 N_0 \right) \right)^{-1} \left(K_i - K_0 \right) \\
&= K_0 + \tilde{V}_0^{-1} \left(\tilde{V}_0^{-1} \left(\tilde{V}_0 M_0 - \tilde{U}_0 N_0 \right) \right)^{-1} \left(K_i - K_0 \right) \\
&= K_0 + \tilde{V}_0^{-1} \left(\tilde{V}_0^{-1} \left(I \right) \right)^{-1} \left(K_i - K_0 \right) \\
&= K_0 + \tilde{V}_0^{-1} \tilde{V}_0 \left(K_i - K_0 \right) \\
&= K_0 + \left(K_i - K_0 \right) \\
&= K_i
\end{aligned}
$$

(2.59)

Finally, the closed loop representation of the LQN/LSN framework is implemented. Note that the relationship form $\begin{bmatrix} w_1 & w_2 \end{bmatrix}^T$ to $\begin{bmatrix} e_1 & e_2 \end{bmatrix}^T$ or $\begin{bmatrix} u & y \end{bmatrix}^T$ of the system in Figure 2.11 for the modified framework is given by Equation where T_1, T_2, T_3, and T_4 depend merely on the choice of K_0 and P_0.

$$\begin{bmatrix}\dot{x}_S\\ \dot{x}_Q\end{bmatrix}=\underbrace{\begin{bmatrix}A_S & B_SC_Q\\ B_QC_S & A_Q\end{bmatrix}}_{\tilde{A}_{QS}(\alpha)}\begin{bmatrix}x_S\\ x_Q\end{bmatrix}+\underbrace{\begin{bmatrix}B_S & 0\\ 0 & B_Q\end{bmatrix}}_{\tilde{B}_{QS}}\begin{bmatrix}d_1\\ d_2\end{bmatrix}$$
$$\begin{bmatrix}r\\ s\end{bmatrix}=\underbrace{\begin{bmatrix}0 & C_S\\ C_Q & 0\end{bmatrix}}_{\tilde{C}_{QS}(\alpha)}\begin{bmatrix}x_S\\ x_Q\end{bmatrix} \tag{2.60}$$

$$\begin{bmatrix}e_1\\ e_2\end{bmatrix}=\left(T_1+T_2H_\alpha T_3\right)\begin{bmatrix}w_1\\ w_2\end{bmatrix} \tag{2.61}$$

$$\begin{bmatrix}u\\ y\end{bmatrix}=\left(T_4+T_2H_\alpha T_3\right)\begin{bmatrix}w_1\\ w_2\end{bmatrix} \tag{2.62}$$

$$T_1=\begin{bmatrix}M_0 & U_0\\ N_0 & V_0\end{bmatrix}\begin{bmatrix}0 & -\tilde{U}_0\\ -\tilde{N}_0 & 0\end{bmatrix} \tag{2.63}$$

$$T_2=\begin{bmatrix}M_0 & U_0\\ N_0 & V_0\end{bmatrix} \tag{2.64}$$

$$T_3=\begin{bmatrix}\tilde{V}_0 & \tilde{U}_0\\ \tilde{N}_0 & \tilde{M}_0\end{bmatrix} \tag{2.65}$$

$$T_4=\begin{bmatrix}M_0 & U_0\\ N_0 & V_0\end{bmatrix}\begin{bmatrix}0 & -\tilde{U}_0\\ -\tilde{N}_0 & 0\end{bmatrix}-I \tag{2.66}$$

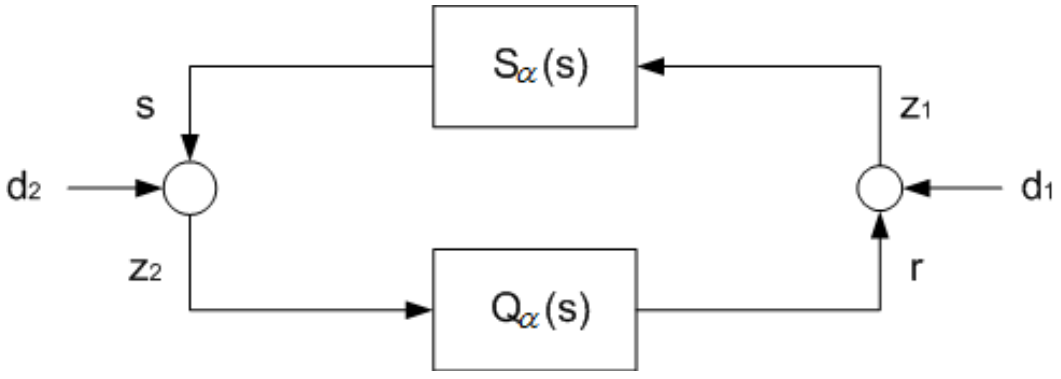

Fig. 2.11 Simplified interconnected LQN/LSN system.

Compared to the Local Q-Network (LQN), the Local S-Network (LSN) is a versatile framework, having been used to capture system variations and model uncertainty [17], [58]. Furthermore, it allows special cases where scheduling variables cannot be measured on-line [77].

The LQN framework for gain-scheduling offers significant advantages such as guaranteed frozen parameter stability, and yet only a few researchers have explored this framework. Niemann and Stoustrup have examined standard LQN approaches [17], [58] [77] and Q-blending with an observer-based control scheme [59], [79]. They have applied their work to power plant control [80], [81] and assessed the performance of the system where modeling errors exist, denoted by a fault tolerant system [60], [82]. Stilwell et al. also discussed this framework under the title "J-Q interpolation" [14], and examined interpolation of controllers by defining a stability-preserving condition corresponding to bound on rate of variation of scheduling variables [83], [84], and a state-space version of Q-blending using state feedback and observer gains [85].

3. YOULA PARAMETER BASED CONTROLLER INTERPOLATION

As discussed previously, guaranteeing global stability of the nonlinear system is a challenging problem in gain-scheduling approaches which has motivated the research presented in this dissertation. This section will examine the gain-scheduling problem with a particular focus on controller interpolation with guaranteed stability of the nonlinear closed loop system. Specifically, an advanced controller interpolation method that guarantees stability of the nonlinear system under arbitrarily fast-varying scheduling is proposed and demonstrated through the simulation case study.

First, the general case of Youla parameterization-based gain-scheduling will be examined to identify degrees of freedom in the design of the gain-scheduled control framework. Second, for the Linear Parameter Varying (LPV) system a particular controller interpolation method utilizing the Youla parameterization will be proposed. Under this framework, quadratic stability is guaranteed by construction of a particular controller interpolation method, while the characteristics of individual controllers designed a priori are recovered at critical design points.

In essence, the proposed approach ensures closed loop stability despite arbitrarily fast transitions which lead naturally to the application of switched linear systems. The efficacy of the method is demonstrated in simulation using a multi-input-multi-output nonminimum phase system while interpolating between two controllers with different sizes and structures.

3.1 Local Controller Network (LCN)/Local Model Network (LMN) Presentation

The Local Model Network (LMN) framework has been widely used in practice and commonly implemented under the assumption that the nonlinear plant is adequately represented by interpolation of local linear models. Under the LCN/LMN framework, local controllers and plant models are assumed to be represented as in Equation 3.1

$$\begin{aligned} \dot{x}_{ki} &= A_{ki}x_{ki} + B_{ki}e_2 \\ u_{ki} &= C_{ki}x_{ki} \end{aligned} \quad \text{and} \quad \begin{aligned} \dot{x}_{pi} &= A_{pi}x_{pi} + B_{pi}e_1 \\ y_{pi} &= C_{pi}x_{pi} \end{aligned} \tag{3.1}$$

By virtue of output blending, the Local Controller Network $K_\alpha(s)$ and Local Model Network $P_\alpha(s)$ can be formed in polytopic representation in Equations 3.2-3, respectively, and the resulting LCN and LMN are a quasi-LPV representation that are affine in the bounded parameters $\alpha_i \in [0,1]$, depicted in Figure 3.1.

$$\begin{bmatrix} \dot{x}_{k1} \\ \vdots \\ \dot{x}_{kn} \end{bmatrix} = \underbrace{\begin{bmatrix} A_{k1} & & 0 \\ & \ddots & \\ 0 & & A_{kn} \end{bmatrix}}_{A_K} \underbrace{\begin{bmatrix} x_{k1} \\ \vdots \\ x_{kn} \end{bmatrix}}_{x_K} + \underbrace{\begin{bmatrix} B_{k1} \\ \vdots \\ B_{kn} \end{bmatrix}}_{B_K} e_2$$

$$u = \underbrace{\begin{bmatrix} \alpha_1 C_{k1} & \cdots & \alpha_n C_{kn} \end{bmatrix}}_{C_K} \begin{bmatrix} x_{k1} \\ \vdots \\ x_{kn} \end{bmatrix} \tag{3.2}$$

$$\begin{bmatrix} \dot{x}_{p1} \\ \vdots \\ \dot{x}_{pn} \end{bmatrix} = \underbrace{\begin{bmatrix} A_{p1} & & 0 \\ & \ddots & \\ 0 & & A_{pn} \end{bmatrix}}_{A_p} \underbrace{\begin{bmatrix} x_{p1} \\ \vdots \\ x_{pn} \end{bmatrix}}_{x_p} + \underbrace{\begin{bmatrix} B_{p1} \\ \vdots \\ B_{pn} \end{bmatrix}}_{B_p} e_1$$

$$y = \underbrace{\begin{bmatrix} \alpha_1 C_{p1} & \cdots & \alpha_n C_{pn} \end{bmatrix}}_{C_p} \begin{bmatrix} x_{p1} \\ \vdots \\ x_{pn} \end{bmatrix} \tag{3.3}$$

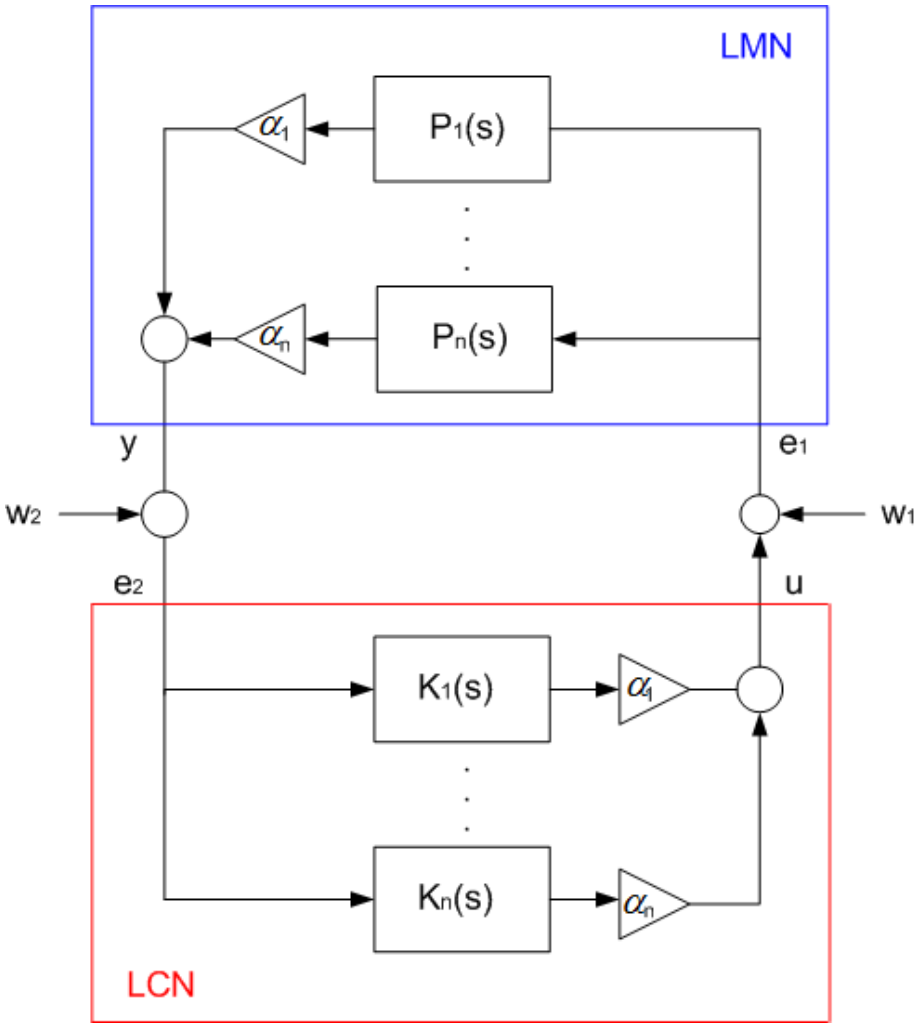

Fig. 3.1. Interconnected LCN/LMN system.

The closed loop system from $[w_1 \quad w_2]^T$ to $[u \quad y]^T$ is given in state-space representation in Equation 3.4, denoted by $G_\alpha(s)$. Again, this system is formed in a polytopic representation of individual models.

$$\begin{bmatrix}\dot{x}_P\\ \dot{x}_K\end{bmatrix}=\underbrace{\begin{bmatrix}A_P & B_PC_K\\ B_KC_P & A_K\end{bmatrix}}_{\tilde{A}_G(\alpha)}\begin{bmatrix}x_P\\ x_K\end{bmatrix}+\underbrace{\begin{bmatrix}B_P & 0\\ 0 & B_K\end{bmatrix}}_{\tilde{B}_G}\begin{bmatrix}w_1\\ w_2\end{bmatrix}$$
$$\begin{bmatrix}u\\ y\end{bmatrix}=\underbrace{\begin{bmatrix}0 & C_P\\ C_K & 0\end{bmatrix}}_{\tilde{C}_G(\alpha)}\begin{bmatrix}x_P\\ x_K\end{bmatrix} \quad (3.4)$$

3.2 Local Q-Network (LQN)/Local S-Network (LSN) Presentation

3.2.1 Closed Loop System Representation

This section discusses general Youla-based gain-scheduling, focusing several design aspects such as plant representation, selection of nominal controller, and the effect of coprime factorizations of the system based on a local model/controller network. Using a dual Youla parameterization, the formulation of the interconnected Local Q-Network (LQN) and Local S-Network (LSN) system is presented in Equation 3.5 and also depicted in Figure 3.2.

$$\begin{bmatrix}\dot{x}_S\\ \dot{x}_Q\end{bmatrix}=\underbrace{\begin{bmatrix}A_S & B_SC_Q\\ B_QC_S & A_Q\end{bmatrix}}_{\tilde{A}_{QS}(\alpha)}\begin{bmatrix}x_S\\ x_Q\end{bmatrix}+\underbrace{\begin{bmatrix}B_S & 0\\ 0 & B_Q\end{bmatrix}}_{\tilde{B}_{QS}}\begin{bmatrix}d_1\\ d_2\end{bmatrix}$$
$$\begin{bmatrix}r\\ s\end{bmatrix}=\underbrace{\begin{bmatrix}0 & C_S\\ C_Q & 0\end{bmatrix}}_{\tilde{C}_{QS}(\alpha)}\begin{bmatrix}x_S\\ x_Q\end{bmatrix} \quad (3.5)$$

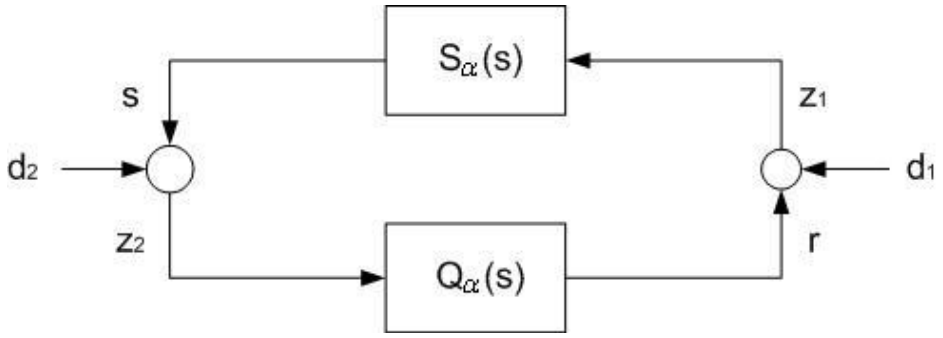

Fig. 3.2. Interconnected LQN/LSN system.

This interconnected system satisfies that Bezout identities can be found based on a choice of feedback gains F_p and F_k such that the matrices $A_k + B_k F_k$ and $A_p + B_p F_p$ have strictly negative eigenvalues [14], and the state space representations of the associated left and right coprime factors are given in Equations 3.6-7 respectively.

$$\begin{bmatrix} M_i & U_j \\ N_i & V_j \end{bmatrix} = \left[\begin{array}{cc|cc} A_{Pi} + B_{Pi}F_{Pi} & 0 & B_{Pi} & 0 \\ 0 & A_{Kj} + B_{Kj}F_{Kj} & 0 & B_{Kj} \\ \hline F_{Pi} & C_{Kj} & I & 0 \\ C_{Pi} & F_{Kj} & 0 & I \end{array}\right] \tag{3.6}$$

$$\begin{bmatrix} \tilde{V}_j & -\tilde{U}_j \\ -\tilde{N}_i & \tilde{M}_i \end{bmatrix} = \left[\begin{array}{cc|cc} A_{Pi} & B_{Pi}C_{Kj} & -B_{Pi} & 0 \\ B_{Kj}C_{Pi} & A_{Kj} & 0 & B_{Kj} \\ \hline F_{Pi} & -C_{Kj} & I & 0 \\ C_{Pi} & -F_{Kj} & 0 & I \end{array}\right] \tag{3.7}$$

The resulting closed loop from $\begin{bmatrix} w_1 & w_2 \end{bmatrix}^T$ to $\begin{bmatrix} u & y \end{bmatrix}^T$ is characterized with the interconnection of LQN and LSN, denoted $H_\alpha(s)$ (Equation 3.5), where T_1, T_2, and T_3 depend on the choice of K_0, P_0, and their coprime factorizations as given in Equation 3.9

$$\begin{bmatrix} u \\ y \end{bmatrix} = \left(T_1 + T_2 H_\alpha T_3\right) \begin{bmatrix} w_1 \\ w_2 \end{bmatrix} \tag{3.8}$$

$$T_1 = \begin{bmatrix} M_0 & U_0 \\ N_0 & V_0 \end{bmatrix} \begin{bmatrix} 0 & -\tilde{U}_0 \\ -\tilde{N}_0 & 0 \end{bmatrix} - I \,,\; T_2 = \begin{bmatrix} M_0 & U_0 \\ N_0 & V_0 \end{bmatrix}, \text{ and } \quad T_3 = \begin{bmatrix} \tilde{V}_0 & \tilde{U}_0 \\ \tilde{N}_0 & \tilde{M}_0 \end{bmatrix} \tag{3.9}$$

Typically, the choice of P_0 should be made so that LSN adequately represents the nonlinear plant, but the K_0 can be chosen somewhat arbitrarily among the controllers designed at each operating point so that the class of acceptable disturbances is maximized. Note that the trivial choice of $K_0 = P_0 = 0$ results in recovery of the LCN/LMN framework.

The choice of coprime factorization presents an additional degree of design freedom that can be exploited to improve stability and performance, and can be equivalent to selectrd matrices F_p and F_k so that $A_k + B_k F_k$ and $A_p + B_p F_p$ are Hurwitz. Clearly, gain-scheduling on the Youla parameters has the interpretation of isolating common controller elements in J_k, and controller differences in Q_i, defined by the coprime factors as $Q_i = \tilde{V}_i (K_i - K_0) V_0$. For the nominal choice $F_p = F_k = 0$, the associated coprime factors are simply $\tilde{V}_i = (I - K_0 P_0)^{-1}$ and $V_0 = I$. Thus, Q_i is simply the controller differences filtered by the loop sensitivity function.

Generally, finding the optimal F_p and F_k that minimizes some performance norm is a nonconvex optimization problem. Even in the simple case of scheduling only two plants/controllers, the resulting closed loop system can be represented as a

constrained state-feedback problem for a polytopic system. For the unconstrained case, this is easily solved by the Linear Matrix Inequality (LMI) [27]

$$A_i Q + Q A_i^T + B_{u,i} Y_i + Y_i^T B_{u,i}^T + B_{w,i} B_{w,i}^T + \frac{1}{\gamma^2} Q C_i^T C_i Q > 0 \qquad (3.10)$$

However, in a constrained case, this is a well-known Bilinear Matrix Inequality (BMI) that may not be computationally feasible [63], [74].

3.2.2 Gain-Scheduled Control of a Mass-Spring–Damper System

The reader knows that the choice of coprime factorization presents a design degree of freedom in Youla-based gain-scheduling and can be implemented by finding the optimal feedback gains F_p and F_k. Although finding the optimal choice of coprime factors remains computationally difficult, a simple example illustrates the value of a few heuristic rules. The illustrative simulation example presented in this section shows the effect of the choice of coprime factors via selecting the optimal F_p and F_k.

As for the simulation case study, consider a nonlinear mass-spring-damper system as given in Figure 3.1. The damping coefficient, c, and spring constant, k, are assumed to vary linearly as a function of displacement and the resulting state space form of the system is presented in Equation 3.11

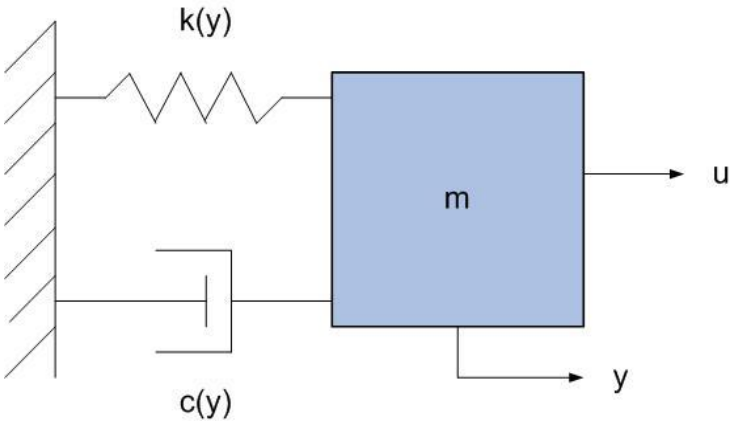

Fig. 3.3. Mass-spring-damper system.

$$\begin{aligned} \dot{x} &= \begin{bmatrix} 0 & 1 \\ -k(y) & -c(y) \end{bmatrix} x + \begin{bmatrix} 0 \\ 1 \end{bmatrix} u \\ y &= \begin{bmatrix} 1 & 0 \end{bmatrix} x \end{aligned} \tag{3.11}$$

where $c \in [0.3,\ 0.7]$, $k \in [0.15,\ 0.05]$, and $m = 1.$

Over the operation envelopes, two design points are chosen at upper end values of the prescribed range. The pole-zero plot for the linear parameter varying plant is shown in Figure 3.4, the step response and bode magnitude/phase plot at the two design points are given in Figures 3.5-3.6 respectively.

To illustrate the effect on the choice of coprime factors, the reference-to-error H_∞ norm of the polytopic system, $\|G_\alpha(s)\|_{L_2 \to L_2}$, is calculated for several cases. Note that the system $G_\alpha(s)$ is defined as Equation 3.12 and H_∞ norm of the system $G_\alpha(s)$ can be calculated by Equation 3.13.

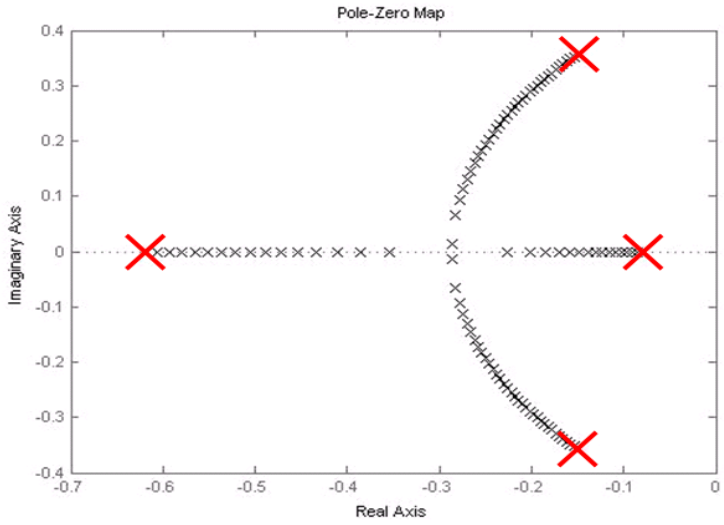

Fig. 3.4. Pole-zero plot for varying k and design points.

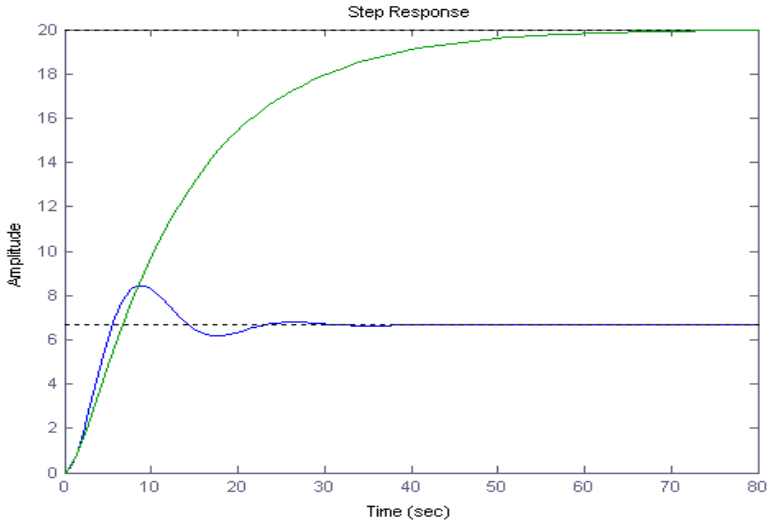

Fig. 3.5. Step responses of two local linear models.

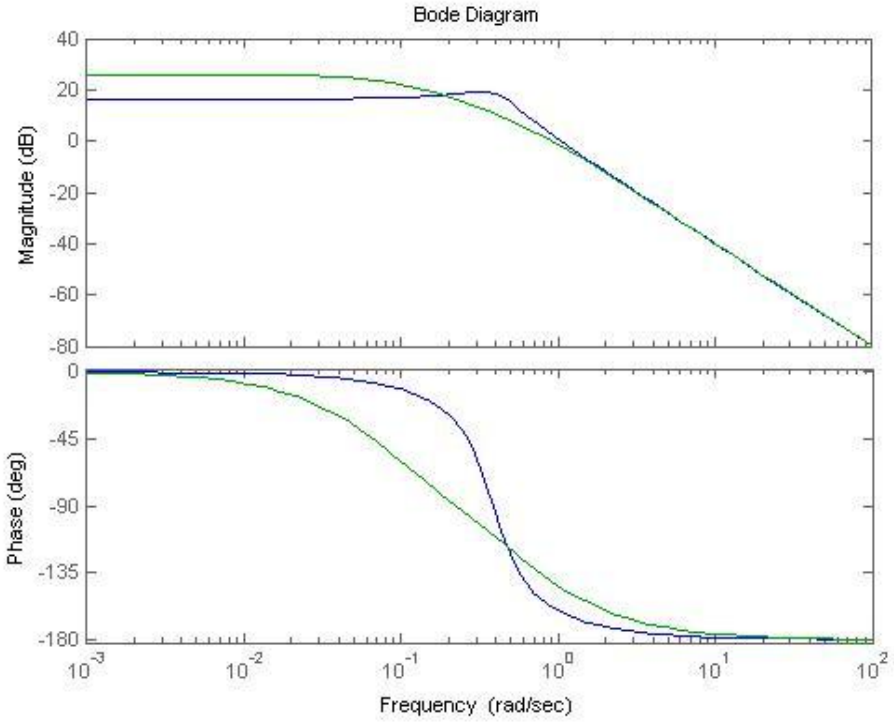

Fig. 3.6. Bode plots of two local linear models.

$$\begin{bmatrix} \dot{x}_P \\ \dot{x}_K \end{bmatrix} = \underbrace{\begin{bmatrix} A_P & B_P C_K \\ B_K C_P & A_K \end{bmatrix}}_{\tilde{A}_G(\alpha)} \begin{bmatrix} x_P \\ x_K \end{bmatrix} + \underbrace{\begin{bmatrix} B_P & 0 \\ 0 & B_K \end{bmatrix}}_{\tilde{B}_G} \begin{bmatrix} w_1 \\ w_2 \end{bmatrix}$$
$$\begin{bmatrix} u \\ y \end{bmatrix} = \underbrace{\begin{bmatrix} 0 & C_S \\ C_Q & 0 \end{bmatrix}}_{\tilde{C}_G(\alpha)} \begin{bmatrix} x_P \\ x_K \end{bmatrix} \tag{3.12}$$

$$\left\| G_\alpha(s) \right\|_\infty = \sup_{\substack{w \in L_2 \\ w \neq 0}} \frac{\|z\|_2}{\|w\|_2} \tag{3.13}$$

First a "good" choice of coprime factors is constructed using LQR techniques to determine the matrices F_P and F_K. Second, a "nominal" choice of coprime factors

determined by $F_P = F_K = 0$ is evaluated. Third, a "bad" choice of coprime factors is constructed by trial and error. For the purpose of comparison, the H_∞ norm of the LCN/LMN approach is also calculated.

The results show that the choice of coprime factors has a significant role in performance bound in stability analysis. This is also evident in the transient response of the nonlinear closed loop system as given in Figure 3.7. Although LQN indicates that it is clearly possible to perform better than the standard method (LCN), there is also the potential to perform worse. Furthermore, the reader can recognize that a key indicator appears to be the maximum H_∞ norm of the Q_i / S_i interconnection in Table 3.1. Note that the H_∞ norm of the interconnected LQN/LSN system with bad coprime factors is several times worse than those of other cases.

Table 3.1. Performance bound on LQN/LSN.

	$\|G_\alpha(s)\|_{L_2 \to L_2}$	$\max_i \|F_\ell(Q_i, S_i)\|_{L_2 \to L_2}$
Good coprime factors	1.42	1.83
Nominal coprime factors	6.76	1.97
Bad coprime factors	10.12	6.69
Local Control Network	1.55	NA

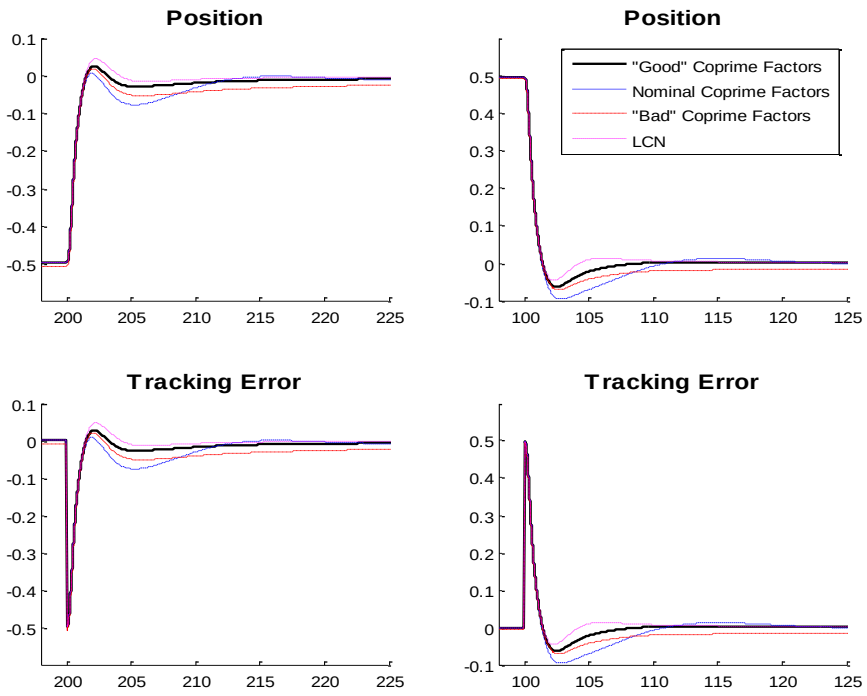

Fig. 3.7. Nonlinear step response depending on choice of coprime factors.

To analyze the results clearly, recall of the closed loop representation of LQN/LSN interconnection system is obtained in Section 3.2.1.

$$\begin{bmatrix} u \\ y \end{bmatrix} = \left(T_1 + T_2 H_\alpha T_3\right) \begin{bmatrix} w_1 \\ w_2 \end{bmatrix} \tag{3.14}$$

$$T_1 = \begin{bmatrix} M_0 & U_0 \\ N_0 & V_0 \end{bmatrix} \begin{bmatrix} 0 & -\tilde{U}_0 \\ -\tilde{N}_0 & 0 \end{bmatrix} - I \,,\; T_2 = \begin{bmatrix} M_0 & U_0 \\ N_0 & V_0 \end{bmatrix}, \text{ and } \quad T_3 = \begin{bmatrix} \tilde{V}_0 & \tilde{U}_0 \\ \tilde{N}_0 & \tilde{M}_0 \end{bmatrix} \tag{3.15}$$

$$\begin{bmatrix}\dot{x}_S\\ \dot{x}_Q\end{bmatrix}=\underbrace{\begin{bmatrix}A_S & B_SC_Q\\ B_QC_S & A_Q\end{bmatrix}}_{\tilde{A}_{QS}(\alpha)}\begin{bmatrix}x_S\\ x_Q\end{bmatrix}+\underbrace{\begin{bmatrix}B_S & 0\\ 0 & B_Q\end{bmatrix}}_{\tilde{B}_{QS}}\begin{bmatrix}d_1\\ d_2\end{bmatrix}$$
$$\begin{bmatrix}r\\ s\end{bmatrix}=\underbrace{\begin{bmatrix}0 & C_S\\ C_Q & 0\end{bmatrix}}_{\tilde{C}_{QS}(\alpha)}\begin{bmatrix}x_S\\ x_Q\end{bmatrix} \tag{3.16}$$

Equation 3.14 indicates that the closed loop performance depends on several time invariant coprime factors, T_1, T_2 and T_3 (Equation 3.15), and the polytopic system which is formed by the Q_i / S_i interconnection as given in Equation 3.16. Thus, intuitively, jointly minimizing Q_i / S_i, formed by the differences between controllers/plants would serve to decrease the system performance norms.

To ensure good performance, the following guideline for the choice of coprime factors will be useful to demonstrate Youla-based gain-scheduled control. First, select the matrices F_P and F_K so that $A_k + B_k F_k$ and $A_p + B_p F_p$ are Hurwitz. This allows for the interpolation of plant/controller that is not open loop stable to be incorporated in the LQN/LSN framework. Second, verify that for the choice of matrices F_P and F_K, the matrix A_{QS} given in Equations 3.17-21 is Hurwitz. This ensures that the individual Q_i / S_i interconnections are stabilized. Third, iterate on the choice of matrices F_P and F_K to minimize an appropriate performance norm.

$$A_{QS}=\begin{bmatrix}A_{QS,11} & A_{QS,12}\\ A_{QS,21} & A_{QS,21}\end{bmatrix} \tag{3.17}$$

$$A_{QS,11} = \begin{bmatrix} A_{p0} & B_{p0}C_{ki} & -B_{p0}F_{p0} & B_{p0}C_{k0} \\ B_{ki}C_{p0} & A_{ki} & B_{ki}C_{p0} & B_{ki}C_{k0} \\ 0 & 0 & A_{p0}+B_{p0}F_{p0} & 0 \\ 0 & 0 & 0 & A_{k0}+B_{k0}F_{k0} \end{bmatrix} \tag{3.18}$$

$$A_{QS,12} = \begin{bmatrix} 0 & 0 & 0 & 0 \\ -B_{ki}F_{p0} & B_{ki}C_{ki} & -B_{ki}F_{p0} & -B_{ki}C_{k0} \\ 0 & 0 & 0 & 0 \\ -B_{ki}F_{p0} & B_{k0}C_{ki} & -B_{ki}F_{p0} & -B_{ki}C_{k0} \end{bmatrix} \tag{3.19}$$

$$A_{QS,21} = \begin{bmatrix} B_{pi}C_{pi} & -B_{p0}F_{k0} & B_{pi}C_{p0} & B_{pi}F_{k0} \\ 0 & 0 & 0 & 0 \\ -B_{p0}C_{pi} & B_{p0}F_{k0} & -B_{p0}C_{p0} & -B_{p0}F_{k0} \\ 0 & 0 & 0 & 0 \end{bmatrix} \tag{3.20}$$

$$A_{QS,22} = \begin{bmatrix} A_{p0} & B_{pi}C_{k0} & -B_{pi}F_{p0} & -B_{pi}C_{k0} \\ B_{k0}C_{pi} & A_{k0} & B_{k0}C_{p0} & B_{k0}C_{k0} \\ 0 & 0 & A_{p0}+B_{p0}F_{p0} & 0 \\ 0 & 0 & 0 & A_{k0}+B_{k0}F_{k0} \end{bmatrix} \tag{3.21}$$

In conclusion, response of bad coprime factors can be found to be worse than that of nominal choice and obviously shows that the choice of coprime factors directly affects the dynamics of the interpolated controller and the closed loop system (Figure 3.8).

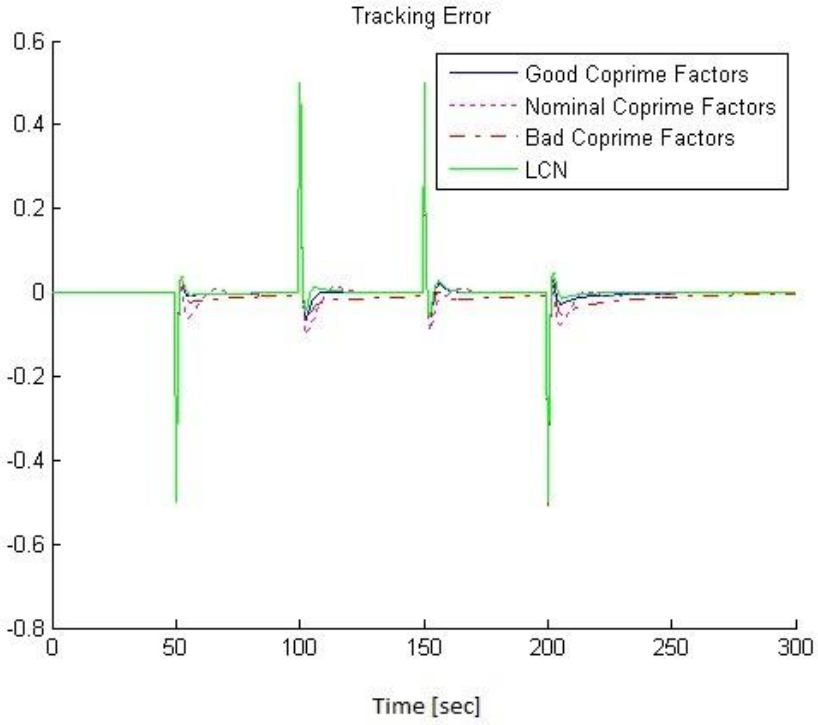

Fig. 3.8. Simulation comparison of LQN and LCN.

3.3 LPV Control with LPV-Q System

The approach in this section is based promarily on the paper [86], [87]. In this section, the specific case of a model represented by an LPV system is considered.

3.3.1 Preliminaries

First, a few mathematical and notational preliminaries are prepared. The transfer function for a Linear Parameter Varying (LPV) system is denoted $G(s,\theta)$. When it is clear from the context, the more compact notation $G(\theta)$ will be used. The associated state space system representation is given by

$$\begin{aligned} \dot{x}_G &= A_G(\theta)x_G + B_G(\theta)u \\ y &= C_G(\theta)x_G + D_G(\theta)u \end{aligned} \tag{3.22}$$

The scheduling parameter θ may be a scalar or vector and is assumed to lie within some predefined range, $\theta \in [\underline{\theta}, \overline{\theta}]$ with the set of critical design points defined by $\theta_i, i = 1,\ldots,n$. As appropriate, we will use the following as an equivalent notation for the system defined in Equation 3.23

$$G(\theta) = \left[\begin{array}{c|c} A_G(\theta) & B_G(\theta) \\ \hline C_G(\theta) & D_G(\theta) \end{array}\right] \tag{3.23}$$

In this section, stability of the closed loop system will be established using common quadratic Lyapunov functions (CQLF) of the form, $V(x) = x^T Px, P > 0$; thus $V(x) > 0$. Assuming an associated LPV dynamic system $\dot{x} = A(\theta)x + B(\theta)u$, if $PA(\theta) + A^T(\theta)P < 0, \forall x \neq 0$, then the LPV system is asymptotically stable [74]. The search for such a common quadratic Lyapunov function typically would require gridding the variable over its predefined range [42] and solving the finite number of associated Linear Matrix Inequalities (LMIs). The number of LMIs is generally reduced considerably for a polytopic LPV system [74] where the system matrices are defined in terms of vertices, at which the LPV system is evaluated at a particular operation point, e.g.

$$G_{polytopic}(\theta) = Co\left\{\left[\begin{array}{c|c} A_G(\theta_j) & B_G(\theta_j) \\ \hline C_G(\theta_j) & D_G(\theta_j) \end{array}\right], \forall j = 1\ldots m\right\} \tag{3.24}$$

At these points the dynamics are denoted simply as:

$$\begin{aligned} \dot{x}_G &= A_{Gj} x_G + B_{Gj} u \\ y &= C_{Gj} x_G + D_{Gj} u \end{aligned} \tag{3.25}$$

The set of all real, rational, proper, and stable transfer functions (real rational subspace of H_∞) is denoted as RH_∞ [67]. A square matrix A is called a Hurwitz matrix if every eigenvalue of A has a strictly negative real part, i.e. $\mathrm{Re}(\lambda(A)) < 0$.

3.3.2 LPV Control with Local Controller Recovery

When nonlinear system models are constructed using first principles, the state variables generally remain tied to the physics of the system. This naturally leads to Linear Parameter Varying (LPV) models where linear models at different operating points share the same state variables, and the state space system matrices are parameterized in terms of the scheduling variable, θ:

$$\begin{aligned} \dot{x}_p &= A_p(\theta) x_p + B_p(\theta) u \\ y &= C_p(\theta) x_p \end{aligned} \tag{3.26}$$

This is in contrast to a set of controllers, defined *a priori*, where there is no physical relationship between state variables. Assume that these local controllers have been designed for a set of critical operating conditions with plant dynamics defined by Equation 3.26 with $\theta = \theta_i$:

$$\alpha_i = 1 \quad \text{and} \quad \alpha_j = 0 \quad \forall \quad j \neq i \tag{3.27}$$

In this case, the Local Control Network (LCN) representation is more appropriate. Assuming individual controllers are represented in state space form as:

$$\begin{aligned} \dot{x}_{ki} &= A_{ki}x_{ki} + B_{ki}z_2 \\ u_{ki} &= C_{ki}x_{ki} + D_{ki}z_2 \end{aligned} \tag{3.28}$$

The full LCN can be constructed as:

$$\begin{aligned} \begin{bmatrix} \dot{x}_{k1} \\ \vdots \\ \dot{x}_{kn} \end{bmatrix} &= \underbrace{\begin{bmatrix} A_{k1} & & 0 \\ & \ddots & \\ 0 & & A_{kn} \end{bmatrix}}_{A_K} \underbrace{\begin{bmatrix} x_{k1} \\ \vdots \\ x_{kn} \end{bmatrix}}_{x_K} + \underbrace{\begin{bmatrix} B_{k1} \\ \vdots \\ B_{kn} \end{bmatrix}}_{B_K} z_2 \\ u &= \underbrace{\begin{bmatrix} \alpha_1 C_{k1} & \cdots & \alpha_n C_{kn} \end{bmatrix}}_{C_K(\alpha)} \begin{bmatrix} x_{k1} \\ \vdots \\ x_{kn} \end{bmatrix} + \underbrace{\begin{bmatrix} \sum_{i=1}^{n} \alpha_i D_{ki} \end{bmatrix}}_{D_K(\alpha)} z_2 \end{aligned} \tag{3.29}$$

The input/output notation is defined consistent with the general feedback control diagram shown in Figure 3.9.

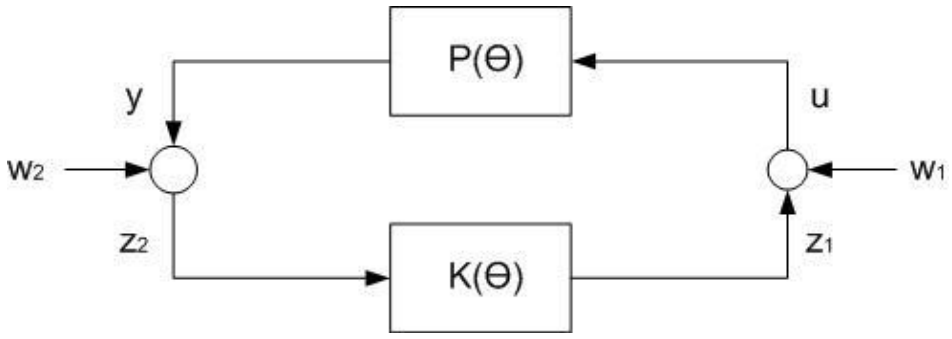

Fig. 3.9. General feedback control diagram.

A sufficient condition for stability of the closed loop system is the existence of a common quadratic Lyapunov function. This can be checked using the finite set of Linear Matrix Inequalities (LMIs):

$$PA_{CL,LPV}(\theta_i) + A_{CL,LPV}(\theta_i)^T P < 0$$

$$\text{where } A_{CL,LPV} = \begin{bmatrix} A_P(\theta_i) + B_P(\theta_i) D_K(\alpha) C_P(\theta_i) & B_P(\theta_i) C_K(\alpha) \\ B_K C_P(\theta_i) & A_K(\alpha) \end{bmatrix} \tag{3.30}$$

When this polytopic system is evaluated at its vertices, the state matrix in Equation 3.30 assumes an upper block triangular structure. By inspection, we may conclude that a necessary precondition for stability is that each controller must be open loop stable. Moreover, we note that the existence of a common Lyapunov function may be computationally elusive, particularly for a large set of controllers. However, using the Youla parameterization as an alternate framework for controller interpolation is possible with less restrictive conditions and with guaranteed stability.

3.3.2.1 Youla Parameter-Based Gain-Scheduling

To create a controller interpolation scheme that satisfies the aforementioned objectives we employ a Youla parameter-based framework. First it is necessary to select a nominal controller $K_0(s,\theta)$

$$\begin{aligned} \dot{x}_{k0} &= A_{k0}(\theta) x_{k0} + B_{k0}(\theta) z_2 \\ u &= C_{k0}(\theta) x_{k0} + D_{k0}(\theta) z_2 \end{aligned} \tag{3.31}$$

Note that this controller need not be an LPV controller. It simply needs to be any controller (LTI or LPV) that stabilizes the LPV plant over the range defined by the scheduling parameter. In most cases, this nominal controller would be designed for robustness, not performance, as the local controllers can be designed to achieve high performance at critical operating points. This aspect of the design process, including particular choices for $K_0(s,\theta)$, will be discussed later in section 3.3.2.5.

Next we decompose the plant and nominal controller into left and right coprime factors, as

$$K_0(s,\theta) = U_0(s,\theta)V_0(s,\theta)^{-1} = \tilde{V}_0(s,\theta)^{-1}\tilde{U}_0(s,\theta) \tag{3.32}$$

$$P(s,\theta) = N(s,\theta)M(s,\theta)^{-1} = \tilde{M}(s,\theta)^{-1}\tilde{N}(s,\theta) \tag{3.33}$$

For the remainder of the paper, we will drop the $K_0(s,\theta)$ notation for the more compact $K_0(\theta)$. These coprime factors are constructed such that $U_0(\theta), \tilde{U}_0(\theta), \mathrm{V}_0(\theta), \tilde{\mathrm{V}}_0(\theta) \in RH_\infty$, and such that they satisfy the double Bezout identity [70]:

$$\begin{bmatrix} M(\theta) & U_0(\theta) \\ N(\theta) & V_0(\theta) \end{bmatrix}\begin{bmatrix} \tilde{V}_0(\theta) & -\tilde{U}_0(\theta) \\ -\tilde{N}(\theta) & \tilde{M}(\theta) \end{bmatrix} = \begin{bmatrix} \tilde{V}_0(\theta) & -\tilde{U}_0(\theta) \\ -\tilde{N}(\theta) & \tilde{M}(\theta) \end{bmatrix}\begin{bmatrix} M(\theta) & U_0(\theta) \\ N(\theta) & V_0(\theta) \end{bmatrix} = \begin{bmatrix} I & 0 \\ 0 & I \end{bmatrix} \tag{3.34}$$

One such factorization can be constructed from the state space representations as:

$$\begin{bmatrix} M(\theta) & U_0(\theta) \\ N(\theta) & V_0(\theta) \end{bmatrix} = \left[\begin{array}{cc|cc} A_p(\theta)+B_p(\theta)F_p(\theta) & 0 & B_p(\theta) & 0 \\ 0 & A_{k0}(\theta)+B_{k0}(\theta)F_{k0}(\theta) & 0 & B_{k0}(\theta) \\ \hline F_p(\theta) & C_{k0}(\theta)+D_{k0}(\theta)F_{k0}(\theta) & I & D_{k0}(\theta) \\ C_p(\theta) & F_{k0}(\theta) & 0 & I \end{array}\right] \tag{3.35}$$

$$\begin{bmatrix} \tilde{V}_0(\theta) & -\tilde{U}_0(\theta) \\ -\tilde{N}(\theta) & \tilde{M}(\theta) \end{bmatrix} = \left[\begin{array}{cc|cc} A_p(\theta)+B_p(\theta)D_{k0}(\theta)C_p(\theta) & B_p(\theta)C_{k0}(\theta) & -B_p(\theta) & B_p(\theta)D_{k0}(\theta) \\ B_{k0}(\theta)C_p(\theta) & A_{k0}(\theta) & 0 & B_{k0}(\theta) \\ \hline F_p(\theta)-D_{k0}(\theta)C_p(\theta) & -C_{k0}(\theta) & I & D_{k0}(\theta) \\ C_p(\theta) & -F_{k0}(\theta) & 0 & I \end{array}\right] \tag{3.36}$$

where $F_p(\theta)$ and $F_k(\theta)$ are feedback gains chosen so that the matrices $A_p(\theta)+B_p(\theta)F_p(\theta)$ and $A_{k0}(\theta)+B_{k0}(\theta)F_{k0}(\theta)$ are Hurwitz. A particular technique

for selecting $F_p(\theta)$ and $F_k(\theta)$ which guarantee stability for time-varying θ will be given later in equations 3.56-57.

The set of all stabilizing controllers for the LPV plant can then be formulated in terms of the interconnection system

$$J_k(\theta) = \begin{bmatrix} U_0(\theta)V_0(\theta)^{-1} & \tilde{V}_0(\theta)^{-1} \\ V_0(\theta)^{-1} & V_0(\theta)^{-1}N(\theta) \end{bmatrix} \tag{3.37}$$

and a Youla parameter Q as shown in Figure 3.10. For implementation, state-space representations of these elements are given by

$$U_0(\theta)V_0(\theta)^{-1} = K_0(\theta) = \left[\begin{array}{c|c} A_{k0}(\theta) & B_{k0}(\theta) \\ \hline C_{k0}(\theta) & D_{k0}(\theta) \end{array}\right] \tag{3.38}$$

$$\tilde{V}_0(\theta)^{-1} = \left[\begin{array}{cc|c} A_p(\theta)+B_p(\theta)F_p(\theta) & 0 & -B_p(\theta) \\ B_{k0}(\theta) & A_{k0}(\theta) & 0 \\ \hline -F_p(\theta)+D_{k0}(\theta)C_p(\theta) & C_{k0}(\theta) & I \end{array}\right] \tag{3.39}$$

$$V_0(\theta)^{-1} = \left[\begin{array}{c|c} A_{k0}(\theta) & B_{k0}(\theta) \\ \hline -F_{k0}(\theta) & I \end{array}\right] \tag{3.40}$$

$$V_0(\theta)^{-1}N(\theta) = \left[\begin{array}{cc|c} A_p(\theta)+B_p(\theta)F_p(\theta) & 0 & B_p(\theta) \\ B_{k0}(\theta)C_p(\theta) & A_{k0}(\theta) & 0 \\ \hline C_p(\theta) & -F_{k0}(\theta) & 0 \end{array}\right] \tag{3.41}$$

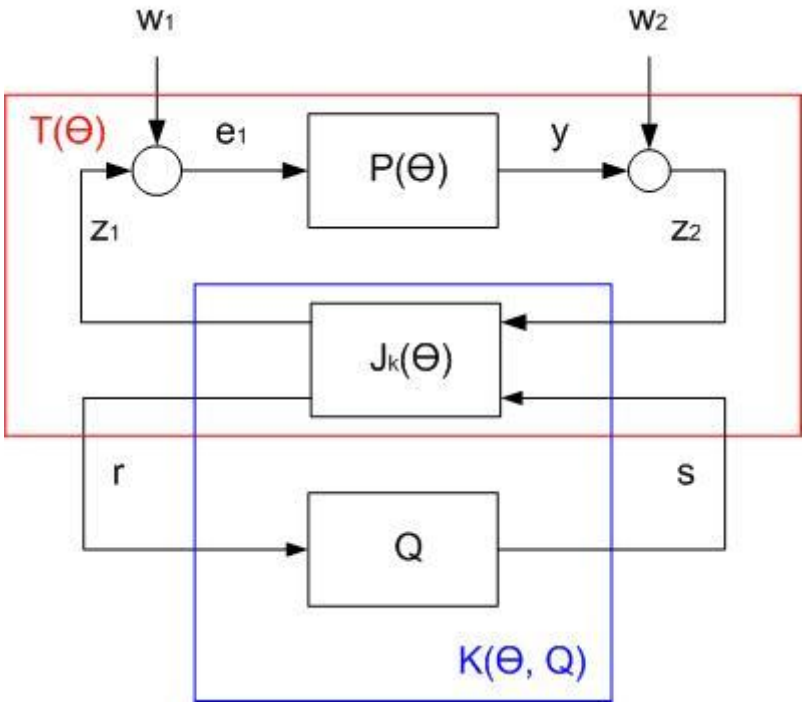

Fig. 3.10. Youla parameter based feedback control system.

3.3.2.2 Local Controller Recovery

The set of all stabilizing controllers is parameterized in terms of system Q. Assuming that the local controller K_i stabilizes the LPV plant with $\theta = \theta_i$, then the local controller can be recovered as $K_i = F_l(J_K, Q_i)$ where F_l is the lower fractional transformation. Q_i is defined as $Q_i = \tilde{U}_i V_0(\theta_i) - \tilde{V}_i U_0(\theta_i) = \tilde{V}_i (K_i - K_0) V_0(\theta_i)$, and the necessary coprime factors are defined as given below to satisfy a similar Bezout identity as in Equation 3.34. Note that by construction $Q_i \in RH_\infty$, and each Q_i is stable.

$$Q_i = -\begin{bmatrix} \tilde{V}_i & -\tilde{U}_i \end{bmatrix} \begin{bmatrix} U_0(\theta_i) \\ V_0(\theta_i) \end{bmatrix} \tag{3.42}$$

$$\begin{bmatrix} M(\theta_i) & U_i \\ N(\theta_i) & V_i \end{bmatrix} = \left[\begin{array}{cc|cc} A_p(\theta_i)+B_p(\theta_i)F_p(\theta_i) & 0 & B_p(\theta_i) & 0 \\ 0 & A_{ki}+B_{ki}F_{ki} & 0 & B_{ki}(\theta) \\ \hline F_p(\theta_i) & C_{ki}+D_{ki}F_{ki} & I & D_{ki} \\ C_p(\theta_i) & F_{ki} & 0 & I \end{array}\right] \quad (3.43)$$

$$\begin{bmatrix} \tilde{V}_i & -\tilde{U}_i \\ -\tilde{N}(\theta_i) & \tilde{M}(\theta_i) \end{bmatrix} = \left[\begin{array}{cc|cc} A_p(\theta_i)+B_p(\theta_i)D_{ki}C_p(\theta_i) & B_p(\theta_i)C_{ki} & -B_p(\theta) & B_p(\theta)D_{k0}(\theta) \\ B_{ki}C_p(\theta_i) & A_{ki} & 0 & B_{k0}(\theta) \\ \hline F_p(\theta_i)-D_{ki}C_p(\theta_i) & -C_{ki} & I & -D_{ki} \\ C_p(\theta_i) & -F_{ki} & 0 & I \end{array}\right] \quad (3.44)$$

$$Q_i = \left[\begin{array}{ccc|c} A_p(\theta_i)+B_p(\theta_i)D_{ki}C_p(\theta_i) & B_p(\theta_i)C_{ki} & B_p(\theta_i)[D_{ki}-D_{k0}(\theta_i)]F_{k0}(\theta_i)-B_p(\theta_i)C_{k0}(\theta_i) & B_p(\theta_i)[D_{ki}-D_{k0}(\theta_i)] \\ B_{ki}C_p(\theta_i) & A_{ki} & B_{ki}F_{k0}(\theta_i) & B_{ki} \\ 0 & 0 & A_{k0}(\theta_i)+B_{k0}(\theta_i)F_{k0}(\theta_i) & B_{k0}(\theta_i) \\ \hline D_{ki}C_p(\theta_i)-F_p(\theta_i) & D_{ki} & [D_{ki}-D_{k0}(\theta_i)]F_{k0}(\theta_i)-C_{k0}(\theta_i) & D_{ki}-D_{k0}(\theta_i) \end{array}\right] \quad (3.45)$$

To show that we do in fact recover the controller K_i at the i[th] operating condition:

$$F_l(J_K(\theta_i), Q_i) = U_0(\theta_i)V_0(\theta_i)^{-1} + \tilde{V}_0(\theta_i)^{-1}Q_i(I + V_0(\theta_i)^{-1}N(\theta_i)Q_i)^{-1}V_0(\theta_i)^{-1} \quad (3.46)$$

Substituting $Q_i = \tilde{V}_i(K_i - K_0(\theta_i))V_0(\theta_i)$ and manipulating yields:

$$F_l(J_K(\theta_i), Q_i) = K_0(\theta_i) + [\tilde{V}_i\tilde{V}_0(\theta_i) + (K_i - K_0(\theta_i))N(\theta_i)\tilde{V}_0(\theta_i)]^{-1}(K_i - K_0(\theta_i)) \quad (3.47)$$

Substituting $K_0(\theta_i) = \tilde{V}_0(\theta_i)^{-1}\tilde{U}_0(\theta_i)$ and $K_i = \tilde{V}^{-1}\tilde{U}_i$, and applying Bezout identities gives the identity:

$$\tilde{V}_i\tilde{V}_0(\theta_i) + (K_i - K_0(\theta_i))N(\theta_i)\tilde{V}_0(\theta_i) = I. \quad (3.48)$$

Thus with some minor algebraic manipulation, $F_l(J_K(\theta_i), Q_i) = K_i$.

3.3.2.3 Stability of the Closed Loop System

The closed loop system can be written as $G(\theta) = F_l(T(\theta), Q)$ as shown in Figure 3.10. After some algebraic manipulation, and application of the Bezout identities, the system $T(\theta)$ is given as:

$$T(\theta) = \begin{bmatrix} T_{11}(\theta) & T_{12}(\theta) \\ T_{21}(\theta) & 0 \end{bmatrix} = \begin{bmatrix} U_0(\theta)\tilde{N}(\theta) & U_0(\theta)\tilde{M}(\theta) & M(\theta) \\ V_0(\theta)\tilde{N}(\theta) & V_0(\theta)\tilde{M}(\theta) & N(\theta) \\ \tilde{N}(\theta) & \tilde{M}(\theta) & 0 \end{bmatrix}, \tag{3.49}$$

where

$$\begin{bmatrix} z_1 \\ z_2 \\ r \end{bmatrix} = T(\theta) \begin{bmatrix} w_1 \\ w_2 \\ s \end{bmatrix}. \tag{3.50}$$

The particular structure of $T(\theta)$ leads to the closed loop system, $\begin{bmatrix} z_1 \\ z_2 \end{bmatrix} = G(\theta) \begin{bmatrix} w_1 \\ w_2 \end{bmatrix}$ being affine in the system Q as:

$$G(\theta) = T_{11}(\theta) + T_{12}(\theta) Q T_{21}(\theta). \tag{3.51}$$

The state matrix of the closed loop system $G(\theta)$ is given as follows (where * indicates nonzero matrix entries):

$$A_G(\theta) = \begin{bmatrix} A_{T11}(\theta) & 0 & 0 & 0 \\ 0 & A_{T12}(\theta) & * & * \\ 0 & 0 & A_Q(\theta) & * \\ 0 & 0 & 0 & A_{T21}(\theta) \end{bmatrix} \tag{3.52}$$

$$A_{T11}(\theta) = \begin{bmatrix} A_{k0}(\theta) + B_{k0}(\theta)F_{k0}(\theta) & B_{k0}(\theta)C_p(\theta) & -B_{k0}(\theta)F_{k0}(\theta) \\ 0 & A_p(\theta) + B_p(\theta)D_{k0}(\theta)C_p(\theta) & B_p(\theta)C_{k0}(\theta) \\ 0 & B_{k0}(\theta)C_p(\theta) & A_{k0}(\theta) \end{bmatrix} \tag{3.53}$$

$$A_{T21}(\theta)=\begin{bmatrix} A_p(\theta)+B_p(\theta)D_{k0}(\theta)C_p(\theta) & B_p(\theta)C_{k0}(\theta) \\ B_{k0}(\theta)C_p(\theta) & A_{k0}(\theta) \end{bmatrix} \tag{3.54}$$

The closed loop system is stable under arbitrarily fast variations in θ if there exists a common quadratic Lyapunov function (CQLF): $V(x)=x^T P_G x>0,\ \forall \mathrm{x}\neq 0$ and $P_G A_G(\theta)+A_G(\theta)^T P_G<0,\ \forall \mathrm{x}\neq 0$. Noting the block diagonal structure of the closed loop system state matrix (Equation 3.51), stability of the system can be guaranteed by ensuring the stability of each sub-block.

First, the state matrix $A_{T21}(\theta)$ is simply the closed loop describing the interaction between the nominal controller and the LPV plant. By assumption, the nominal controller, fixed or LPV, stabilizes the LPV plant, such that there exists a corresponding CQLF:

$$P_{T21}A_{T21}(\theta)+A_{T21}^T(\theta)P_{T21}<0 \tag{3.55}$$

Second, assuming that the state feedback gains for the coprime factors, $F_p(\theta)$ and $F_k(\theta)$, are chosen such as $F_p(\theta)=X(\theta)P_p^{-1}$ and $F_k(\theta)=Y(\theta)P_k^{-1}$, so that the following Linear Matrix Inequalities (LMIs) are satisfied, then $A_{T12}(\theta)$ is also guaranteed to be quadratically stable:

$$A_p(\theta)P_p+P_pA_p(\theta)^T+B_p(\theta)X(\theta)+X(\theta)^T B_p(\theta)^T<0, \tag{3.56}$$

$$A_k(\theta)P_k+P_kA_k(\theta)^T+B_k(\theta)Y(\theta)+Y(\theta)^T B_k(\theta)^T<0. \tag{3.57}$$

(Note that for polytopic LPV systems, these conditions can be written as a finite set of LMIs.) Finally, we assume that the interpolation scheme is designed so that there exists a quadratic Lyapunov function P_Q such that:

$$P_Q A_Q + A_Q{}^T P_Q < 0. \tag{3.58}$$

Methods for creating such an interpolation scheme will be given in the next section. As the state matrix of the closed loop system is block diagonal, then the block diagonal CQLF $P_G = diag\{P_k, P_{21}, P_p, P_Q, P_{21}\}$ is sufficient for guaranteeing stability of the system under arbitrarily fast transitions of scheduling variables.

3.3.2.4 Construction of LPV-Q System

The previous sections discuss how to form Q_i so that each local controller K_i is recovered at the corresponding operating point, and showhow the stability of the resulting closed loop system can be guaranteed, assuming there exists a CQLF for the interpolated Q. In this section we present a method for interpolating between these Q_i while guaranteeing the existence of a CQLF for the interpolated Q, and limiting the state dimension of the eventual controller.

The standard LCN approach to interpolation would be to simply create a weighted average of the output signals from each Q_i based on the current operating point (Equation 3.59). The stability of the resulting polytopic system can be established with a simple CQLF (Equation 3.60)

$$\begin{bmatrix} \dot{x}_{Q1} \\ \vdots \\ \dot{x}_{Qn} \end{bmatrix} = \begin{bmatrix} A_{Q1} & \cdots & 0 \\ \vdots & \ddots & \vdots \\ 0 & \cdots & A_{Qn} \end{bmatrix} \begin{bmatrix} x_{Q1} \\ \vdots \\ x_{Qn} \end{bmatrix} + \begin{bmatrix} B_{Q1} \\ \vdots \\ B_{Qn} \end{bmatrix} z$$

$$u = \begin{bmatrix} \alpha_1 C_{Q1} & \cdots & \alpha_n C_{Qn} \end{bmatrix} \begin{bmatrix} x_{Q1} \\ \vdots \\ x_{Qn} \end{bmatrix} + \begin{bmatrix} \sum_{i=1}^{n} \alpha_i D_{Qi} \end{bmatrix} \tag{3.59}$$

$$P_Q = diag\{P_{Q1}, P_{Q2}, \ldots, P_{Qn}\} \tag{3.60}$$

However, utilizing a large number of local controllers within a LCN/LQN can lead to significant computational problems, as the state dimension of the resulting nonlinear controller can become very large. In contrast to plant models where the physical nature of the dynamic states naturally leads to LPV representations, the states of a set of local controllers do not share any physical significance. Thus LPV controllers generally only arise from direct synthesis, and do not allow separate control design at specified operating conditions. However, a notable advantage of LPV controller implementation is the limited number of dynamic state variables required. Thus we propose an alternative formulation of the gain-scheduled interpolated controller where states are shared, leading to an LPV controller formulation which enjoys a significantly lower state dimension than the Local Controller Network approach but retains the benefits of local controller recovery.

First, note that if the local controllers K_i have different state dimensions, the corresponding Q_i would also have different state dimensions. In this case, stable, unobservable/uncontrollable states are augmented to the state space representations of

Q_i such that the augmented $\hat{Q}_i$ has equal state dimensions to the highest dimensional Q_i.

$$\hat{Q}_i = \left[\begin{array}{cc|c} A_{Qi} & 0 & B_{Qi} \\ 0 & -\mu & 0 \\ \hline C_{Qi} & 0 & D_{Qi} \end{array}\right] \tag{3.61}$$

Each $\hat{Q}_i$ is guaranteed to be stable by construction, and therefore there exists an associated QLF, $P_{\hat{Q}_i}$. For the purposes of this paper, the following finite set of LMIs will be solved to obtain the matrices $P_{\hat{Q}_i}$ that guarantee stability and also ensure that $\left\|\hat{Q}_i\right\|_\infty < \gamma_i$,

$$\begin{bmatrix} P_{\hat{Q}_i} A_{\hat{Q}_i} + A_{\hat{Q}_i}^T P_{\hat{Q}_i} + C_{\hat{Q}_i}^T C_{\hat{Q}_i} & P_{\hat{Q}_i} B_{\hat{Q}_i} + C_{\hat{Q}_i}^T D_{\hat{Q}_i} \\ B_{\hat{Q}_i}^T P_{\hat{Q}_i} + D_{\hat{Q}_i}^T C_{\hat{Q}_i} & D_{\hat{Q}_i}^T D_{\hat{Q}_i} - {\gamma_i}^2 I \end{bmatrix} < 0 \tag{3.62}$$

Next, note that a state transformation can be applied to each augmented system $\hat{Q}_i$ without affecting its input-output nature. Applying a similarity transformation defined by $(P_{\hat{Q}_i})^{\frac{1}{2}}$, to each $\hat{Q}_i$ system yields:

$$\hat{\hat{Q}}_i = \left[\begin{array}{c|c} P_{\hat{Q}_i}^{\frac{1}{2}} A_{\hat{Q}_i} P_{\hat{Q}_i}^{-\frac{1}{2}} & P_{\hat{Q}_i}^{\frac{1}{2}} B_{Qi} \\ \hline C_{\hat{Q}_i} P_{\hat{Q}_i}^{-\frac{1}{2}} & D_{Qi} \end{array}\right]. \tag{3.63}$$

It is straightforward to verify that under this similarity transformation, the LMI norm bound becomes:

$$\begin{bmatrix} A_{\hat{\hat{Q}}_i} + A_{\hat{Q}}^T + C_{\hat{Q}}^T C_{\hat{\hat{Q}}_i} & B_{\hat{\hat{Q}}_i} + C_{\hat{Q}}^T D_{\hat{\hat{Q}}_i} \\ B_{\hat{Q}}^T + D_{\hat{Q}}^T C_{\hat{\hat{Q}}_i} & D_{\hat{Q}}^T D_{\hat{\hat{Q}}_i} - \gamma_i^{\,2} I \end{bmatrix} < 0. \tag{3.64}$$

Thus the polytopic system formed by the transformed systems (Equation 3.65) is guaranteed stable with CQLF $P_{Q(\theta)} = I$, and with guaranteed norm bound $\left\|Q(\theta)\right\|_\infty = \max \left\|\hat{Q}_i\right\|_\infty < \gamma_{\max}$.

$$Q(\theta) = Co\left\{ \left[\begin{array}{c|c} A_{\hat{\hat{Q}}_i} & B_{\hat{\hat{Q}}_i} \\ \hline C_{\hat{\hat{Q}}_i} & D_{\hat{\hat{Q}}_i} \end{array} \right] \right\}. \tag{3.65}$$

Note that the stability of the nonlinear closed loop does not depend on how the state matrices of the particular $\hat{\hat{Q}}_i$ are interpolated to form $Q(\theta)$; this offers an additional element of design freedom. In general the weighting functions are designed such that $\alpha_i \in [0,1]$ and $\sum \alpha_i = 1$, with the magnitude based on the relative distance to the respective design point in the scheduling space (e.g. Figure 3.11).

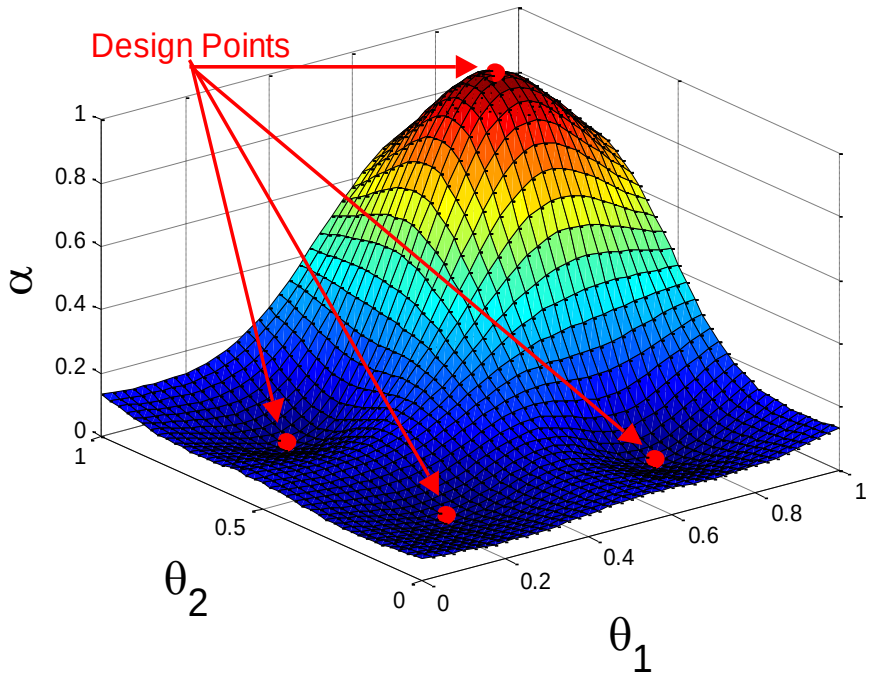

Fig. 3.11. Quadratic weighting function for a 2-dimensional scheduling space.

A summary of the design procedure is given as follows:

Step 1) Design fixed linear controllers at key operating conditions $K_i(s)$.

Step 2) Select a nominal controller $K_0(\theta)$ that stabilizes the system for the entire operating envelope (see section V for a detailed discussion).

Step 3) Utilizing the LPV representation of the system dynamics, solve equations 3.56-57 for feedback gains as $F_p(\theta) = X(\theta)P_p^{-1}$ and $F_k(\theta) = Y(\theta)P_k^{-1}$. These are used to construct the coprime factors given in Equations 3.35-36.

Step 4) Formulate the interconnection system $J_k(\theta)$ given in equation 3.37 and the individual Youla parameters $Q_i(s)$ as given in Equation 3.45.

Step 5) As necessary, augment the states of the individual Q_i systems as given in Equation 3.61 to ensure equal state dimension among controllers.

Step 6) Use the LMIs given in Equation 3.62 to determine the state transformation specified in Equation 3.63, and formulate the LPV representation of $Q(\theta)$ as in Equation 3.65, and select the weighting functions $\alpha = f(\theta)$.

Step 7) The final controller is implemented as the interconnection of $J_k(\theta)$ and $Q(\theta)$.

3.3.2.5 Application to Control of Switched Linear Systems

The capability of the proposed interpolation approach to guarantee closed loop stability for arbitrarily fast changes in the scheduling variable leads naturally to application of switched linear systems. If the transitions between critical operating conditions occur infinitely fast (instantly), the LPV plant model can be represented by a switched linear system using standard notation [52]:

$$\dot{x}_p = A_{p,\sigma} x_p + B_{p,\sigma} u$$

$$y = C_{p,\sigma} x_p \tag{3.66}$$

where σ denotes the switching signal. Application of the techniques presented above result in stable switching between controllers of arbitrary size/structure if there exists a nominal control strategy $K_0(s,\sigma)$ that stabilizes the switched system so that there exists a common quadratic Lyapunov function

$$PA_{PK,\sigma} + A_{PK,\sigma}^T P < 0 \tag{3.67}$$

where

$$A_{PK,\sigma} = \begin{bmatrix} A_{p,\sigma} + B_{p,\sigma} D_{k,\sigma} C_{p,\sigma} & B_{p,\sigma} C_{k,\sigma} \\ B_{k,\sigma} C_{p,\sigma} & A_{k,\sigma} \end{bmatrix} \tag{3.68}$$

If any such nominal stabilizing controller exists, then the above framework allows local control strategies to be parameterized in terms of this nominal controller so that the characteristics of the local controllers are recovered exactly, but the stability of the closed loop system is guaranteed. This technique provides a promising alternative to standard switched systems control methodologies such as dwell-time or switching sequencing approaches [52].

3.4 Special-Cases: Choice of Nominal Controller

The approach outlined in the previous section provides a general method of constructing a gain-scheduled controller for LPV system with local controller recovery. Additionally, an interpolation approach is given that results in an LPV controller, significantly reducing the large state dimensions resulting from simple controller blending. However, a prerequisite to this design methodology is the existence of a nominal controller $K_0(\theta)$ that stabilizes the plant for the entire range of operating conditions. The synthesis of a single fixed controller that meets these conditions is the well-known, and provably difficult, simultaneous stabilization problem, while the synthesis of a stabilizing LPV controller relies on existing design methods available in the literature. However, in practice, a far simpler method involves selecting one of the fixed controllers and attempting to verify stability by determining an appropriate

common Lyapunov function. In this section, two specific choices for nominal controller are discussed, where the approach for verifying stability is more formulaic and the state dimensions of the final controller can be further reduced. These special cases result when the nominal controller is selected as a state feedback/estimator controller or as a simple static output feedback controller.

3.4.1 State Estimate/State Feedback Controller

A common choice when implementing Youla-based controller interpolation schemes is to use state estimate/state feedback controllers. If the nominal controller is selected as such, the result is similar to that presented in [88] where the authors use a Youla based LPV controller and self-schedule the *Q*-parameter to optimize L_2-gain performance. However, instead of focusing on LPV controller synthesis, we will examine this choice of nominal control from the perspective of ensuring local controller recovery.

Assuming a state estimate/feedback controller $K_0(\theta)$ of the form:

$$\dot{x}_{k0} = [A_p(\theta) + B_p(\theta)F_p(\theta) + H_p(\theta)C_p(\theta)]x_{k0} - H_p(\theta)z_2$$

$$u = F_p(\theta)x_{k0} \tag{3.69}$$

where the state feedback and observer gains are calculated as $F_p(\theta) = X(\theta)P_f^{-1}$ and $H_p(\theta) = P_h^{-1}W(\theta)$, such that the following Linear Matrix Inequalities (LMIs) are satisfied:

$$A_p(\theta)P_f + P_f A_p(\theta)^T + B_p(\theta)X(\theta) + X(\theta)^T B_p(\theta)^T < 0 \tag{3.70}$$

$$A_p(\theta)^T P_h + P_h A_p(\theta) + W(\theta)C_p(\theta) + C_p(\theta)^T W(\theta)^T < 0 \tag{3.71}$$

As before, for polytopic LPV systems, these conditions can be written as a finite set of LMIs, and a feasible solution to the LMIs is necessary to guarantee stability.

For controllers of this form, a doubly coprime factorization satisfying the Bezout identities for the LPV plant and nominal LPV controller $K_0(\theta)$ can be constructed as:

$$\begin{bmatrix} M(\theta) & U_0(\theta) \\ N(\theta) & V_0(\theta) \end{bmatrix} = \left[\begin{array}{c|cc} A_p(\theta)+B_p(\theta)F_p(\theta) & B_p(\theta) & -H_p(\theta) \\ \hline F_p(\theta) & I & I \\ C_p(\theta) & I & 0 \end{array}\right], \text{ and} \qquad (3.72)$$

$$\begin{bmatrix} \tilde{V}_0(\theta) & -\tilde{U}_0(\theta) \\ -\tilde{N}(\theta) & \tilde{M}(\theta) \end{bmatrix} = \left[\begin{array}{c|cc} A_p(\theta)+H_p(\theta)C_p(\theta) & -B_p(\theta) & H_p(\theta) \\ \hline F_p(\theta) & I & I \\ C_p(\theta) & I & 0 \end{array}\right]. \qquad (3.73)$$

With only the state estimate/feedback controller, the resulting closed loop LPV system is guaranteed to be quadratically stable by construction. But to recover the local controller behavior at each operating condition, we define the coprime factors at the i[th] operating condition as given previously in Equation 3.43-44, and the individual Youla parameters as:

$$Q_i = -\begin{bmatrix} \tilde{V}_i & -\tilde{U}_i \end{bmatrix}\begin{bmatrix} U_0(\theta_i) \\ V_0(\theta_i) \end{bmatrix} = \left[\begin{array}{ccc|c} A_p(\theta_i)+B_p(\theta_i)D_{ki}C_p(\theta_i) & B_p(\theta_i)C_{ki} & B_p(\theta_i)[F_{k0}(\theta_i)+D_{ki}C_p(\theta_i)] & B_p(\theta_i)D_{ki} \\ B_{ki}C_p(\theta_i) & A_{ki} & B_{ki}C_p(\theta_i) & B_{ki} \\ 0 & 0 & A_{k0}(\theta_i)+B_{k0}(\theta_i)F_{k0}(\theta_i) & -H_p(\theta_i) \\ \hline D_{ki}C_p(\theta_i)-F_p(\theta_i) & C_{ki} & D_{ki}C_p(\theta_i)-F_p(\theta_i) & D_{ki} \end{array}\right] \qquad (3.74)$$

The system $J_k(\theta)$ is constructed simply as:

$$J_k(\theta) = \begin{bmatrix} U_0(\theta)V_0(\theta)^{-1} & \tilde{V}_0(\theta)^{-1} \\ V_0(\theta)^{-1} & V_0(\theta)^{-1}N(\theta) \end{bmatrix} = \left[\begin{array}{c|cc} A_p(\theta)+B_p(\theta)F_p(\theta) & -H_p(\theta) & B_p(\theta) \\ \hline F_p(\theta) & 0 & I \\ C_p(\theta) & I & 0 \end{array}\right]. \qquad (3.75)$$

3.4.2 Static Output Feedback

Another technique for reducing the dimension of the interpolated controller is to select the nominal controller to be as simple as possible namely static output feedback control: $K_0(s,\theta) = D_{k0}(\theta)$. Although many nonlinear systems can be stabilized by static output feedback control (constant or scheduled with θ), the synthesis problem of solving Equation 3.76 is nonconvex in general. Thus for the purposes of the approach proposed in this paper, the authors advocate selecting a static output feedback gain and *verifying* stability in place of attempting to *synthesize* a stabilizing gain.

$$[A_p(\theta) + B_p(\theta)D_{k0}(\theta)C_p(\theta)]^T P + P[A_p(\theta) + B_p(\theta)D_{k0}(\theta)C_p(\theta)] < 0 \qquad (3.76)$$

This choice of controller does in fact simplify the resulting interpolated controller. Assuming this choice for the nominal stabilizing controller, the associated coprime factorizations would be:

$$\begin{bmatrix} M(\theta) & U_0(\theta) \\ N(\theta) & V_0(\theta) \end{bmatrix} = \left[\begin{array}{c|cc} A_p(\theta)+B_p(\theta)F_p(\theta) & B_p(\theta) & 0 \\ F_p(\theta) & I & D_{k0}(\theta) \\ \hline C_p(\theta) & 0 & I \end{array}\right] \qquad (3.77)$$

$$\begin{bmatrix} \tilde{V}_0(\theta) & -\tilde{U}_0(\theta) \\ -\tilde{N}(\theta) & \tilde{M}(\theta) \end{bmatrix} = \left[\begin{array}{c|cc} A_p(\theta)+B_p(\theta)D_{k0}(\theta)C_p(\theta) & -B_p(\theta) & B_p(\theta)D_{k0}(\theta) \\ F_p(\theta)-D_{k0}(\theta)C_p(\theta) & I & D_{k0}(\theta) \\ \hline C_p(\theta) & 0 & I \end{array}\right] \qquad (3.78)$$

Again, we define the coprime factors at the i[th] operating condition as given previously in equation 3.43-44, and the individual Youla parameters as:

$$Q_i = -\begin{bmatrix} \tilde{V}_i & -\tilde{U}_i \end{bmatrix}\begin{bmatrix} U_0(\theta_i) \\ V_0(\theta_i) \end{bmatrix} = \left[\begin{array}{cc|c} A_p(\theta_i)+B_p(\theta_i)D_{ki}C_p(\theta_i) & B_p(\theta_i)C_{ki} & B_p(\theta_i)[D_{ki}-D_{k0}(\theta_i)] \\ B_{ki}C_p(\theta_i) & A_{ki} & B_{ki} \\ \hline D_{ki}C_p(\theta_i)-F_p(\theta_i) & C_{ki} & D_{ki}-D_{k0}(\theta_i) \end{array}\right] \qquad (3.79)$$

The interconnection system is then given as:

$$J_k(\theta)=\begin{bmatrix} U_0(\theta)V_0(\theta)^{-1} & \tilde{V}_0(\theta)^{-1} \\ V_0(\theta)^{-1} & V_0(\theta)^{-1}N(\theta) \end{bmatrix}=\left[\begin{array}{c|cc} A_p(\theta)+B_p(\theta)F_p(\theta) & 0 & B_p(\theta) \\ \hline F_p(\theta)-D_{K0}(\theta)C_p(\theta) & D_{K0}(\theta) & I \\ C_p(\theta) & I & 0 \end{array}\right] \quad (3.80)$$

To show the recovery of the controller K_i at the i[th] operating condition, the lower fractional transformation of $J_K(\theta)$ and Q_i is explored, while once again the notation $U_0(\theta_i)$ is dropped for the simpler $U_{0,i}$:

$$F_{LFT}\left(J_K(\theta_i),Q_i\right)=U_{0,i}{V_{0,i}}^{-1}+\tilde{V}_{0,i}{}^{-1}Q_i\left(I+{V_{0,i}}^{-1}N_{0,i}Q_i\right)^{-1}V_{0,i} \quad (3.81)$$

An equivalent expression is given by:

$$F_{LFT}\left(J_K(\theta_i),Q_i\right)=\left(U_{0,i}+M_{0,i}Q_i\right)\left(V_{0,i}+N_{0,i}Q_i\right)^{-1} \quad (3.82)$$

By substituting the definition of the Youla parameters Q_i, above equation is termed in:

$$F_{LFT}\left(J_K(\theta_i),Q_i\right)=\left(U_{0,i}+M_{0,i}\left(\tilde{U}_{Ki}V_{0,i}-\tilde{V}_{Ki}U_{0,i}\right)\right)\left(V_{0,i}+N_{0,i}\left(\tilde{U}_{Ki}V_{0,i}-\tilde{V}_{Ki}U_{0,i}\right)\right)^{-1} \quad (3.83)$$

and simplifying yields:

$$F_{LFT}\left(J_K(\theta_i),Q_i\right)=\left(U_{0,i}+M_{0,i}\tilde{U}_{Ki}V_{0,i}-M_{0,i}\tilde{V}_{Ki}U_{0,i}\right)\left(V_{0,i}+N_{0,i}\tilde{U}_{Ki}V_{0,i}-N_{0,i}\tilde{V}_{Ki}U_{0,i}\right)^{-1} \quad (3.84)$$

Using the Bezout identities, it can be replaced as:

$$F_{LFT}\left(J_K(\theta_i),Q_i\right)=\left(U_{0,i}+\left(U_{Ki}\tilde{M}_{0,i}\right)V_{0,i}-\left(I+U_{Ki}\tilde{N}_{0,i}\right)U_{0,i}\right)\left(V_{0,i}+\left(V_{Ki}\tilde{M}_{0,i}-I\right)V_{0,i}-\left(V_{Ki}\tilde{N}_{0,i}\right)U_{0,i}\right)^{-1} \quad (3.85)$$

After collecting terms and simplifying, recovery of the a priori designed controller at design point can be achieved as given by:

$$F_{LFT}\left(J_K\left(\theta_i\right),Q_i\right)=\left(U_{Ki}\left(\tilde{M}_{0,i}V_{0,i}-\tilde{N}_{0,i}U_{0,i}\right)\right)\left(V_{Ki}\left(\tilde{M}_{0,i}V_{0,i}-\tilde{N}_{0,i}U_{0,i}\right)\right)^{-1}$$
$$=U_{Ki}{V_{Ki}}^{-1}=K_i \tag{3.86}$$

3.4.3 Gain-scheduled Control of a Quadruple Tank System

To demonstrate efficacy of the proposed gain-scheduling framework, a quadruple tank system is selected as a simulated model. This system is a well known multivariable control example and has been discussed in detail in [89]. A schematic diagram of the quadruple tank system is shown in Figure 3.12. The two inputs to the system are the input voltages to pumps 1 and 2, and two outputs of interest are the fluid levels in tanks 1 and 2. Two valves divide the flow from each of the pumps to the upper and lower tanks. The upper tanks (tanks 3 and 4) drain into the lower tanks (tanks 1 and 2) which drain into a reservoir. The cross flow from pump 1 to tank 4 and from pump 2 to tank 3 creates interesting dynamic phenomena.

This system can be modeled using mass balances and Bernoulli's law. The resulting nonlinear model is given in Equation 3.45 where A is the tank cross-sectional area, a is the orifice cross-sectional area, h is the fluid level, u is the pump input with a scalar gain k_u. The valve parameters $\gamma \in [0,1]$ determine the flow to each tank. The selected outputs are the fluid levels of tanks 1 and 2 and are measured with a scalar gain k_y. The linearized version of this model is determined by Jacobian linearization given in [89].

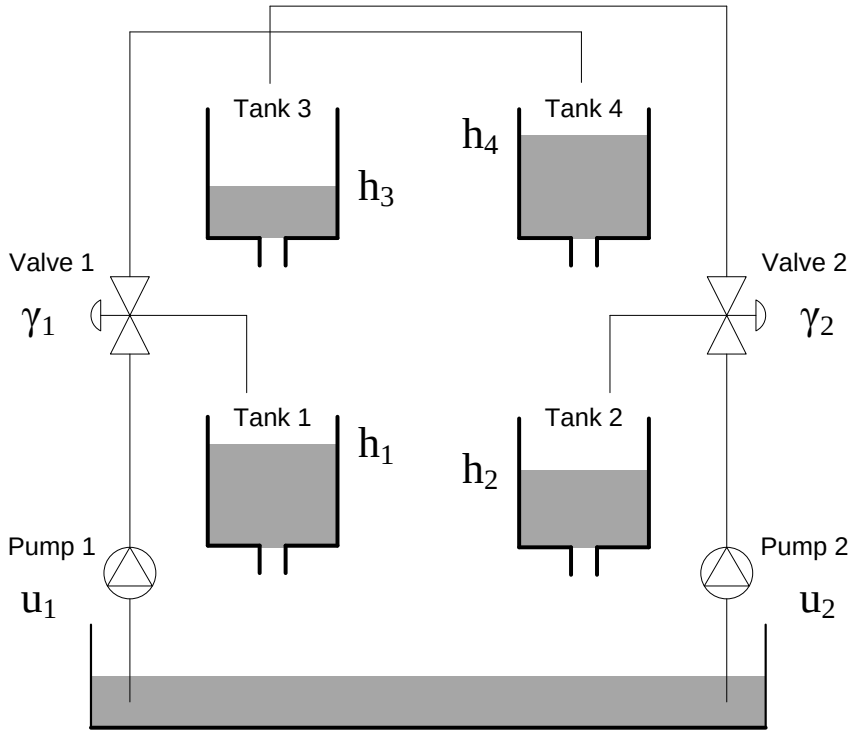

Fig. 3.12. Diagram of a quadruple tank system.

$$
\begin{aligned}
A_1\dot{h}_1 &= -a_1\sqrt{2gh_1} + a_3\sqrt{2gh_3} + \gamma_1 k_{u1}u_1 \\
A_2\dot{h}_2 &= -a_2\sqrt{2gh_2} + a_4\sqrt{2gh_4} + \gamma_2 k_{u2}u_2 \\
A_3\dot{h}_3 &= -a_3\sqrt{2gh_3} + (1-\gamma_2)k_{u2}u_2 \\
A_4\dot{h}_4 &= -a_4\sqrt{2gh_4} + (1-\gamma_1)k_{u1}u_1
\end{aligned}
\tag{3.87}
$$

This system was chosen as simulation model for several notable reasons. First, this is a well known multivariable controls example with a validated modeling approach available in the literature. Second, the poles of the system strongly depend on the nominal fluid height in the tanks; thus as the fluid heights, the system dynamics change significantly. Third, the system has a multivariable zero that can be arbitrarily placed in the right or left half plane.

For control design purposes, a quasi-LPV representation of the dynamics can be constructed from the nonlinear model as shown in Equation 3.88, with equilibrium defined by Equation 3.89:

$$\begin{bmatrix}\dot{h}_1\\ \dot{h}_2\\ \dot{h}_3\\ \dot{h}_4\end{bmatrix}=\begin{bmatrix}-\left(\frac{a_1}{A_1}\right)\sqrt{\frac{2g}{h_1}} & 0 & \left(\frac{a_3}{A_1}\right)\sqrt{\frac{2g}{h_3}} & 0\\ 0 & -\left(\frac{a_2}{A_2}\right)\sqrt{\frac{2g}{h_2}} & 0 & \left(\frac{a_4}{A_2}\right)\sqrt{\frac{2g}{h_4}}\\ 0 & 0 & -\left(\frac{a_3}{A_3}\right)\sqrt{\frac{2g}{h_3}} & 0\\ 0 & 0 & 0 & \left(\frac{a_4}{A_4}\right)\sqrt{\frac{2g}{h_4}}\end{bmatrix}\begin{bmatrix}h_1\\ h_2\\ h_3\\ h_4\end{bmatrix}+\begin{bmatrix}\frac{\gamma_1 k_u}{A_1} & 0\\ 0 & \frac{\gamma_1 k_u}{A_2}\\ 0 & \frac{(1-\gamma_2)k_u}{A_3}\\ \frac{(1-\gamma_2)k_u}{A_4} & 0\end{bmatrix}\begin{bmatrix}u_1\\ u_2\end{bmatrix} \tag{3.88}$$

$$\begin{bmatrix}u_1^0\\ u_2^0\end{bmatrix}=\left(\frac{1}{k_u(1-\gamma_1-\gamma_2)}\right)\begin{bmatrix}-\gamma_2 & 1-\gamma_2\\ 1-\gamma_1 & -\gamma_1\end{bmatrix}\begin{bmatrix}a_1\sqrt{2gh_1^0}\\ a_2\sqrt{2gh_2^0}\end{bmatrix} \tag{3.89}$$

A slight variation of the parameter values published in [89] is used for the simulations presented here. The values of tank and orifice areas, and input/output scaling, depending on the units used, are given in Table 3.2. The gravity is given as 9.81 [m/s^2], and the steady state values at the chosen operating conditions (both minimum and non-minimum phase) are given in Table 3.3.

Table 3.2. Tank and orifice areas [m2] / Input/output Scaling

A_1	2.8E-03	a_1	7.1E-06		V	3.33E-06
A_2	3.2E-03	a_2	5.7E-06	k_u	m^3/s	1.0
A_3	2.8E-03	a_3	7.1E-06		m	1.0
A_4	3.2E-03	a_4	5.7E-06	k_y	Pa	9.81E+03

Table 3.3. Operating condition (minimum phase, non-minimum phase)

h_1^0	(0.12, 0.12) [m]	u_1^0	(2.44, 3.80) [V]
h_2^0	(0.12, 0.12) [m]	u_2^0	(3.80, 2.44) [V]
h_3^0	(0.081, 0.037) [m]	γ_1	(0.7, 0.4) [-]
h_4^0	(0.052, 0.014) [m]	γ_2	(0.6, 0.3) [-]

The valve parameters γ_1 and γ_2 determine the flow ratio of lower to upper tank. Low values of γ signify a significant amount of cross-flow, thus resulting in non-minimum phase behavior. In this case a multivariable right half plane zero will be present when $\gamma_1 + \gamma_2 < 1$ as depicted in Figure 3.13.

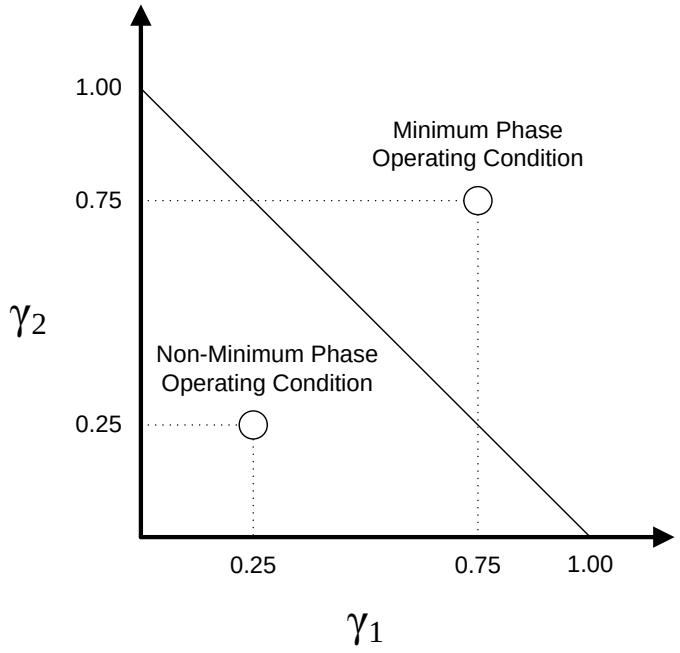

Fig. 3.13. Controller design points in minimum and nonminimum phase region.

For this example, γ_1 and γ_2 are selected as the scheduling variables. External changes to these variables will change the underlying system dynamics, as well as a disturbance to the closed loop system attempting to regulate the fluid height of the lower tanks. Two operating points in a quasi-LPV model [2] are selected: one in the minimum phase region and the other in the nonminimum phase region, depicted in Figure 3.13. As advocated in [43], a decoupled PID controller is designed for the minimum phase condition. A static decoupling matrix $W(s) = G^{-1}(0)$ is used and PID controllers are designed (Equation 3.90-91). Similarly, a set of PI controllers is designed at the minimum-phase phase operating point as given in Equation 3.92:

$$K_{PID}(s) = \begin{bmatrix} 1.26 + \frac{0.042}{s} + 0.019s & 0 \\ 0 & 1.29 + \frac{0.029}{s} + 0.028s \end{bmatrix} \tag{3.90}$$

$$W(s) = \begin{bmatrix} 0.54064 & -0.28962 \\ -0.27032 & 0.50204 \end{bmatrix} \tag{3.91}$$

$$K_{PI}(s) = \begin{bmatrix} 1.26 + \frac{0.042}{s} & 0 \\ 0 & 1.29 + \frac{0.029}{s} \end{bmatrix} \tag{3.92}$$

For the nonminimum phase operating point, [87] suggests the use of an H_∞ controller [90]. Using standard design and model reduction procedures, a 4th order H_∞ controller is designed as given in Equation 3.93. These controllers are not necessarily selected for optimal performance, but to demonstrate the full capabilities of the proposed interpolation approach. Not only do the two controllers have different state dimensions, but they are designed for fundamentally different plant dynamics. The PI and PID controller has pure integrators that prevent the controller from being strictly stable.

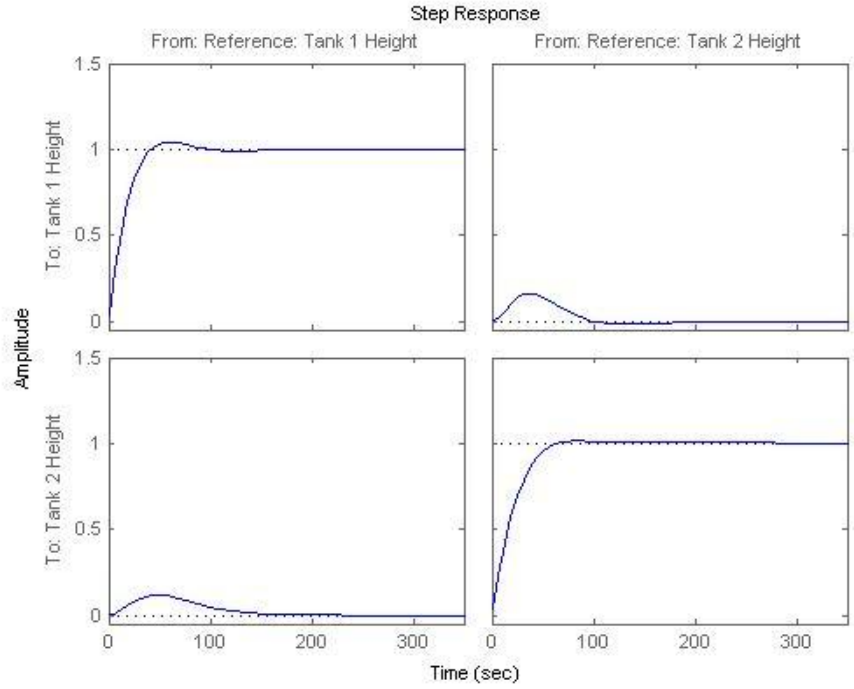

Fig. 3.14. Step response of PID controlled system at minimum phase design point.

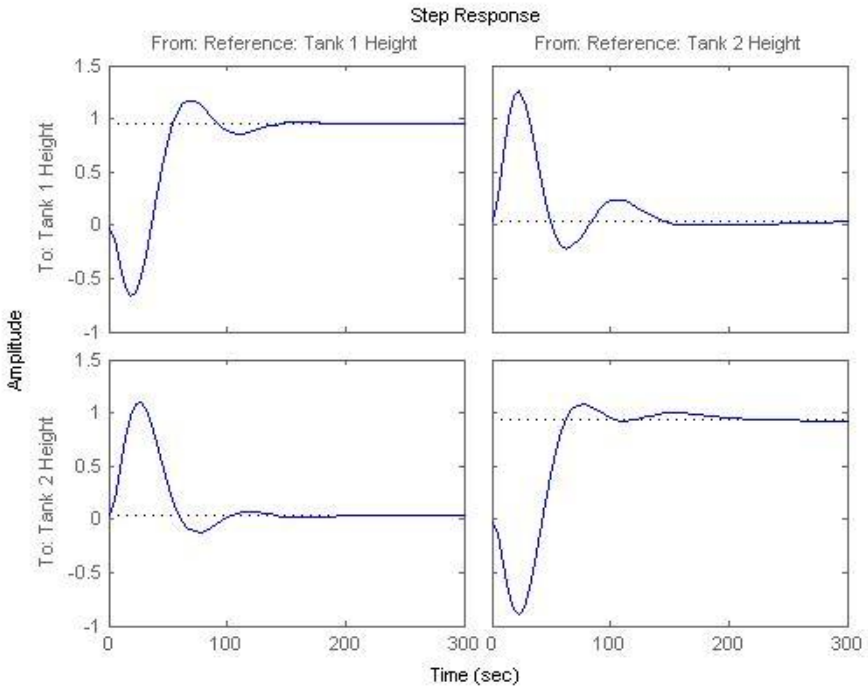

Fig. 3.15. Step response of H_∞ controlled system at minimum phase design point.

$$H_\infty = \left[\begin{array}{c|c} A_{H_\infty} & B_{H_\infty} \\ \hline C_{H_\infty} & D_{H_\infty} \end{array}\right]$$

$$= \left[\begin{array}{cccc|cc} -0.00125 & -0.00061 & 0.01279 & -0.00201 & -0.1116 & 0.0143 \\ -0.00037 & -0.00181 & 0.01026 & -0.00557 & -0.0218 & 0.1110 \\ 0.00878 & 0.01859 & -0.16460 & 0.15750 & 0.6230 & -0.7261 \\ 0.00207 & 0.00549 & -0.15760 & -0.00086 & 0.0450 & -0.0456 \\ \hline -0.02317 & -0.11190 & 0.68900 & -0.05296 & -0.1998 & -0.6641 \\ 0.11010 & 0.01625 & -0.66390 & 0.03595 & -0.7687 & -0.2333 \end{array}\right] \quad (3.93)$$

As a result, both controllers perform adequately around their respective design points, and are easily able to track reference changes in the desired fluid height. Note that Figure 3.14 and Figure 3.15 shows the step responses of the PID and H_∞ controller respectively and Figure 3.16 depicts the step response of PI and H_∞ controlled systems.

Table 3.4. Closed loop system poles.

PI controller with minimum phase plant: -0.095, -0.033, -0.040±0.032j, -0.022±0.012j
PI controller with nonminimum phase plant: **+0.016**, -0.023, -0.012±0.035j, -0.034±0.009j
$\mathcal{H}_\infty$ controller with nonminimum phase plant: -0.087, -0.009, -0.037±0.067j, -0.018±0.025j, -0.017±0.001j
$\mathcal{H}_\infty$ controller with minimum phase plant: **+0.074**, -0.220, -0.009, -0.014, -0.056±0.026j, -0.029±0.019j

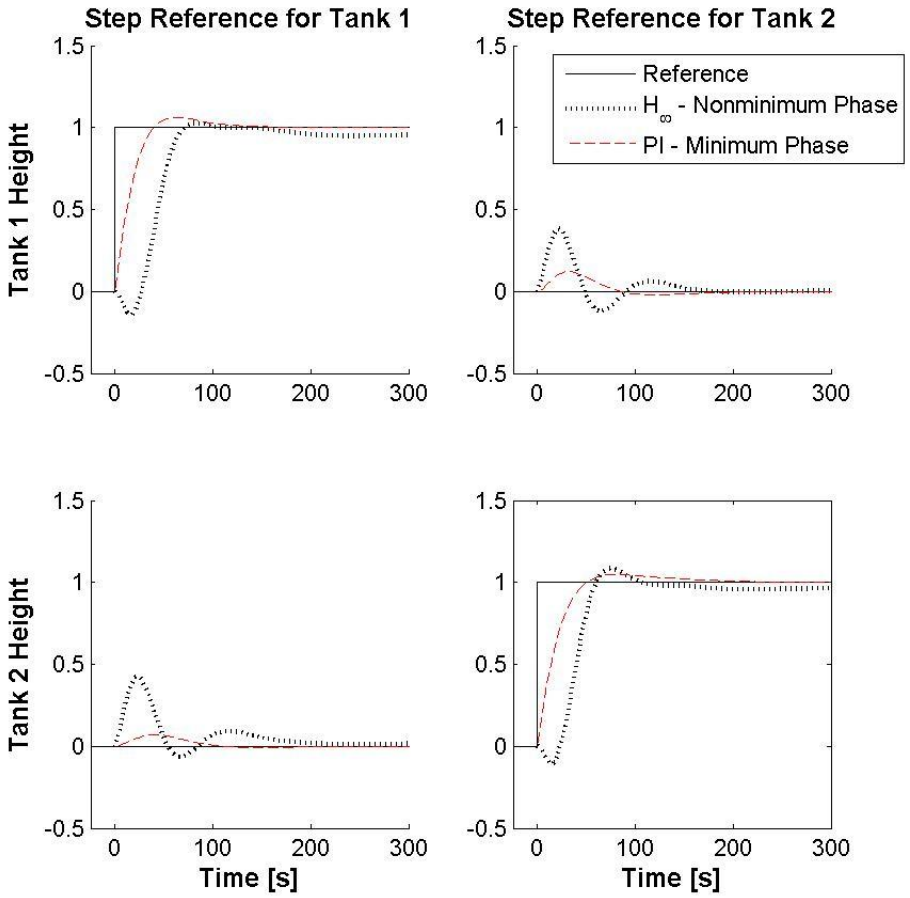

Fig. 3.16. Step response of PI and H_∞ controlled systems at design points.

Although the step response of the H_∞ controlled system displays significant undershoot, this is an expected strong non-minimum phase nature of the plant. However, these controllers are not effective at controlling the system at off-design conditions, and in fact are destabilizing. Figure 3.17 (a) and (b) show this destabilizing effectively and Table 3.4 gives the closed loop poles for the four possible combinations of plant/controller.

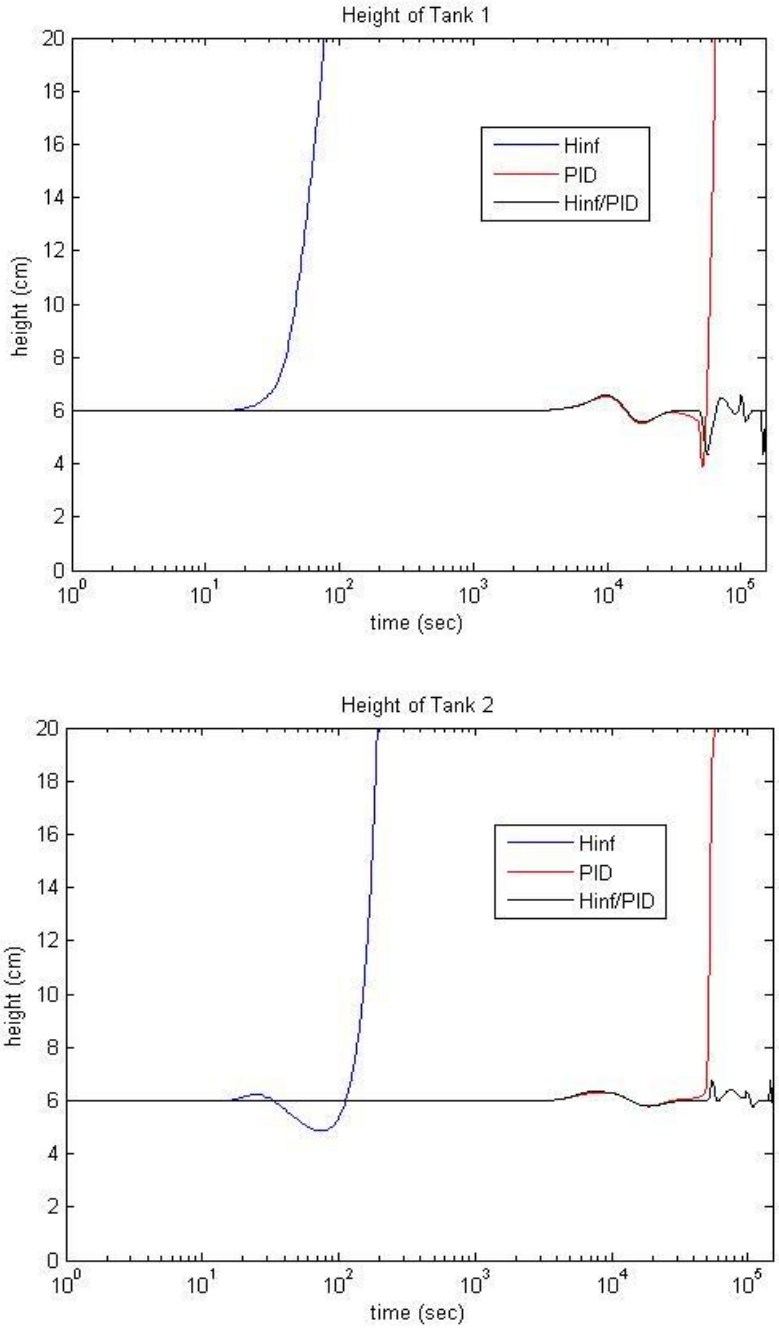

Fig. 3.17. Fluid heights in lower tank 1 and tank 2 (log scale).

A principal advantage of the LQN framework for controller interpolation is ability to interpolate controllers of different dimensions and structure or open-loop unstable controllers. As described in previous sections, a nominal LPV observer-based controller is designed for the system, and *Q* parameters are calculated so that the original MIMO-PI and H_∞ controller are recovered near the design point, blended by the exponential weighting function. The resulting controller is evaluated in simulation as applied to the nonlinear system dynamics. The interpolated controller retains the abilities of the local controller designs, and is capable of rejecting disturbances and regulating the lower tank fluid heights to the desired levels at both nonminimum phase and minimum phase conditions.

For example, Figure 3.18 shows the closed loop system response to instantaneous disturbances applied to individual tank fluid heights. More importantly, the interpolated controller can transition smoothly and stably from one design point to another. Figure 3.19 shows the system response to rapid changes in γ_1 and γ_2, which both induce disturbances on the system and change the underlying system dynamics from minimum phase to nonminimum phase. As the scheduling variables change, the exponential weighting factors allow smooth transitioning between the two *Q* functions. The control input voltages remain within reasonable bounds and fluid heights in the two lower tanks are effectively regulated.

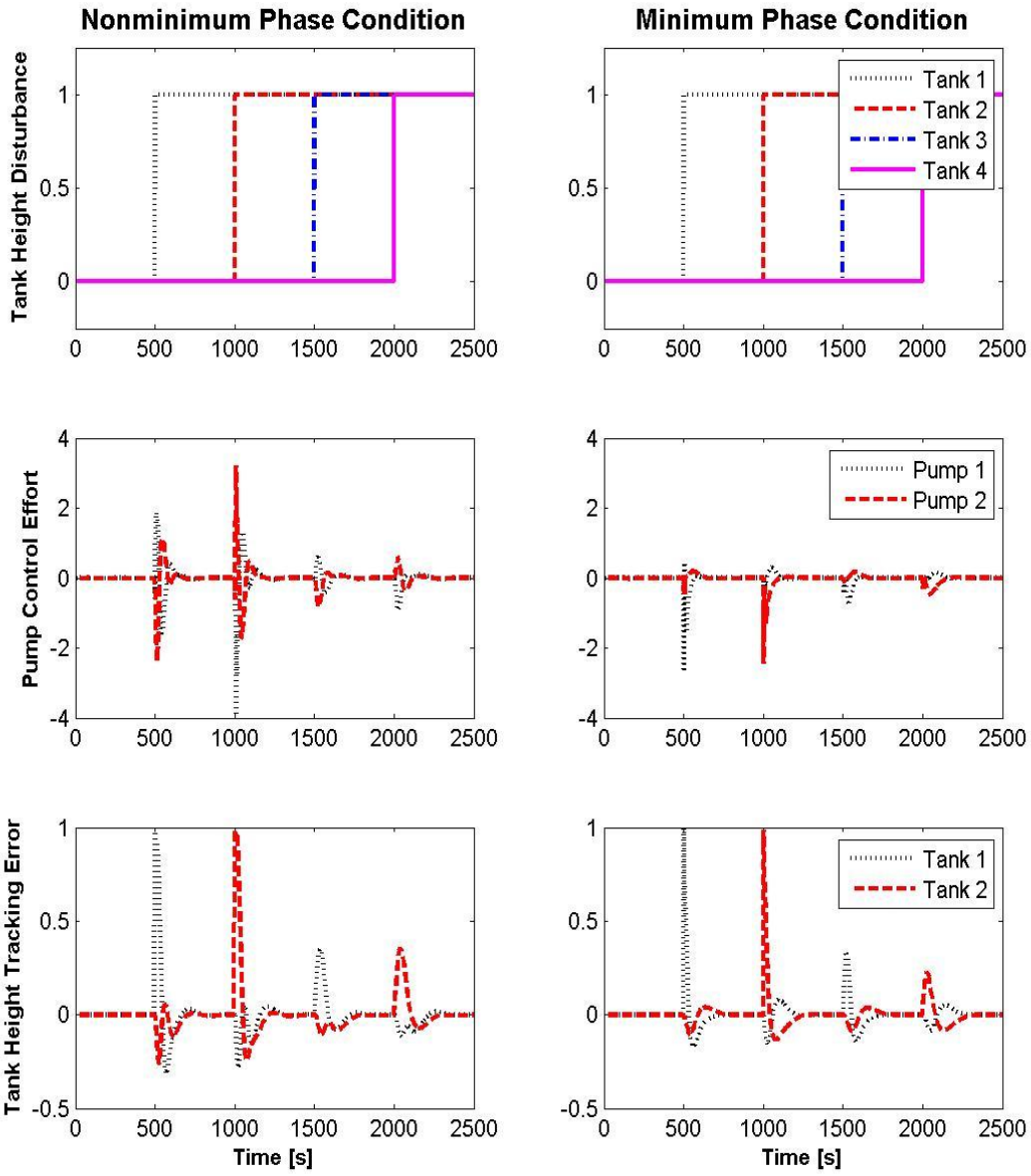

Fig. 3.18. Disturbance rejection at design conditions.

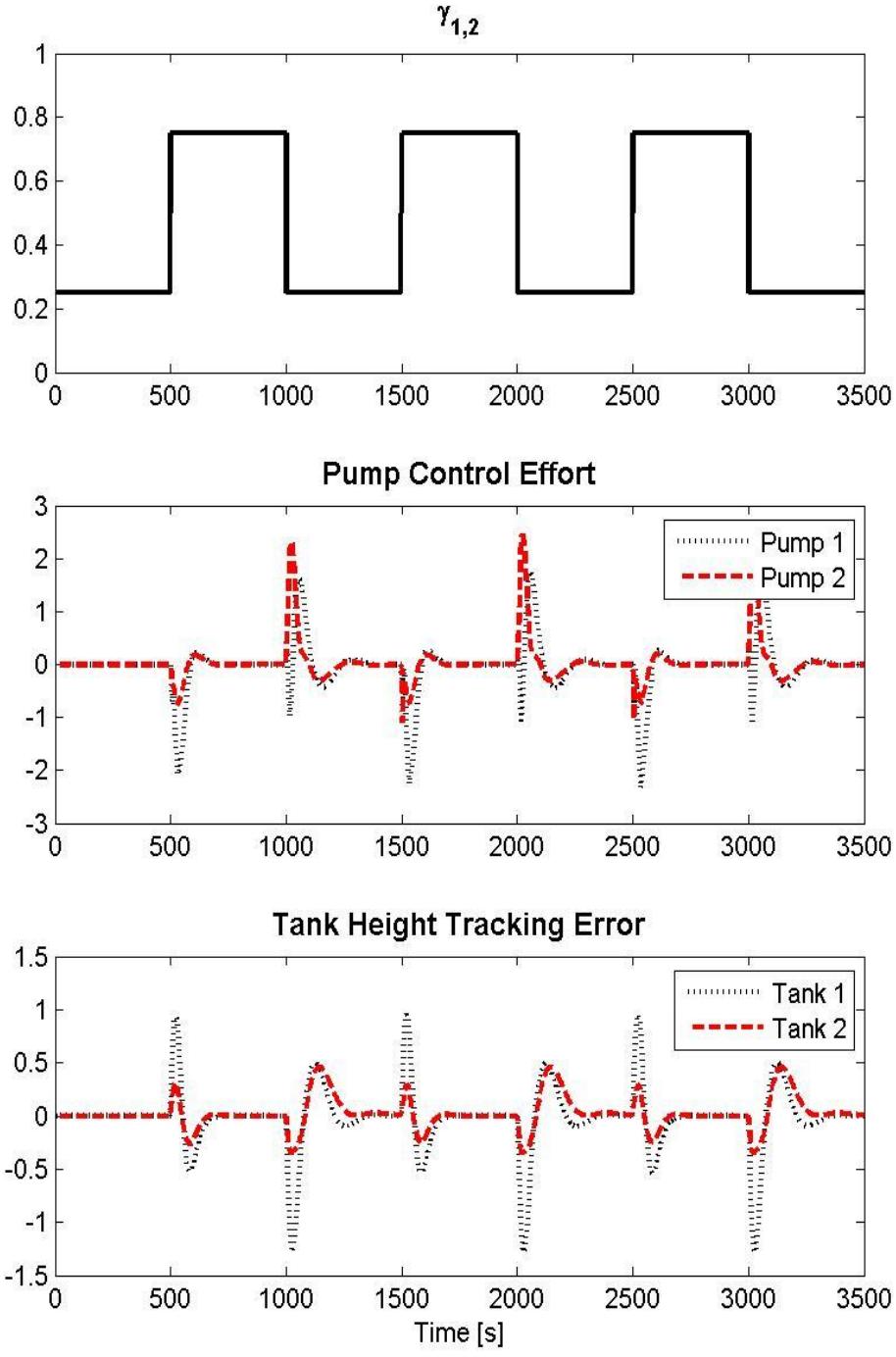

Fig. 3.19. Tracking during transition between operating conditions.

4. ROBUST STABILITY OF GAIN SCHEDULED CONTROL SYSTEM

When LPV plant models include uncertainty in scheduling variables or modeling error in plant model and these factors affect the system dynamics significantly, the plant model may not reflect the nonlinear system precisely and the associated conventional stability analyses may not be sufficient to guarantee the stability of nonlinear system in practice [3].

In this section, we extend the stability analysis in Section 3 to robustness and performance, focusing the guarantees of robust stability when the LPV plant model is assumed to include the modeling errors. A proposed framework can guarantee a global level of the stability of the perturbed nonlinear system by minimizing the L_2 gain that remained within desired bounds over the operating envelope.

4.1 Uncertain System Modeling

4.1.1 Uncertainty Description

An uncertain system is often defined as a system that does not have a completely accurate representation of a real system although the modeling difference between system representation and real system may exist in practice. There are several ways in which systems will be considered to be uncertain [3]:

The local controllers may be of different state dimensions and possibly open-loop unstable. Research achievements include:

- System's external inputs, e.g., exogenous disturbances, significantly affect the behaviors of the system, but separation between system and environment cannot be implemented
- Uncertainty in the accuracy of a system model itself is a central source when dynamic model of the system will neglect some physical phenomena. Any control method using this model will neglect some operating regimes and result in the failure of the controlled system

Note that any of these factors may result in uncertainty significantly included in the system. In any case, the control objective is to minimize the effects of unknown initial conditions and external influences on the behavior of the system, subject to the lack of a suitable system representation.

Among those uncertainty descriptions, the third definition of uncertain system is quite attractive in the gain-scheduling paradigm since the plant model used in gain-scheduling strategies virtually alleviates the requirement of exact structure or mathematical model. However, it may cause the failure of the desired stability or performance of the system when the plant model cannot reflect real dynamics of the system precisely at certain operating points. Thus an uncertainty consideration could be useful to achieve the desired stability and performance of the real systems in practice.

Several uncertainty modeling methods have been proposed in the literature but mainly categorized into two classes: 1) Parametric uncertainty and 2) neglected/unmodelled dynamics uncertainty [3]. The former is based on the structure of the model that is known but some of the parameters are uncertain. This class of

uncertainty is often called structured uncertainty since it models the uncertainty in a structured manner. In contrast, the latter appears when the model is in error because of missing dynamics, usually at high frequencies, either through deliberate neglect or because of a lack of understanding of the physical process. Note that any plant model will possibly contain this source of uncertainty [3].

Parametric uncertainty is often avoided in that it usually requires large efforts to real perturbations which are more difficult to deal with numerically, especially when it comes to controller synthesis. Thus unstructured modeling uncertainty will preferably be considered for the robust stability analysis demonstrated in this dissertation. This class of uncertainty can be addressed when one chooses to work with a simple nominal model which represents neglected dynamics as uncertainty which is unstructured.

Among uncertainty representations, additive and multiplicative uncertainty representations are most commonly used, denoted in Equation 4.18-9, respectively, and also depicted in Figure 4.1 where G is plant model, W is weighting function, and Δ is unstructured modeling uncertainty [3].

Additive uncertainty:

$$G_p(s) = G(s) + W_A(s)\Delta_A(s); \quad \left|\Delta_A(j\omega)\right| \le 1, \ \forall\omega \tag{4.18}$$

Multiplicative uncertainty:

$$G_p(s) = G(s)(1 + W_I(s)\Delta_I(s)); \quad \left|\Delta_I(j\omega)\right| \le 1, \ \forall\omega \tag{4.19}$$

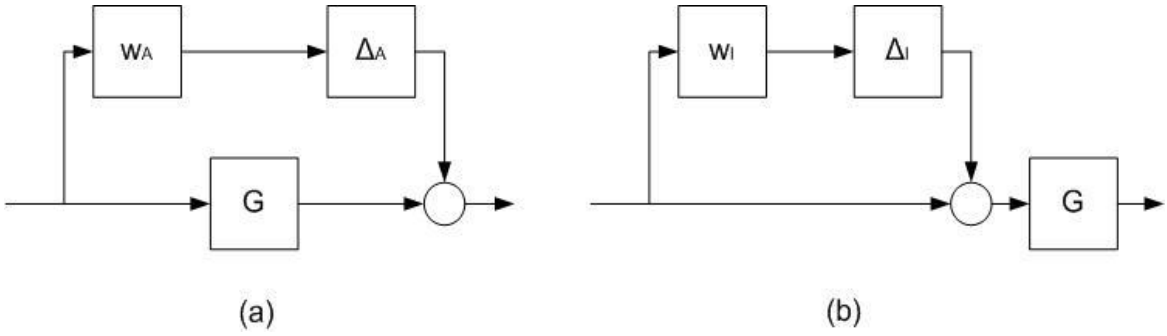

Fig. 4.1. Uncertainty representations:

(a) additive uncertainty (b) multiplicative input uncertainty

4.1.2 General Uncertain System Representation

Consider a feedback control system with input uncertainty as depicted in Figure 4.2 where Δ_I is input multiplicative uncertainty, W_I is a normalized weight for Δ_I, and W_P is performance weight. This feedback loop can be converted into a standard closed loop system with a generalized plant P to allow more flexibility in analysis, depicted in Figure 4.3 [3].

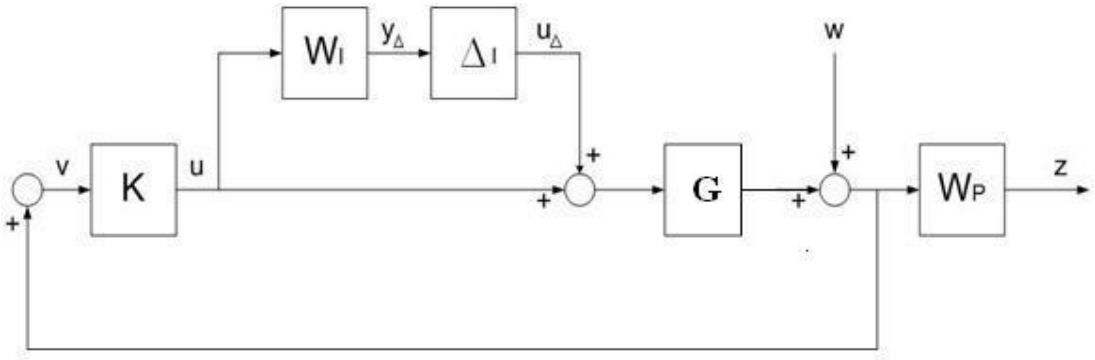

Fig. 4.2. Closed loop configuration of uncertain system.

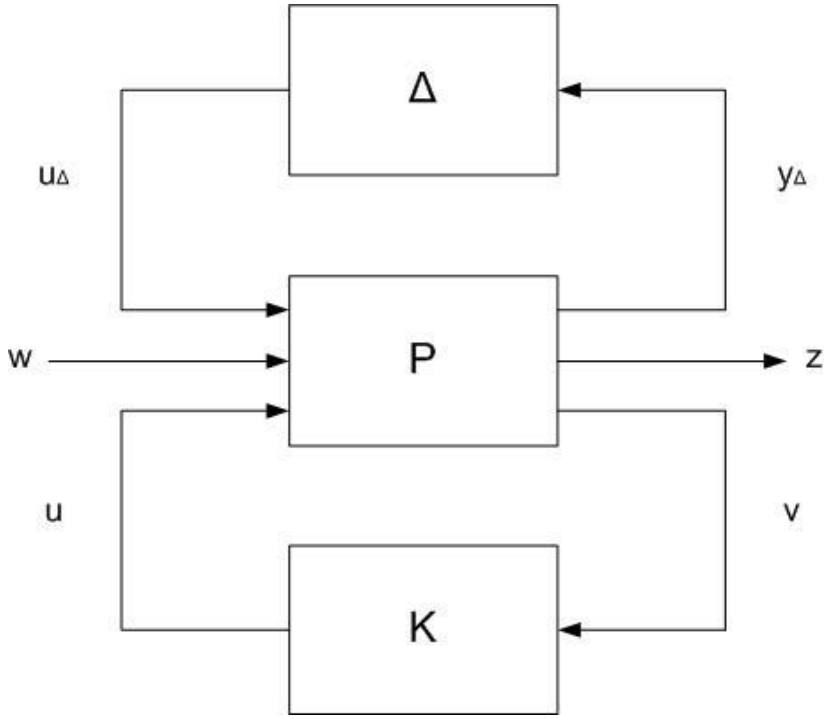

Fig. 4.3. General configuration of uncertain system for controller synthesis.

A suitable representation of generalized plant P can be sought based on the subsystems appearing in Figure 4.3. The closed loop from $[u_\Delta \quad w \quad u]$ to $[y_\Delta \quad z \quad v]$ in Figure 4.3 is determined by:

$$\begin{bmatrix} y_\Delta \\ z \\ v \end{bmatrix} = P \begin{bmatrix} u_\Delta \\ w \\ u \end{bmatrix} = \begin{bmatrix} 0 & 0 & W_I \\ W_P G & W_P & W_P G \\ -G & -I & -G \end{bmatrix} \begin{bmatrix} u_\Delta \\ w \\ u \end{bmatrix} \tag{4.20}$$

where u_Δ is uncertainty output, y_Δ is uncertainty input, w is disturbance input (exogenous input), z is performance output, u is control output, and v is control input. As shown in Equation 4.20, transfer function from u_Δ to y_Δ, upper left elements in P,

is zero since u_Δ has no direct effect on y_Δ except through a controller K. Thus partitioning P to be compatible with K can be simply implemented by:

$$\begin{bmatrix} y_\Delta \\ z \end{bmatrix} = P_{11}\begin{bmatrix} u_\Delta \\ w \end{bmatrix} + P_{12}u,\ v = P_{21}\begin{bmatrix} u_\Delta \\ w \end{bmatrix} + P_{22}u \tag{4.21}$$

$$\begin{aligned} P_{11} &= \begin{bmatrix} 0 & 0 \\ W_P G & W_P \end{bmatrix}, \quad P_{12} = \begin{bmatrix} W_I \\ W_P G \end{bmatrix} \\ P_{21} &= \begin{bmatrix} -G & -I \end{bmatrix}, \quad P_{22} = \mathrm{G} \end{aligned} \tag{4.22}$$

Then the uncertain system representation, called "$N-\Delta$ structure," is constructed in which N is an interconnected system between a generalized plant P and a controller K; Linear Fractional Transformation (LFT) effectively shows this interconnection [76]. Using the system configuration in Figure 4.4, N is simply modified by a lower LFT of P and K [3]:

$$N = F_l(P,K) \equiv P_{11} + P_{12}K(I - P_{22}K)^{-1}P_{21} \tag{4.23}$$

Similarly, the closed loop transfer function from w to z is related to N and Δ by upper LFT:

$$F = F_u(N,\Delta) \equiv N_{22} + N_{21}\Delta(I - N_{11}\Delta)^{-1}N_{12} \tag{4.24}$$

By pulling out the perturbation block and nominal system, the system in Figure 4.4 is rearranged by "$M-\Delta$ structure" of Figure 4.5 where $M = N_{11}$ is the transfer function from the output to the input of the perturbation block Δ. Under this framework, the reader can easily focus on the input-to-output properties of the perturbed system for the robust stability.

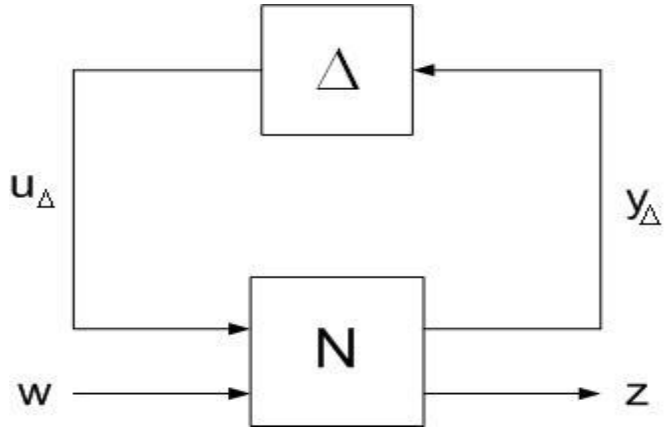

Fig. 4.4. $N-\Delta$ system.

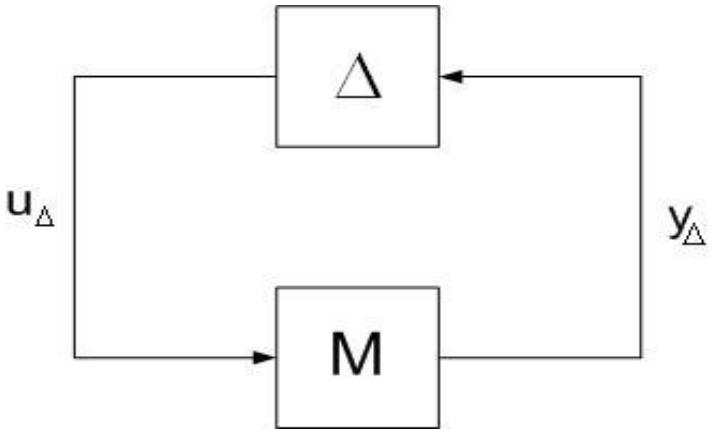

Fig. 4.5. $M-\Delta$ system.

When the state matrix of the system is formed in block-diagonal by a particular state transformation, the stability of the resulting system is guaranteed where preliminary condition, $\|\Delta\|_\infty < 1$, is satisfied. This particular state transformation that ensures block-diagonal system matrix will be demonstrated later in this section.

Furthermore, state space models of each component of the system will be sought for the stability analysis gain-scheduled control framework. The associating state space model of individual components can be derived by:

Controller K:

$$\begin{aligned} \dot{x}_k &= A_k x_k + B_k v \\ u &= C_k x_k + D_k v \end{aligned} \tag{4.25}$$

Plant G:

$$\begin{aligned} \dot{x}_p &= A_p x_p + B_p (u + u_\Delta) \\ y &= C_p x_p \end{aligned} \tag{4.26}$$

Input uncertainty weight function W_I:

$$\begin{aligned} \dot{x}_{W_I} &= A_{W_I} x_{W_I} + B_{W_I} u \\ y_\Delta &= C_{W_I} x_{W_I} \end{aligned} \tag{4.27}$$

Performance weight function W_P:

$$\begin{aligned} \dot{x}_{W_P} &= A_{W_P} x_{W_P} + B_{W_P} v \\ z &= C_{W_P} x_{W_P} \end{aligned} \tag{4.28}$$

Based on these state space models, the $M-\Delta$ system is derived following state space representation from $\begin{bmatrix} u_\Delta & w \end{bmatrix}^T$ to $\begin{bmatrix} y_\Delta & z \end{bmatrix}^T$ where subscripts of the system matrices k, p, w_I are controller, plant, and weight on input uncertainty, respectively. Note that the state matrix of this system is given by a block-diagonal structure constructed by system matrices of controller, plant, and input weight.

$$\begin{bmatrix} \dot{x}_K \\ \dot{x}_P \\ \dot{x}_{W_I} \end{bmatrix} = \underbrace{\begin{bmatrix} A_K & B_K C_P & 0 \\ B_P C_K & A_P + B_P D_K C_P & 0 \\ B_{W_I} C_K & B_{W_I} D_K C_P & A_{W_I} \end{bmatrix}}_{A_M} \begin{bmatrix} x_K \\ x_P \\ x_{W_I} \end{bmatrix} + \underbrace{\begin{bmatrix} 0 & B_K \\ B_P & B_P D_K \\ 0 & B_{W_I} D_K \end{bmatrix}}_{B_M} \begin{bmatrix} u_\Delta \\ w \end{bmatrix}$$
$$\begin{bmatrix} y_\Delta \\ z \end{bmatrix} = \underbrace{\begin{bmatrix} 0 & 0 & C_{W_I} \\ 0 & 0 & 0 \end{bmatrix}}_{C_M} \begin{bmatrix} x_K \\ x_P \\ x_{W_I} \end{bmatrix} \tag{4.29}$$

4.2 Robust Stability Analysis

4.2.1 Robust Stability Description

Before discussing robust stability of the uncertain system, addressing the background of the robust stability and performance could be helpful in understanding the key ideas of this section.

Definition 4.1) [3]

Robust stability analysis: Determines whether the system remains stable for all plants in uncertainty set with a given controller K.

Robust performance analysis: If robust stability is satisfied, determines how large the transfer function from exogenous inputs to outputs may be for all plants in the uncertainty set.

For the $N-\Delta$ system, sufficient conditions for guarantees of the stability and performance can be summarized using Definition 4.1 as follows:

Definition 4.2) [3]

Nominal stability: N is internally stable

Nominal performance: $\|N_{22}\|_\infty < 1$ with satisfying nominal stability

Robust stability: $F = F_u(N,\Delta)$ in Equation 4.24 is stable $\forall\Delta, \|\Delta\|_\infty \le 1$ with satisfying nominal stability

Robust performance: $\|F\|_\infty < 1,\ \forall\Delta, \|\Delta\|_\infty \le 1$ with satisfying robust stability

The primary interest of this section is to guarantee the stability of the perturbed system, thus recall the general system configuration for robust stability analysis that is prepared in Section 4.1. Consider the $N-\Delta$ system for which the transfer function from w to z is given by

$$F = F_u(N,\Delta) \equiv N_{22} + N_{21}\Delta(I - N_{11}\Delta)^{-1}N_{12} \tag{4.30}$$

Supposing that system N is nominally stable and Δ is also assumed to be stable, one can directly see the only possible source of instability is the feedback term $(I - N_{11}\Delta)^{-1}$. Thus when nominal stability is guaranteed, the stability of the $N-\Delta$ system would be equivalent to the stability of the $M-\Delta$ system in Figure 4.5 where $M = N_{11}$.

Seeking the direct method to evaluate stability of the $M-\Delta$ system uses Nyquist stability theorem as follows [3]:

Theorem 4.1) Determinant stability condition for perturbations [3]

Supposing that the nominal system $M(s)$ and the perturbations $\Delta(s)$ are stable and considering the convex set of perturbations Δ, then the $M-\Delta$ system is stable for all allowed perturbations if and only if

- Nyquist plot of $\det(I-M\Delta(s))$ does not encircle the origin , $\forall\Delta$ (4.31)

$\Leftrightarrow$ $\det(I-M\Delta(s))\neq 0$, $\forall w, \forall\Delta$ (4.32)

Proof:

The statement in Equation (4.31) is simply a generalized Nyquist theorem applied to a positive feedback system with a stable loop transfer function $M\Delta(s)$ as the generalized Nyquist theorem is given in Lemma 4.1 [3]:

Lemma 4.1)

The closed loop system with loop transfer function $L(s)$ and negative feedback are stable if, and only if, the Nyquist plot of $\det(I+L(s))$ makes i) n anti-clockwise encirclements of the origin and ii) does not pass through the origin.

Also, a sufficiency of the statement in Equation (4.31) to the form in Equation (4.32) can be proved by statement 2) in Lemma 4.1, “no encirclement of the origin”. For

the necessity, please see Theorem 8.1 in [3]. Using the spectral radius definition, the equivalent theorem will be prepared as follows:

Theorem 4.2) Spectral radius condition for perturbations [3]

Suppose that nominal system $M(s)$ and perturbations $\Delta(s)$ are stable. Considering the convex set of perturbations Δ **,** then the $M-\Delta$ system is stable for all allowed perturbations if, and only if,

$$\rho(M\Delta(jw))<1,\ \ \forall w,\forall\Delta$$

$$\Leftrightarrow \max_{\Delta}\rho(M\Delta(jw))<1,\quad \forall w \tag{4.32}$$

where ρ **(** $\bullet$ **)** is spectral radius, the largest of absolute eigenvalues of system **(** $\bullet$ **)**, $\rho(\bullet)\equiv\max_i|\lambda_i(\bullet)|$.

Proof: See [44] (simply proved by the definition of spectral radius)

Now, considering the special case where the perturbation block $\Delta(s)$ is allowed to be any full complex transfer function matrix satisfying $\|\Delta\|_\infty\le 1$ which is often referred to as unstructured uncertainty. To get a final form of stability theorem, the mathematical relationship between spectral radius (ρ) and eigenvalues (σ) of the system is modified and holds [3]:

$$\max_{\Delta}\rho(M\Delta)=\max_{\Delta}\bar{\sigma}(M\Delta)=\max_{\Delta}\bar{\sigma}(\Delta)\bar{\sigma}(M)=\bar{\sigma}(M) \tag{4.33}$$

Finally, we can conclude the robust stability of the system using Theorem 4.1-2 and Equation 4.29, presented as follows:

Theorem 4.3) Robust stability for perturbations [3]

Supposing that the nominal system $M(s)$ and the perturbations $\Delta(s)$ are stable and considering the convex set of perturbations Δ, then the $M-\Delta$ system is stable for all allowed perturbations if, and only if,

$$\sigma(M(j\omega))<1 \quad \forall\omega \qquad \Leftrightarrow \qquad \|M\|_{\infty}<1 \tag{4.34}$$

Proof: See [3]

4.2.2 LPV-Q System Modification

In this section, the proposed LPV-Q system will be formed in a suitable representation for robust stability. First, $\tilde{T}-Q\Delta$ representation is constructed using $M-\Delta$ system in Figure 4.6. Note that tilde (~) on T represents the difference between system T constructed in Section 3.4. Figure 4.6 shows a general configuration of the LPV-Q system with uncertainty and Figure 4.7 depicts the $\tilde{T}-Q\Delta$ representation. Note that the controller in the LQN closed loop system can simply be decomposed into an interconnection system J_k and Youla system Q. Referring to Figure 4.7, the transfer function $\tilde{T}$, from $\begin{bmatrix}u_\Delta & s\end{bmatrix}^T$ to $\begin{bmatrix}y_\Delta & r\end{bmatrix}^T$, is constructed by interconnecting plant P with system J_k [30]:

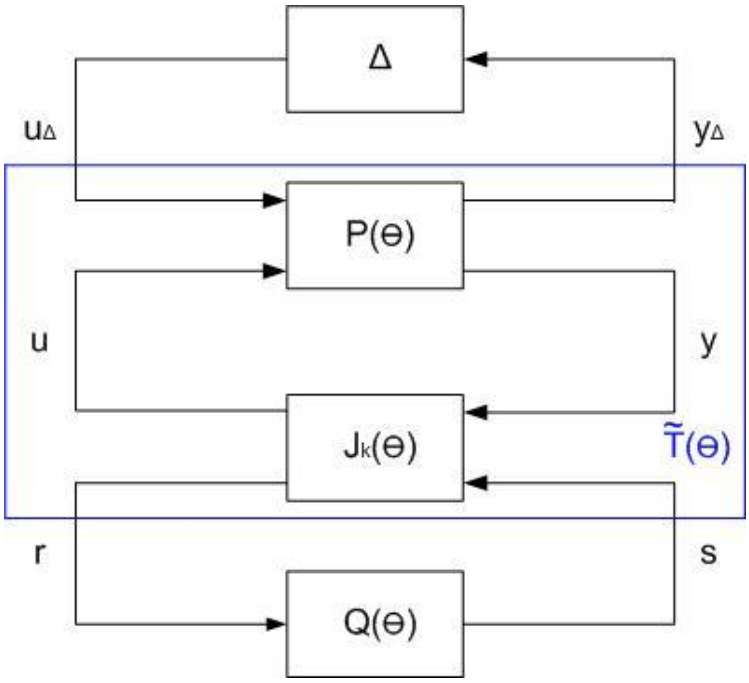

Fig. 4.6. Closed loop of perturbed system for all stabilizing controllers.

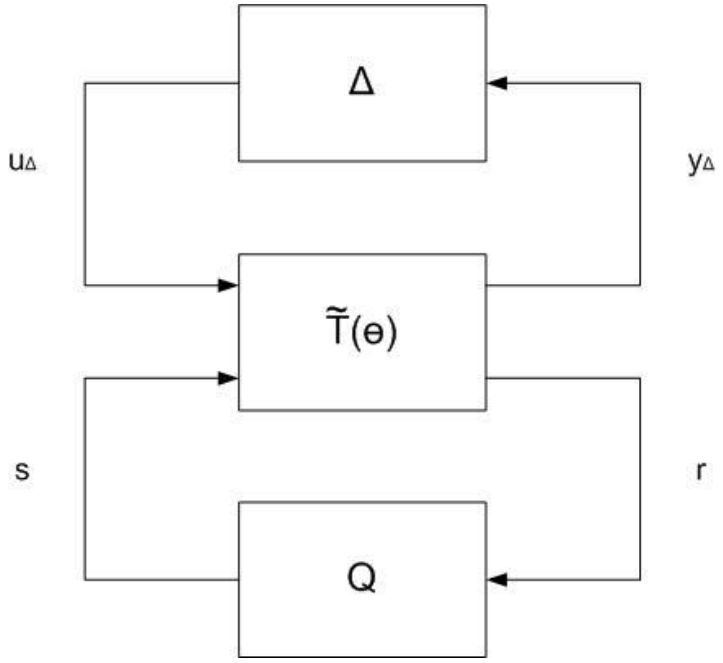

Fig. 4.7. $\tilde{T} - Q\,\Delta$ system.

$$\begin{bmatrix} y_\Delta \\ y \end{bmatrix} = \begin{bmatrix} P_{11} & P_{12} \\ P_{21} & P_{22} \end{bmatrix} \begin{bmatrix} u_\Delta \\ u \end{bmatrix} = \begin{bmatrix} P_{11} & P_{12} \\ P_{21} & G \end{bmatrix} \begin{bmatrix} u_\Delta \\ u \end{bmatrix} \tag{4.35}$$

$$\begin{bmatrix} u \\ r \end{bmatrix} = \begin{bmatrix} J_{K,11} & J_{K,12} \\ J_{K,21} & J_{K,22} \end{bmatrix} \begin{bmatrix} y \\ s \end{bmatrix} = \begin{bmatrix} K & \tilde{V}^{-1} \\ V^{-1} & -V^{-1}N \end{bmatrix} \begin{bmatrix} y \\ s \end{bmatrix} \tag{4.36}$$
$$s = Qr$$

Then the variable u and y can be eliminated using the coprime factorization of the plant $G = \tilde{M}^{-1}\tilde{N}$ and controller $K = \tilde{V}^{-1}\tilde{U}$. The useful coprime factorization of interconnected system that simplifies the system representation can be derived using the double Bezout identities given by [30]:

$$(I - J_{11}P_{22})^{-1} = (I - \tilde{V}^{-1}\tilde{U}NM^{-1})^{-1} = M\tilde{V} \tag{4.37}$$

Using Equation 4.37, the resulting state space representation of system $\tilde{T}$ can be derived as [30]:

$$\begin{bmatrix} y_\Delta \\ r \end{bmatrix} = \begin{bmatrix} \tilde{T}_{11} & \tilde{T}_{12} \\ \tilde{T}_{21} & \tilde{T}_{22} \end{bmatrix} \begin{bmatrix} u_\Delta \\ s \end{bmatrix} = \begin{bmatrix} P_{11} + P_{12}U\tilde{M}P_{21} & P_{12}M \\ \tilde{M}P_{21} & 0 \end{bmatrix} \begin{bmatrix} u_\Delta \\ s \end{bmatrix} \tag{4.38}$$

In Equation 4.38, $\tilde{T}_{22}$ is always zero under any choice of plant and controller representation. Using this result, the closed loop transfer function from u_Δ to y_Δ is given by:

$$y_\Delta = F_Q u_\Delta = (\tilde{T}_{11} + \tilde{T}_{12}Q\tilde{T}_{21})u_\Delta \tag{4.39}$$

Note that this closed loop representation allows the convex optimization of Q by minimizing disturbance responses where $\tilde{T}$, Q, and F_Q are Hurwitz. Also, the affine characteristic of the F_Q system in Youla parameter Q enables feasibility in computation.

4.2.3 LPV-Q Closed Loop System

The reader knows that the transfer function F_Q could be a direct indicator of robust stability of the closed loop system. In the LPV-Q system, transfer function F_Q is determined by plugging general coprime factors of subsystems, J_k, Q, and $\tilde{T}$ (Equation 4.40.-44) that can be defined using Youla parameterization into F_Q.

$$J_K(\theta) = \left[\begin{array}{c|cc} A_p(\theta)+B_p(\theta)F_p(\theta) & 0 & B_p(\theta) \\ \hline F_p(\theta)-D_K(\theta)C_p(\theta) & D_K(\theta) & I \\ C_p(\theta) & I & 0 \end{array}\right] \tag{4.40}$$

$$Q(\theta_i) = \left[\begin{array}{ccc|c} A_P(\theta_i)+B_P(\theta_i)D_K(\theta_i)C_P(\theta_i) & B_P(\theta_i)C_K(\theta_i) & -B_P(\theta_i)C_K(\theta_i) & 0 \\ B_K(\theta_i)C_P(\theta_i) & A_K(\theta_i) & B_K(\theta_i)F_K(\theta_i) & B_K(\theta_i) \\ 0 & 0 & A_K(\theta_i)+B_K(\theta_i)F_K(\theta_i) & B_K(\theta_i) \\ \hline D_K(\theta_i)C_P(\theta_i)-F_P(\theta_i) & C_K(\theta_i) & -C_K(\theta_i) & 0 \end{array}\right] \tag{4.41}$$

$$\tilde{T}_{11}(\theta) = P_{11}(\theta) + P_{12}(\theta)U\tilde{M}P_{21}(\theta)$$

$$= \left[\begin{array}{ccc|c} A_k(\theta)+B_k(\theta)F_k(\theta) & B_k(\theta)C_p(\theta) & -B_k(\theta)F_k(\theta) & B_k(\theta) \\ 0 & A_p(\theta)+B_p(\theta)D_k(\theta)C_p(\theta) & B_p(\theta)C_k(\theta) & B_p(\theta)D_k(\theta) \\ 0 & B_k(\theta)C_p(\theta) & A_k(\theta) & B_k(\theta) \\ \hline F_k(\theta) & C_p(\theta) & -F_k(\theta) & 0 \end{array}\right] \tag{4.42}$$

$$\tilde{T}_{12}(\theta) = P_{12}(\theta)M(\theta) = \left[\begin{array}{c|c} A_p(\theta)+B_p(\theta)F_p(\theta) & B_p(\theta) \\ F_p(\theta) & I \\ \hline C_p(\theta) & 0 \end{array}\right] \tag{4.43}$$

$$\tilde{T}_{21}(\theta) = \tilde{M}(\theta)P_{21}(\theta)$$

$$= \left[\begin{array}{cc|cc} A_p(\theta)+B_p(\theta)D_k(\theta)C_p(\theta) & B_p(\theta)C_k(\theta) & -B_p(\theta) & B_p(\theta)D_k(\theta) \\ B_k(\theta)C_p(\theta) & A_k(\theta) & 0 & B_k(\theta) \\ \hline C_p(\theta) & F_k(\theta) & 0 & I \end{array}\right] \tag{4.44}$$

For nominal controller, a doubly coprime factorization satisfying the Bezout identities for the LPV plant and static output feedback LPV controller $K_0(\theta)$ can be constructed as:

$$\begin{bmatrix} M(\theta) & U_0(\theta) \\ N(\theta) & V_0(\theta) \end{bmatrix} = \left[\begin{array}{c|cc} A_p(\theta)+B_p(\theta)F_p(\theta) & B_p(\theta) & 0 \\ F_p(\theta) & I & D_{k0}(\theta) \\ \hline C_p(\theta) & 0 & I \end{array}\right] \tag{4.45}$$

$$\begin{bmatrix} \tilde{V}_0(\theta) & -\tilde{U}_0(\theta) \\ -\tilde{N}(\theta) & \tilde{M}(\theta) \end{bmatrix} = \left[\begin{array}{c|cc} A_p(\theta)+B_p(\theta)D_{k0}(\theta)C_p(\theta) & -B_p(\theta) & B_p(\theta)D_{k0}(\theta) \\ F_p(\theta)-D_{k0}(\theta)C_p(\theta) & I & D_{k0}(\theta) \\ \hline C_p(\theta) & 0 & I \end{array}\right] \tag{4.46}$$

4.3 Robust Stability of LPV-Q System

4.3.1 LMI-Based Robust Stability

Theorem 4.3 describes a necessary and sufficient condition so that the nonlinear system is robustly stable. This is a well-known criterion that evaluates the closed loop stability of the system according to the H_∞ performance of a given system in that it requires a less conservative assumption and enables simple analysis [91] [92]. Consider the $\tilde{T} - Q\,\Delta$ structure of the proposed LPV-Q system. By applying the theorem 4.3 to the $\tilde{T} - Q\,\Delta$ system, a revised version of necessary and sufficient condition for the robust stability of the LPV-Q system is given by Theorem 4.4.

Theorem 4.4) Robust stability of perturbed systems [63]

Suppose that the system $\tilde{T}(s)$ and the perturbations $\Delta(s)$ are stable with stable $Q(s)$. Let Δ be convex set of perturbations, then the LPV/LQN system is guaranteed to be robustly stable for all perturbations Δ satisfying $\|\Delta\|_\infty < 1$ if, and only if,

$$\left\|F_Q\right\|_\infty < 1 \tag{4.47}$$

Proof: See [63]

It is interesting to note that the closed loop transfer function $F_Q(=\tilde{T}_{11}+\tilde{T}_{12}Q\tilde{T}_{21})$ is affine in Youla system Q that allows the convex optimization in performance evaluation. Often norm-based performance of the system is calculated using Linear Matrix Inequality (LMI) techniques that alleviate the complexity in computation [74]. The LMI form of the H_∞ performance and its Schur complement of the closed loop system are given as:

$$A_{F_Q}{}^T P + PA_{F_Q} + C_{F_Q}{}^T C_{F_Q} + \frac{1}{\gamma^2} PB_{F_Q} B_{F_Q}{}^T P < 0 \tag{4.48}$$

$$\begin{bmatrix} A_{F_Q}{}^T P + PA_{F_Q} + C_{F_Q}{}^T C_{F_Q} & PB_{F_Q} \\ B_{F_Q}{}^T P & -\gamma^2 I \end{bmatrix} < 0 \tag{4.49}$$

Note that the Schur complement has been widely used in analytical studies because of computational flexibility. The alternative formula adapted to LMI toolbox in Matlab is given by [93]:

$$\begin{pmatrix} I & 0 \\ A_{F_Q} & B_{F_Q} \\ 0 & I \\ C_{F_Q} & 0 \end{pmatrix}^T \begin{pmatrix} 0 & P & 0 & 0 \\ P & 0 & 0 & 0 \\ 0 & 0 & -\gamma I & 0 \\ 0 & 0 & 0 & \frac{1}{\gamma} I \end{pmatrix} \begin{pmatrix} I & 0 \\ A_{F_Q} & B_{F_Q} \\ 0 & I \\ C_{F_Q} & 0 \end{pmatrix} < 0 \tag{4.50}$$

In the gain-scheduling paradigm, the desired level of stability is easily guaranteed at local operating points, but guarantees of the stability over the entire operating envelop is much more difficult to achieve. However, even though the quadratic Lyapunov function P can be found at each local operating point so that the H_∞ norm, i.e., L_2 gain, of the system remains within a desired bound, finding a

common quadratic Lyapunov function (CQLF) to guarantee global stability is still a challenging problem [93].

4.3.2 Robust Stability via Optimizing Coprime Factors

In Section 4.3.1, we know that robust stability of the system is globally guaranteed by the existence of CQLF so that the L_2 gain of the system remains within a desired bound over operating envelopes. To guarantee the global stability of the LPV-Q system, consider $\tilde{T} - Q\Delta$ representative of the system and find the degree of freedom included in the closed loop transfer function F_Q. The subsystems $\tilde{T}_{11}$, $\tilde{T}_{12}$, and $\tilde{T}_{21}$ consist of system matrices and associating feedback gains of plant and controller so that $A_P + B_P F_P$ and $A_K + B_K F_K$ are Hurwitz (Equation 4.41-44). It is interestingly note that $\tilde{T}_{11}$ and $\tilde{T}_{21}$ merely include the feedback gain of controller F_k and $\tilde{T}_{12}$ includes the feedback gain of plant, F_p.

By virtue of gain-scheduling, the choice of feedback gains of plant and controller would be an additional freedom where they merely meet the restriction so that the state matrices of the state feedback system are Hurwitz. Also, the reader can find the particular relationships between those feedback gains and subsystem matrices by carefully noting that subsystems T_{11} and T_{21} include only F_P while F_K merely appears in T_{12}. Thus finding the optimal subsystem is implemented through optimizing feedback gains in sub systems that minimize the H_∞ norm to guarantee global stability and performance. Alternatively, guaranteeing the closed loop stability of the system is

achieved through retaining the H_∞ norm globally within specific bounds and also minimizing the difference between L_2 gains calculated locally and globally.

4.3.3 Case Study: Robust Stability on Gain Scheduled Control System

In Section 4.3.2, we know that robust stability of the LPV-Q system is globally guaranteed by the optimal choices of coprime factors of Youla system. In essence, choice of coprime factors is design degree of freedom but significantly affects stability and performance of the system as illustrated in Section 3.2. This section illustrates a simple example of robust stability of the Youla based gain-scheduled control system.

To find the optimal feedback gains of plant model and controller F_P and F_K, we employ the LQR technique. By virtue of state feedback control, LQR control provides optimal gain matrices F_P and F_K by minimizing cost function included Q and R thus choice of these weighting matrices would be an additional freedom where they merely are positive-definite.

Equations 4.51-52 present state-space forms of LPV plant model at controller design points and state-space forms of two LQR controllers with integrators are given in Equations 4.53-54, respectively. Note that plant models are defined as LPV way, $P(\theta) = P_i$ at $\theta=\theta_i$, $i = 1,2$, so that each plant model shares the states.

$$\begin{aligned} \dot{x} &= \begin{bmatrix} -0.2499 & -0.1055 \\ -0.1520 & -0.2134 \end{bmatrix} x + \begin{bmatrix} -0.0275 & -0.0171 \\ -0.0129 & -0.0316 \end{bmatrix} u \\ y &= \begin{bmatrix} 1 & 0 \\ 0 & 1 \end{bmatrix} x \end{aligned} \tag{4.51}$$

$$\dot{x} = \begin{bmatrix} -0.1815 & -0.0274 \\ -0.0979 & -0.1246 \end{bmatrix} x + \begin{bmatrix} -0.0194 & -0.0050 \\ -0.0030 & -0.0192 \end{bmatrix} u$$
$$y = \begin{bmatrix} 1 & 0 \\ 0 & 1 \end{bmatrix} x \tag{4.52}$$

$$\dot{x} = \begin{bmatrix} 0 & 0 \\ 0 & 0 \end{bmatrix} x + \begin{bmatrix} 1 & 0 \\ 0 & 1 \end{bmatrix} u$$
$$y = \begin{bmatrix} 0.9942 & -0.1077 \\ 0.1077 & 0.9942 \end{bmatrix} x + \begin{bmatrix} 6.592 & -0.4746 \\ 0.4195 & 6.223 \end{bmatrix} u \tag{4.53}$$

$$\dot{x} = \begin{bmatrix} 0 & 0 \\ 0 & 0 \end{bmatrix} x + \begin{bmatrix} 1 & 0 \\ 0 & 1 \end{bmatrix} u$$
$$y = \begin{bmatrix} 0.9924 & -0.1229 \\ 0.1229 & 0.9924 \end{bmatrix} x + \begin{bmatrix} 6.539 & -1.502 \\ 0.5627 & 8.565 \end{bmatrix} u \tag{4.54}$$

Table 4.1 Performance bounds on LPV-Q system.

	$\left\|F_Q(s)\right\|_{L_2 \to L_2}$
Fixed at θ_1	0.6029
Fixed at θ_2	0.4799
$LPV(\theta)$	0.6032

Table 4.1 indicates H_∞ performance bounds on LPV-Q closed loop system. First, we examine the performance bounds of LPV-Q system at controller design points. Before optimizing coprime factors, we initially guessed reasonable values of Q and R matrices in LQR control design.

$$Q_{K,P} = \begin{bmatrix} 1 & 0 \\ 0 & 1 \end{bmatrix} \text{ and } R_{K,P} = \begin{bmatrix} 1 & 0 \\ 0 & 1 \end{bmatrix} \tag{4.55}$$

Then we optimized coprime factors such that H_∞ norm of the system is minimized.

As given in Table 4.1, LPV-Q closed loop system is robustly stable at design points since H_∞ norm of the system is less than one where $\|\Delta\|_\infty < 1$ satisfies. Furthermore, the reader can recognize that H_∞ norm of the system remains within acceptable bounds over operating envelope. Thus we can conclude that LPV-Q system is guaranteed to be robustly stable with optimal choice of coprime factors. Note that norm bound using initially guessed values is 2.5743 which remains out of desired bound.

5. MULTI EVAPORATOR VAPOR COMPRESSION SYSTEM CONTROL

Gain-scheduled control is known to be a powerful solution for nonlinear systems that are highly nonlinear and vary arbitrarily fast in a wide range of operating regions. In this section, the efficacy of the proposed controller interpolation method is demonstrated in experimentation using a multi-evaporator vapor compression system. The dynamics of the vapor compression system are highly nonlinear but gain-scheduled control has the potential to achieve the desired stability and performance of the system. Clearly, this section demonstrates the experimental study of gain-scheduled control as applied to a multi-evaporator vapor compression system, while the thermal efficiency and cooling capacity of the system are subsequently improving.

5.1 Introduction

Vapor compression systems have been widely used for various residential and industrial purposes. A huge amount of energy is consumed for air conditioning, becoming one of the largest sources of energy consumption in the world [70]. Thus the thermal efficiency of these systems is a key aspect in energy saving since the energy demand for air conditioning systems will be reduced by achieving desired energy efficiency of vapor compression systems, via developing accurate system model and advanced control strategies. Energy saving air conditioning systems have significant effects on the economy as well as the environment. This situation has been widely studied for many years [71].

Unfortunately, the dynamics of this system are known to be highly nonlinear and also vary arbitrarily fast over the operating envelopes. Although a very strictly designed controller could possibly stabilize the system, significant performance would be sacrificed. To guarantee desired global stability, an advanced gain-scheduled control approach can be an intuitive solution for this problem [5].

In this section, the proposed gain-scheduled control strategy will be applied to a vapor compression system to achieve the desired energy efficiency. The efficacy of the proposed controller interpolation method will be demonstrated in experimental studies on multi-evaporator vapor compression system.

5.2 Vapor Compression Cycle

To build an advanced control framework for vapor compression systems, an in-depth understanding of the characteristics of these systems would be helpful. Consider a standard air conditioning system operating on a vapor compression cycle. As shown in Figure 5.1, a standard vapor compression system consists of four components - compressor, condenser, expansion device, and evaporator [72]. Assume that refrigerant steadily circulates through each of components in the cycle. First, the refrigerant enters the evaporator as a two-phase liquid-vapor mixture at a lower pressure. In the evaporator, some of the refrigerant changes phase from liquid to vapor as a result of heat transfer from the region of low temperature to the refrigerant then exits as a superheated vapor at a lower pressure.

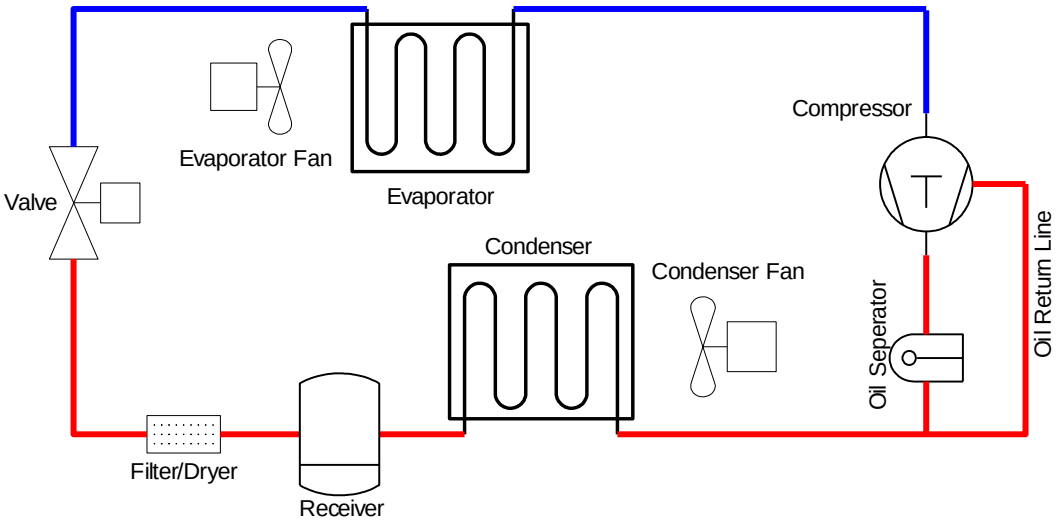

Fig. 5.1. Vapor compression system.

Then the refrigerant is compressed to a high pressure by the compressor. During compression, the temperature of the refrigerant goes up to a temperature that is higher than ambient temperature. Next, the refrigerant passes from the compressor into the condenser where it changes phase from a saturated vapor to a saturated liquid as a result of the heat transfer to a region of high temperature and, then exits the condenser as a subcooled liquid at a higher pressure. However, the refrigerant at a two-phase flow may result in a choked flow problem thus a receiver is placed at the exit of condenser to avoid the two-phase refrigerant [72].

The refrigerant returns to the inlet of the evaporator by expanding through the expansion device. In this process, the temperature goes down from a high to low temperature and there is a drop in pressure. The $P-h$ diagram of each of the vapor compression processes is shown in Figure 5.2.

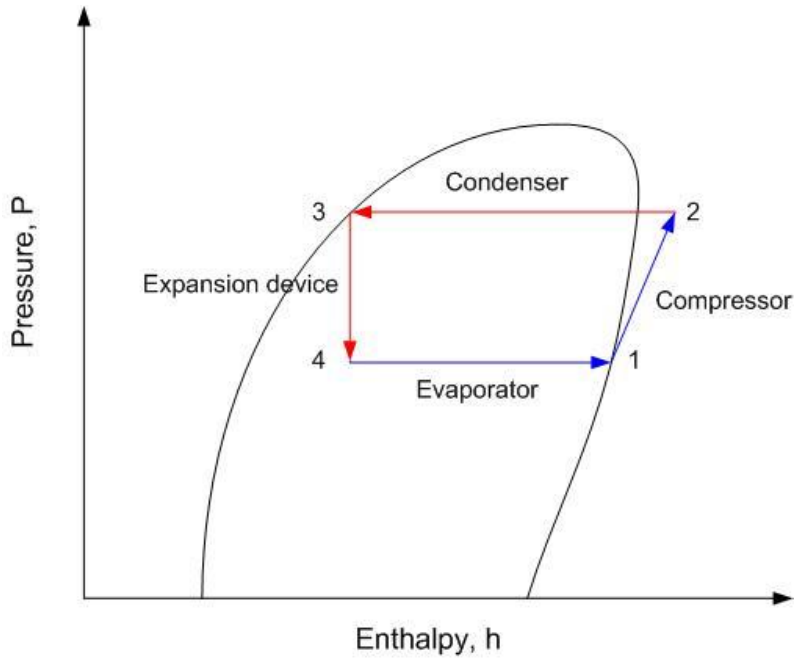

Fig. 5.2. $P-h$ diagram of vapor compression cycle.

The characteristics of vapor compression systems are affected by the thermodynamic states of refrigerant at various components in the vapor compression cycle such as evaporator pressure, condenser pressure, and evaporator superheat temperature. To evaluate the system's efficiency, key thermodynamic properties, i.e., cooling capacity (refrigerant capacity) and coefficient of performance (COP), are commonly used. The former is modulated as a desired cooling requirement while the latter is regulated to be maximized for energy saving [94], [95].

Cooling capacity is defined as the amount of heat transferred from the refrigerant region resulting in the vaporization of the refrigerant [72]. As refrigerant passes through the evaporator, the mass and energy balance are reduced to give the heat transfer rate per unit mass of refrigerant flow where $\dot{m}$ is the mass flow rate of the refrigerant, and h_4

and h_1 are the enthalpy at evaporator inlet and outlet, respectively. In Equation 5.1, heat transfer rate $\dot{Q}_{in}$ refers to cooling capacity, normally expressed in kW.

$$\frac{\dot{Q}_{in}}{\dot{m}} = h_1 - h_4 \tag{5.1}$$

Cooling efficiency or COP indicates the efficiency of the vapor compression system. For the Carnot system, COP is simply given as:

$$COP_C = \frac{T_{low}}{T_{high} - T_{low}} \tag{5.2}$$

However, the Carnot vapor compression cycle is an ideal thermodynamic cycle, generated under conservative theoretical assumptions and cannot be realized in real systems. Thus the COP of the real vapor compression system at steady-state can be presented as [72]:

$$COP_R = \frac{h_1 - h_4}{h_2 - h_1} \tag{5.3}$$

Note that the enthalpy at the evaporator outlet plays a significant role in cooling capacity. The COP of real systems and maximum thermal efficiency can be achieved via minimal evaporator superheat, i.e., maximizing the two-phase region of the evaporator, since heat transferred from the cold temperature region to liquid refrigerant is much higher than when transferred to vapor refrigerant. However, liquid refrigerant may result in the failure of the compressor, thus improving the cooling capacity. The COP of the vapor compression system should be achieved by optimal choice of evaporator superheat temperature.

Four components of the vapor compression system can be categorized into two classes – heat exchanger and actuator. The evaporator and condenser function as heat exchangers in that they add (remove) heat from (to) the ambient region, respectively, while the compressor and expansion valves function as actuators. In heat exchangers, heat is removed from the refrigerant as it flows at a constant pressure through the condenser and heat is transferred into the refrigerant as it flows at constant pressure through the evaporator. The two principle actuators, expansion valve and compressor, modulate the mass flow rate of the system at each state. The change of mass flow rate results in the change of operating pressures and the resulting two-phase and superheat region in heat exchangers that directly affect the cooling of the system. Among various expansion devices, an electronic expansion valve (EEV) has been widely used since a stepping motor is used to open or close the valve by control action that can be directly applied to voltage signal of motor [96], [97].

Multi-evaporator vapor compression systems whose evaporators serve different cooling zone, has been used in this dissertation, depicted in Figure 5.3, and $P-h$ diagram of the system is presented in Figure 5.4. Typically, a static discharge valve (SDR) is installed on the secondary evaporator to regulate a pressure difference between evaporators; thus each evaporator provides individually cooling under different operating conditions [71]. More details on this strategy will be addressed later in Section 5.4.

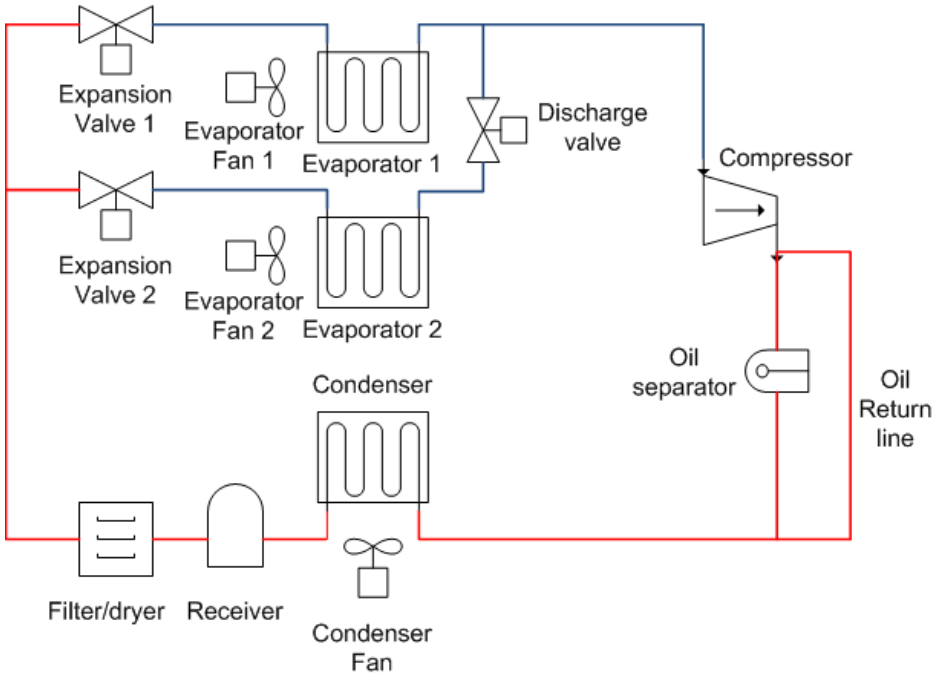

Fig. 5.3. Multi-evpaorator vapor compression system.

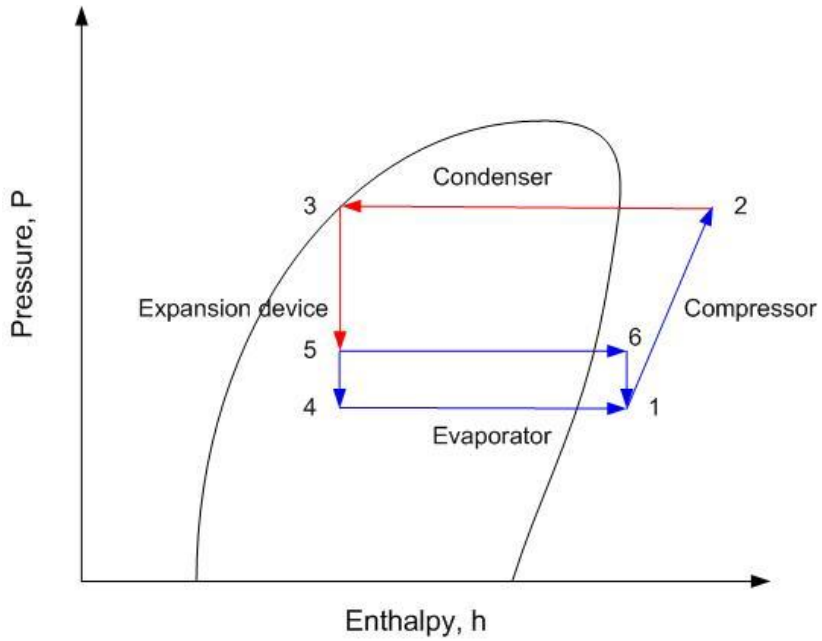

Fig. 5.4. $P-h$ diagram of two-evaporator vapor compression system.

5.3 Vapor Compression System Control

5.3.1 Experimental Vapor Compression System

The experimental vapor compression system for the research presented in this dissertation is two-evaporator water chiller system. This system has been built in Thermo-Fluids Control Laboratory for research of model validation, control design, and fault detection. The primary (refrigerant) system consists of four components of vapor compression system – compressor, condenser, expansion valve, and two evaporators – and the secondary (water) system is constructed to circulate water. Figures 5.5-5.7 present primary and secondary loop of the system, and experimental system respectively. Note that two evaporators serve different cooling zones since static discharge valve has been installed at the outlet of second evaporator, regulating evaporator pressure individually. The reader can find more detail about the system in [71].

5.3.2 Control Aspects in Vapor Compression System

Thermal efficiency of vapor compression systems would have a notable effect on energy savings in both industrial and residential air conditioning systems, but primary interests in control paradigms depend on the class of system operation [5]. For residential purposes, a prompt response in the start-up process has the potential to reduce energy consumption and automotive air-conditioning systems rarely operate at steady state conditions since the driving and external conditions are continuously changed [4].

In both cases, air conditioning systems operate in transient but these transients are different.

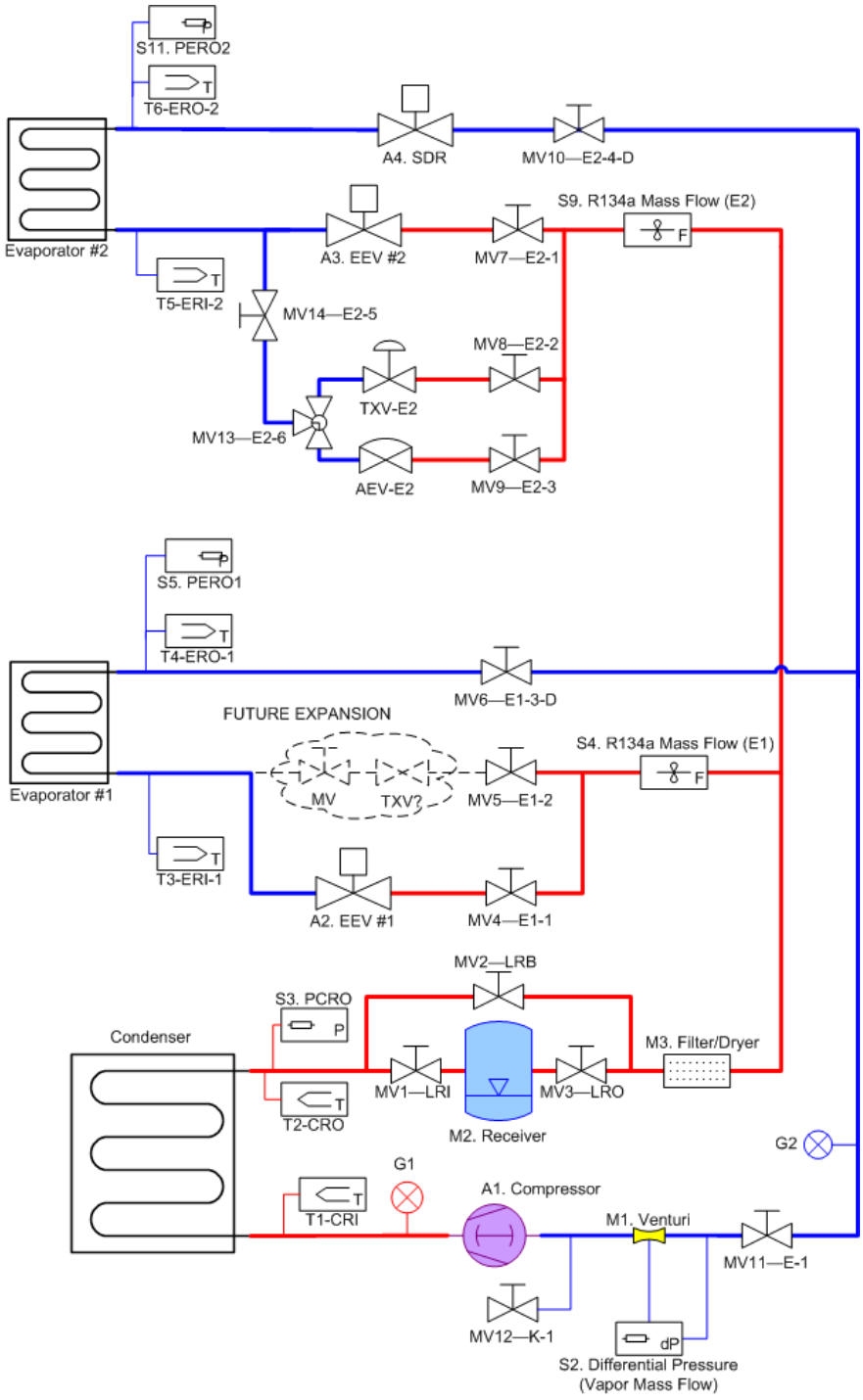

Fig. 5.5. Primary (refrigerant) loop of experimental vapor compression system.

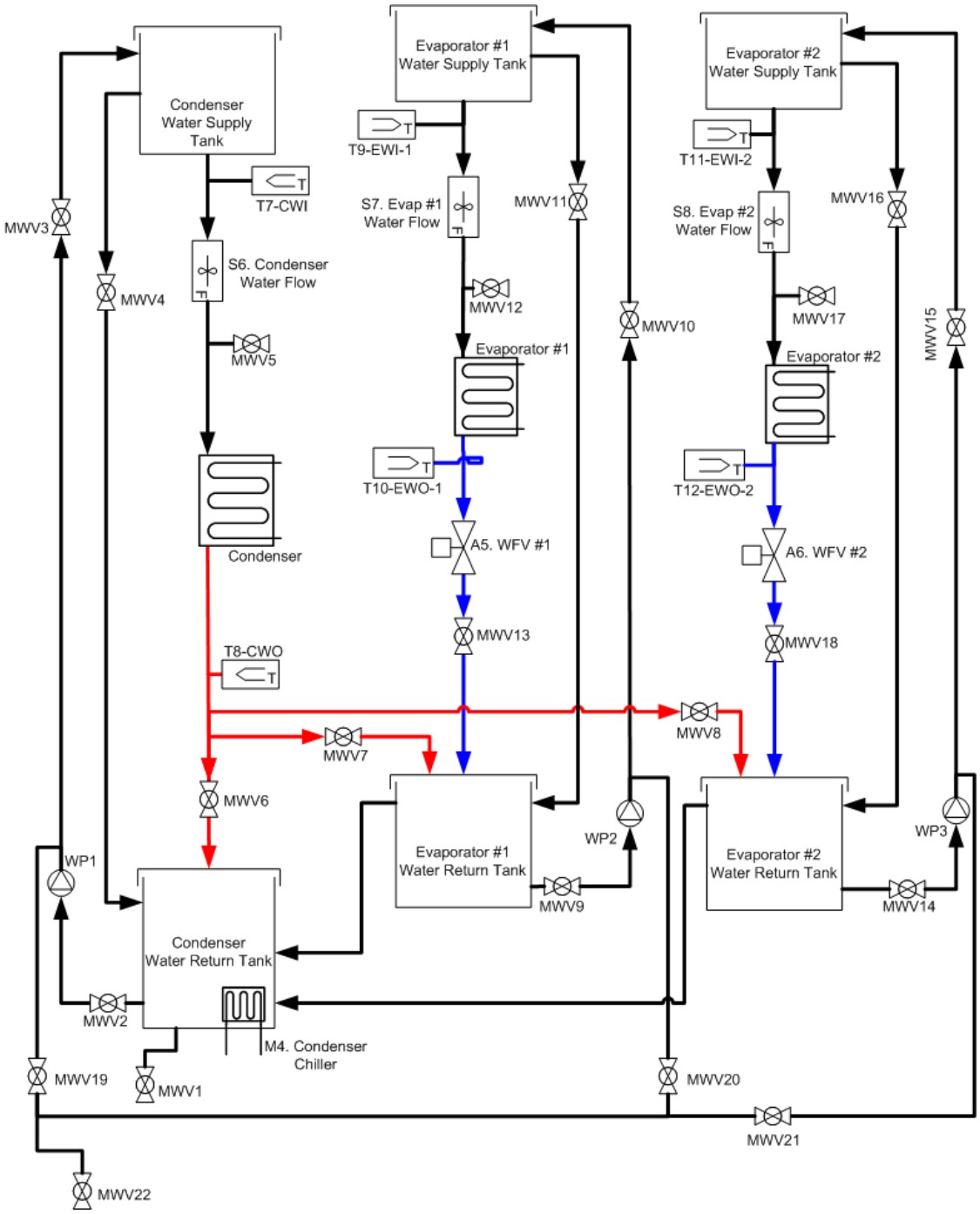

Fig. 5.6. Secondary (water) loop of experimental vapor compression system.

Fig. 5.7. Experimental vapor compression system.

5.3.3 Control of Vapor Compression System

As mentioned in Section 5.1, thermal efficiency of vapor compression systems would have a notable effect on energy savings in both industrial and residential air conditioning systems, but primary interests in control paradigms depend on the class of system operation [5]. For residential purposes, a prompt response in the start-up process has the potential to reduce energy consumption and automotive air-conditioning systems rarely operate at steady state conditions since the driving and external conditions are continuously changed [4]. In both cases, air conditioning systems operate in transient but these transients are different.

To improve thermal efficiency of the system while maximizing the cooling effect, the portion of two-phase flow in the evaporator needs to be maximized since the amount of heat transferred between liquid and evaporator walls is much higher than the amount of heat transferred between vapor and evaporator walls. Furthermore, the two-phase portion of the evaporator enhances the cooling capacity of the system. However to operate the compressor safely, the fluid entering the compressor must be completely vaporized so the placement of the receiver at the evaporator exit can ensure safe operation of the compressor while maximizing the evaporator's performance. In essence, evaporator superheat and cooling capacity of the system are control objectives in this section.

Among various control strategies, a simple on/off control or classical single-input-single-output (SISO) control method has been widely used both in industrial and residential air conditioning systems. However, the on/off control significantly diminishes

system efficiency due to larger power consumption at start-up. Furthermore, classical methods in vapor compression system controls generally employ multiple SISO loops where superheat and cooling capacity are modulated by expansion valve opening and compressor speed respectively, i.e., superheat is regulated by using the expansion valve and cooling is regulated by the compressor. However, performance of the superheat regulation has been limited due to the difficulty in tuning the feedback gains under SISO control strategies. It has been shown that there are strong cross-coupling effects between superheat and compressor speed thus a proper coordination between expansion valve opening and compressor speed using MIMO control strategy can improve the superheat regulation of the system. Furthermore, not only superheat, but other essential cycle variables including evaporating pressure and condensing pressure can be properly regulated through the coordination of these actuators [4].

Typically, evaporator superheat is modulated by opening the expansion valve but may often result in unexpected oscillations in the amount of superheated vapor at the evaporator exit, often observed in practice. This phenomenon, called “valve-hunting,” is usually solved by adjusting the valve parameters and resulting in decreased performance [5]. Using multivariable control schemes, these fluctuations could be avoided while allowing the system to function at more efficient operating levels.

To modulate the cooling capacity supplied from the evaporator, evaporator temperature has been commonly used as control input in classical control of vapor compression systems. Alternatively, evaporator pressure can be employed since it is closely related to the evaporator saturation temperature. The associating enthalpy at

evaporator inlet/outlet in cooling calculation is a function of both evaporator pressure and temperature which affect subsequent cooling capacity. Furthermore, pressure response is much faster than temperature response, increasing the bandwidth of the output sensing [71].

Thus multivariable control paradigms have been developed to achieve multiple objectives, i.e., maximizing thermal efficiency with desired cooling capacity, through the cross-coupling effect between superheat regulation and compressor speed. This dissertation demonstrates the effectiveness of advanced MIMO coordination-based control strategies in both simulation and experiment.

5.3.4 MIMO Control of Vapor Compression Systems

In Section 5.3.2, the shortcomings of classical SISO control in vapor compression system are addressed to stimulate the development of a MIMO control strategy to prevent the cross-coupling of two actuators, expansion valve and compressor. Furthermore, to match the thermal load (cooling capacity) with thermal efficiency (superheat) requires an MIMO control system that meets multiple control objectives.

Typically, a vapor compression system has various controllable inputs for feedback control: electronic expansion valve (EEV) opening, compressor speed, condenser fan speed, and water flow valve opening. The fan speed of the evaporator and condenser affect the amount of heat transferred across the evaporator and condenser, respectively, but compared to EEV and the compressor, these effects on superheat and

cooling capacity are not as significant and will not be considered as control inputs in this dissertation.

A general MIMO feedback control system is built to achieve the proper superheat regulation as well as match the load of cooling capacity, depicted in Figure 5.8, where Q is cooling capacity [kW] and T_{SH} is superheat temperature of the evaporator [℃]. The controller in Figure 5.8 regulates compressor speed [rpm] and the electronic expansion valve (EEV) opening [%] with respect to the difference between reference and current values of cooling capacity and superheat in the evaporator. Constructing the cascade expansion valve-compressor control strategy will follow in the next section.

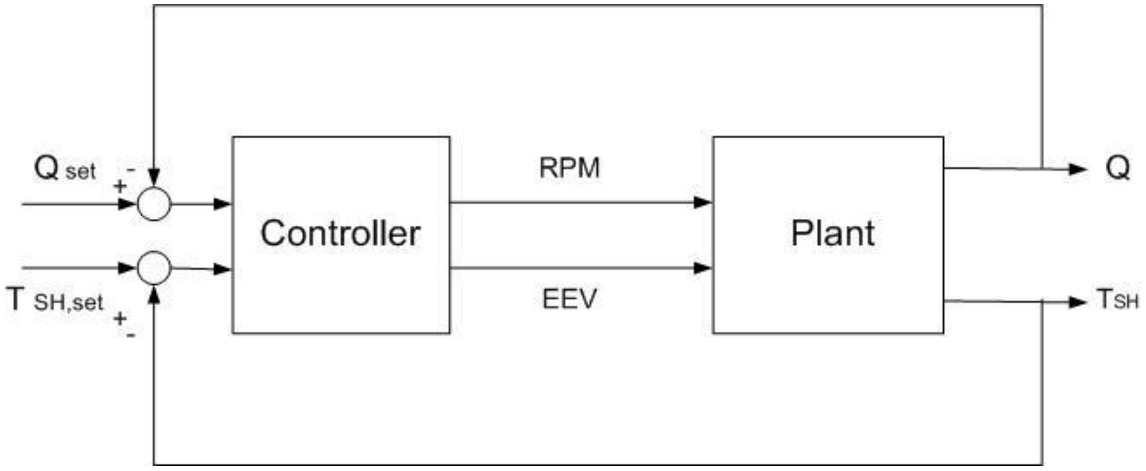

Fig. 5.8. MIMO control of vapor compression system.

5.3.5 MIMO Cascade Control for Vapor Compression Systems

In Section 5.3.3, a general MIMO control paradigm was introduced for the control of superheat and cooling capacity of vapor compression systems. This control

paradigm may perform the desired control of multi-evaporator vapor compression systems but may possibly be limited for employing aggressive control action due to strong nonlinearities. It is difficult to construct an exact plant model using system identification. Typically, strong nonlinearities create difficulties in plant modeling using system identification techniques and the resulting control design using those models may not achieve the desired stability and performance of nonlinear systems; thus sluggish or weak control action is merely acceptable in practice [98], [99].

In this section, we employ the cascade MINO control paradigm which prevents the shortcomings of conventional MIMO control for superheat and cooling capacity regulation. By virtue of the cascade control paradigm, an indirect relationship between control outputs and system outputs allows more exact plant modeling and aggressive control action can be applied to construct a plant model [67], [71].

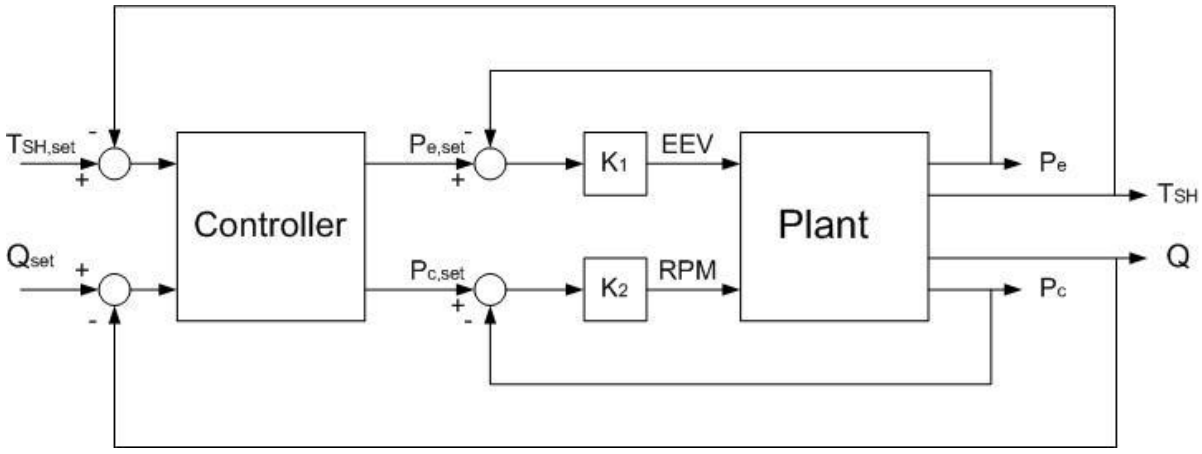

Fig. 5.9. MIMO cascade control of vapor compression system.

Figure 5.9 illustrates an equivalent control algorithm to Figure 5.8 using a cascade control paradigm. Instead of EEV opening and compressor speed, evaporating pressure and condensing pressure have been used as controller outputs where proportional gains K_1 and K_2 are determined from experimentation. Under the cascade framework, a plant model of the nonlinear system is constructed changing evaporating and condensing pressures to superheat and cooling capacity; thus any model can more precisely reflect the dynamics of a nonlinear system.

5.4 Gain-Scheduled Control for Multi-Evaporator Vapor Compression Systems

In this section, a proposed Youla-based gain-scheduled control approach is applied to a multi-evaporator vapor compression system. To demonstrate the gain-scheduled control, we follow a conventional control design process of gain-scheduling for nonlinear systems: First, select control variables and adjustable parameters such as control inputs, outputs, states, and scheduling variables according to the control objectives. Second, construct the LPV plant model from empirical models. In this case, empirically identified models constructed using system identification techniques that closely reflect the physical system at prescribed operating conditions, then the LPV model was created from system identification models using particular state transformation. Note that empirical models have no common states and states of each model don’t have any physical meanings thus a state transformation forces the LPV model to share the states.

Third, linear controllers were designed at each operating condition according to empirical models constructed by system identification. Finally, linear controllers designed at local operating points were interpolated using the proposed controller interpolation method. The stability/performance of the closed loop system was evaluated using LMI-based Lyapunov stability.

The remainder of this section is organized as follows. Section 5.4.1 describes closed loop system formulation with selection of control variables. Section 5.4.2 examines empirical modeling using system identification and LPV plant modeling. Local control design using linear control design at local design points will be presented in Section 5.4.3 and an LPV-LQN feedback system will be discussed in Section 5.4.4. Section 5.4.5 prepares experimental results and analyses.

5.4.1 Closed Loop Formulation

In this section, feedback control system is formulated with a choice of control variables and adjustable parameters. As discussed in Section 5.3, MIMO control framework ensures that desired performance will match the thermal load (cooling capacity) with maximizing thermal efficiency (superheat) so that two evaporator superheats are primary system output regulated as desired values. Instead of direct regulation of cooling capacity supplied from an evaporator, condensing pressure is selected as the secondary system output. Clearly, the crux of multi-evaporator vapor compression system is to provide cooling individually from the demand of each evaporator thus water flow rates are selected as scheduling variables in this dissertation.

Another significant decision is a proper choice of actuators. As presented in Section 5.3, two expansion valves and a compressor are the primary manipulators to alter the mass flow rate of refrigerant, thus these three actuators are employed to modulate superheats and condensing pressure as desired values. Also, water flow valves have been used as disturbance inputs to regulate cooling capacities of the two evaporators since they alter heat transfer from refrigerant to water. Note that condensing pressure is not changed significantly by any actuators of the system. Compressor speed doesn't affect superheat responses while superheats are strongly regulated by expansion valves. A schematic diagram of cascade feedback control system is depicted in Figure 5.10.

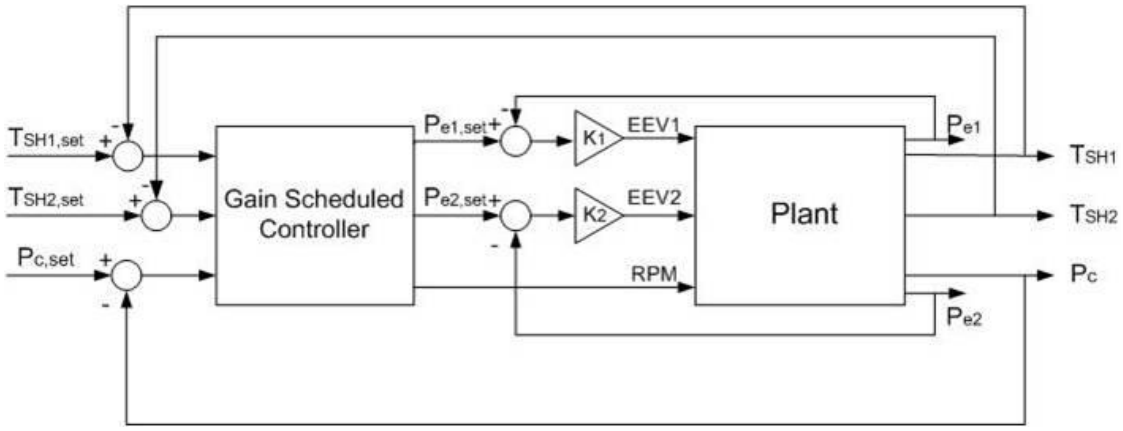

Fig. 5.10. MIMO cascade feedback control Loop.

Under this framework, gain-scheduled controller modulates two expansion valve positions and compressor speed to track the reference inputs. Two superheat and

condensing pressure and local design points are determined in terms of scheduling variable (second water flow valve opening).

5.4.2 MIMO System Identification and LPV Plant Modeling

To create an empirical model to design a controller at local operating conditions through investigating the dynamics of vapor compression system, a set of data-driven models are constructed at prescribed design points using standard system identification techniques. First, the system is operated at a steady state then a pseudo-random binary signal (PRBS) input is applied. This procedure was then repeated: the first run was used for model identification and the second run for model validation [100].

When preparing data for the model identification, experimental data was scaled properly to modulate the effects of each input into each output equivalently. Among various identification models, prediction error method (PEM) was used to define the estimating parameter model formed in a state-space representation since it reduces the prediction error fit by minimizing a quadratic prediction error criterion [100].

Before demonstrating the system identification of the vapor compression system, key operating conditions were selected in scheduling space. In this dissertation, water flow valves are scheduling variables. The sudden change of water flow rate affects the cooling capacities as disturbance input.

Figure 5.11 illustrates local design points in scheduling space where three different operating conditions are selected for cooling of two evaporators. Note that design point 1 and 2 present full and half openings of water flow valve #2 while two

evaporators are running, and point 3 presents a zero opening of water flow valve #2 while evaporator #2 is closed. Using prediction error method (PEM) as a system identification technique [100], 2nd order state space models for each input/output pair are created at three operating conditions as follows ($i = 1,2,3$).:

$$\begin{aligned} \dot{x} &= A_{P,i}x + B_{P,i}u \\ y &= C_{P,i}x \end{aligned} . \tag{5.4}$$

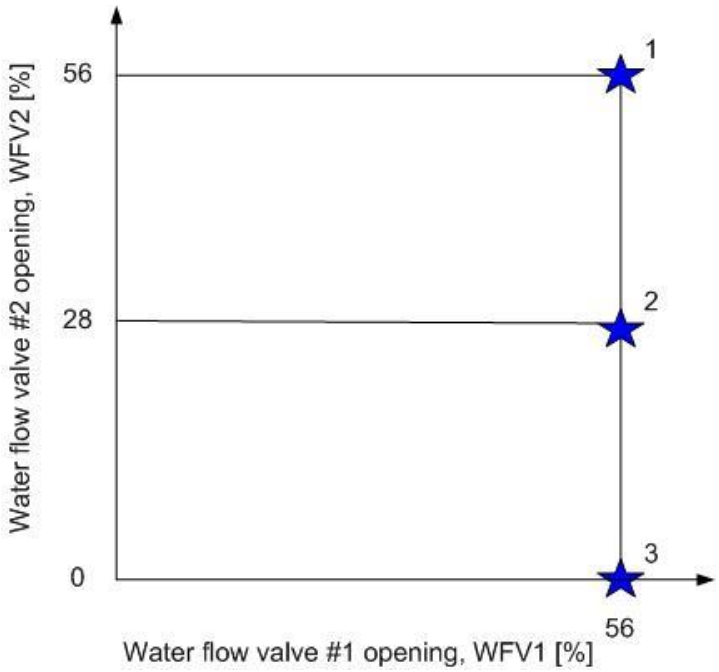

Fig. 5.11. System identification points in scheduling space.

The reader recognizes that empirical models defined at fixed operating conditions would not have common states. Thus a particular state transformation technique, i.e., Cholesky Transformation, has been employed to force the LPV model to share the states where T_i is Cholesky matrix, $C_{P,i}$ in this dissertation.

$$\begin{aligned} \dot{x} &= T_i A_{P,i} T_i^{-1} x + T_i B_{P,i} u = C_{P,i} A_{P,i} C_{P,i}^{-1} x + C_{P,i} B_{P,i} u \\ y &= C_{P,i} T_i^{-1} x = Ix \end{aligned} . \quad (5.5)$$

Finally, LPV plant model is constructed in a form of scheduling variable where $\rho = [0 \quad 1]$.

$$\begin{aligned} \dot{x} &= (A_1 + 2(1-\rho)(A_2 - A_1)x + (B_1 + 2*(1-\rho)(B_2 - B_1)u \\ y &= Ix \end{aligned} . \quad (5.6)$$

To construct LPV plant model, initial guesses are made from individual system identification runs then refined them using PEM technique. Note that the LPV plant model can be recovered at design points where full, half, and zero water flow valve openings present 1, 0.5, and 0 of weighting on scheduling ρ, respectively.

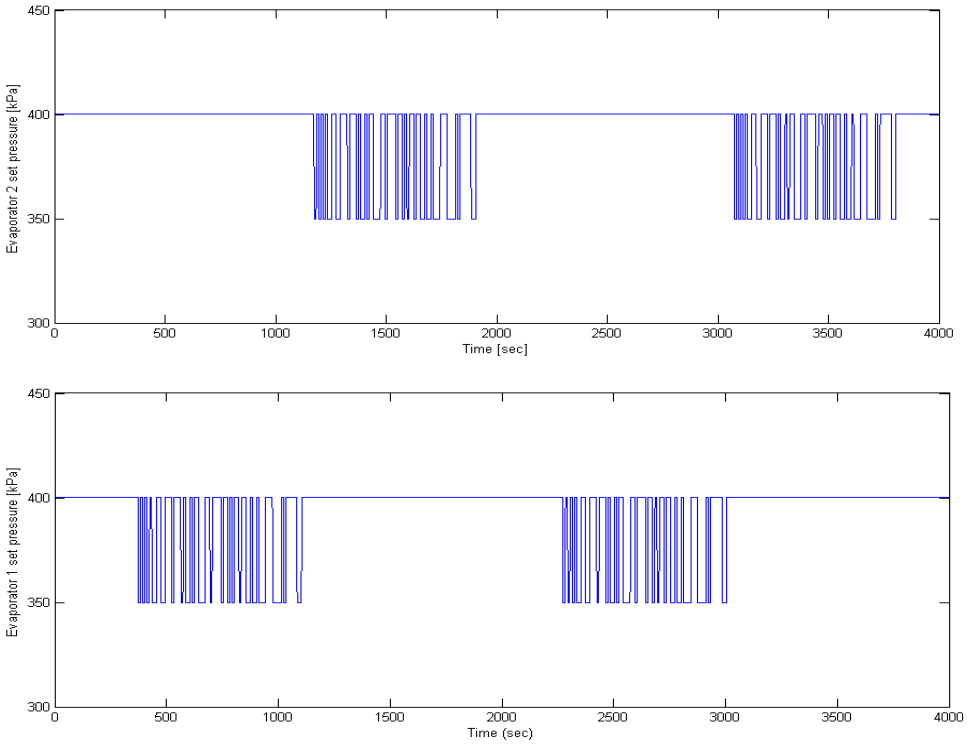

Fig. 5.12. Pseudo random bias input of evaporator set pressures.

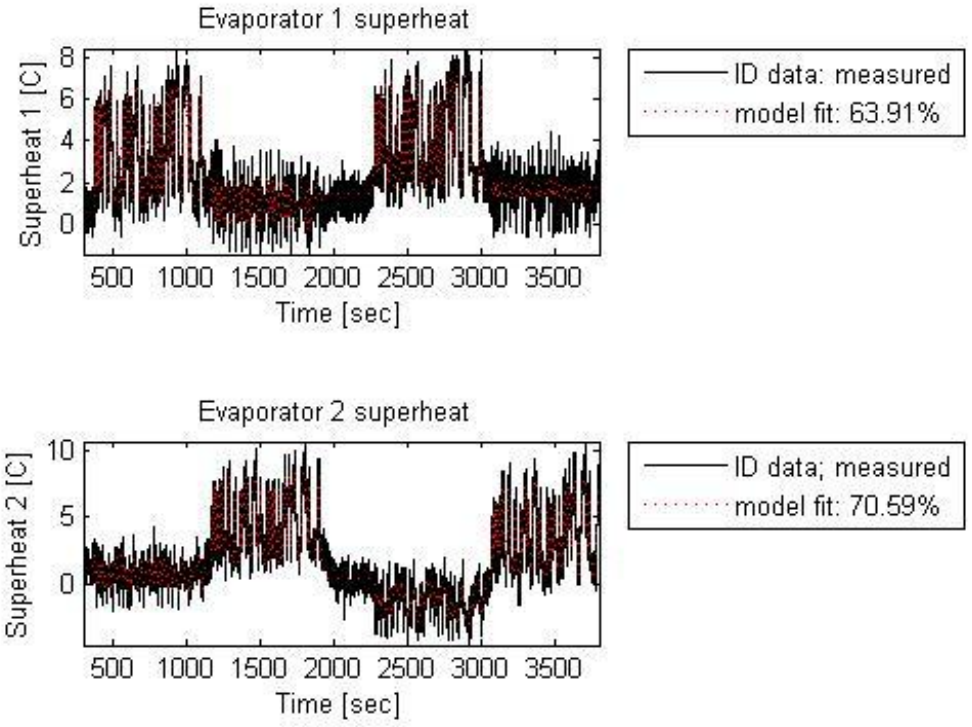

Fig. 5.13. Model identification and validation.

Model identification and validation are performed using the system identification toolbox in Matlab [100]. Figures 5.12-13 illustrate model validation of experimental data for system identification models at operating conditions 1 and 2. As discussed previously, pseudo-random binary signal (PRBS) input was applied to system inputs, two evaporator set pressures, then prediction error method (PEM) was used to define the estimating parameter model using these data which reflect input/output characteristics of system.

Also, state space representations of three LPV identification models are presented in Equation 5.7.

Operating condition 1:

$$\dot{x} = \begin{bmatrix} -0.2499 & -0.1055 \\ -0.1520 & -0.2134 \end{bmatrix} x + \begin{bmatrix} -0.0275 & -0.0171 \\ -0.0129 & -0.0316 \end{bmatrix} u$$
$$y = \begin{bmatrix} 1 & 0 \\ 0 & 1 \end{bmatrix} x \tag{5.7}$$

Operating condition 2:

$$\dot{x} = \begin{bmatrix} -0.1815 & -0.0274 \\ -0.0979 & -0.1246 \end{bmatrix} x + \begin{bmatrix} -0.0194 & -0.0050 \\ -0.0030 & -0.0192 \end{bmatrix} u$$
$$y = \begin{bmatrix} 1 & 0 \\ 0 & 1 \end{bmatrix} x \tag{5.8}$$

Operating condition 3:

$$\dot{x} = \begin{bmatrix} -0.1132 & 0.0506 \\ -0.0437 & -0.0357 \end{bmatrix} x + \begin{bmatrix} -0.0113 & -0.0071 \\ 0.0069 & -0.0068 \end{bmatrix} u$$
$$y = \begin{bmatrix} 1 & 0 \\ 0 & 1 \end{bmatrix} x \tag{5.9}$$

Using an LPV plant model constructed from those system identification models, a proposed controller interpolation is applied to vapor compression system.

5.4.3 Local Controller Design

By virtue of gain-scheduled control paradigm, any linear controller design tools can be applied to design linear controller that stabilizes the plant at fixed operating condition. In this dissertation, LQR and PI control methods have been employed to design stabilizing controllers. Despite being most commonly used in practice, the LQR design method does not consider a reference input nor does it provide for command following. To achieve the desired performance of the system, a good disturbance

rejection and good command following need to be considered in designing a control system [101]. Good command following is implemented by properly introducing the reference input into the system equations.

For the purpose of command following, robust tracking can be achieved by utilizing integral control in that the result from a standard LQR controller is not robust because any change in the plant parameters would result in the steady state error to be nonzero. Integral control is a special case of tracking a signal that does not go to zero in the steady state.

To modify the LQR control representation included integrator, integral control is augmented the state vector with desired dynamics. Consider a standard plant representation with reference [101]:

$$\begin{aligned} \dot{x} &= Ax + Bu \\ y &= Cx \end{aligned} \tag{5.10}$$

integral error, $e = y - r$, and the state of the plant x, by augmenting the plant state with the extra state x_I that yields the differential equation as:

$$\dot{x}_I = Cx - r \tag{5.11}$$

where

$$\dot{x}_I = \int_0^t e\, dt \tag{5.12}$$

Then the augmented state equations will be:

$$\begin{bmatrix} \dot{x} \\ \dot{x}_I \end{bmatrix} = \begin{bmatrix} A & 0 \\ C & 0 \end{bmatrix} \begin{bmatrix} x_I \\ x \end{bmatrix} + \begin{bmatrix} B \\ 0 \end{bmatrix} u \tag{5.13}$$

where the feedback law is:

$$u = -\begin{bmatrix} K_0 & K_1 \end{bmatrix} \begin{bmatrix} e \\ x_I \end{bmatrix} \tag{5.14}$$

The integral control structure of LQR control is depicted in Figure 5.14.

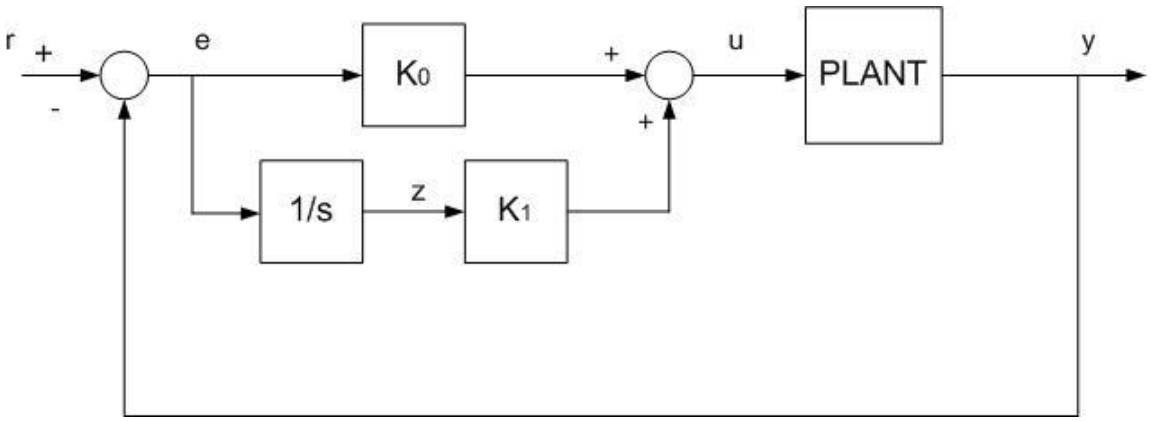

Fig. 5.14. LQR control with integral structure.

Also, state space representation of LQR and PI controller can be represented respectively as follows:

$$\begin{aligned} \dot{x} &= \begin{bmatrix} 0 & 0 \\ 0 & 0 \end{bmatrix} x + \begin{bmatrix} 1 & 0 \\ 0 & 1 \end{bmatrix} e \\ u &= \begin{bmatrix} K_1 \end{bmatrix} x + \begin{bmatrix} K_0 \end{bmatrix} e \end{aligned} \tag{5.15}$$

$$\begin{aligned} \dot{x} &= \begin{bmatrix} 0 & 0 \\ 0 & 0 \end{bmatrix} x + \begin{bmatrix} 1 & 0 \\ 0 & 0 \end{bmatrix} e \\ u &= \begin{bmatrix} K_{I1} & 0 \\ 0 & K_{I2} \end{bmatrix} x + \begin{bmatrix} K_{P1} & 0 \\ 0 & K_{P2} \end{bmatrix} e \end{aligned} \tag{5.16}$$

where K_{P1} and K_{P2} are proportional gains, and K_{I1} and K_{I2} are integral gains of PI controller.

5.4.4 LPV-Q Feedback System

An LPV-Q feedback system is prepared using an LPV plant model and local controllers. To achieve the desired performance levels across the entire operating envelop an Youla-based gain-scheduling controller is constructed using the local controllers, based on the LPV-Q framework outlined in Section 3. A schematic diagram of LPV-Q feedback system is depicted in Figure 5.15 [86].

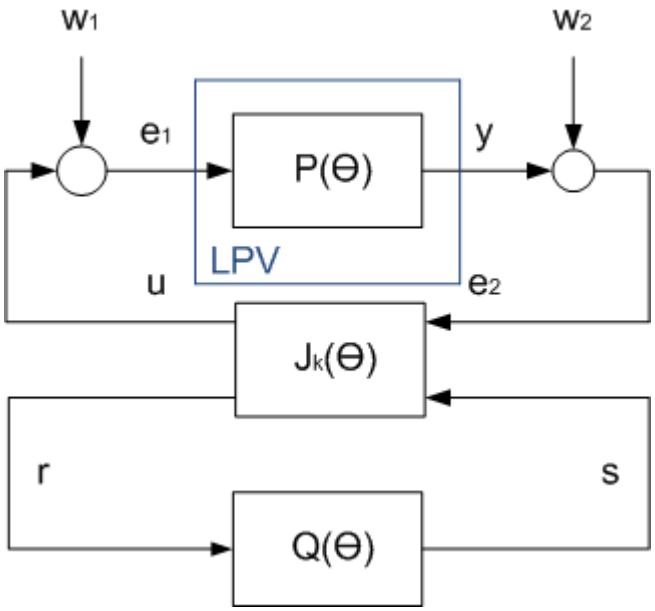

Fig. 5.15. LPV-Q feedback system.

5.4.5 Gain-scheduled Control on Vapor Compression System

Finally, a proposed Youla-based gain-scheduled control approach is experimentally demonstrated on a multi-evaporator vapor compression system in this section. The LPV plant model indicates that the system dynamics of the system change

with a variation in the water flow rate applied to the second evaporator. Assuming that the water flow valve which regulates water flow rate remains fully opened and applied to the first evaporator, compressor speed will not significantly affect the evaporator superheat.

To demonstrate the gain-scheduled control, controller interpolation/switching is implemented among the three controllers that were designed at high, medium, and zero water flow conditions and experimentally evaluated. Note that two controllers are designed at high and medium water flow conditions where two evaporators are working using an LQR design method; the third controller is designed at a zero water flow condition using the PI control method. A desired gain-scheduled control can be achieved via interpolating two LQR controllers when water flow rate varies within a range between high and medium flow while simultaneous switching between an LQR controller designed at medium flow condition and PI controller designed at zero condition is implemented when the water flow valve is instantly closed.

Variation of water flow rate and the associating weighting functions are shown in Figure 5.16. Water flow rate [kg/s] is regulated by changing the water flow valve opening [%] electronically over operating conditions and closing manually after 1800 seconds to implement controller switching. As shown in Figure 5.16, linear weighting functions properly reflect change of the water flow condition. Note that weighting function 1, α_1, and weighting function 2, α_2, vary nearly linearly with scheduling variable between high and medium operating conditions. Weighting function 3, α_3, dominates the control switching when the water flow valve is instantly closed.

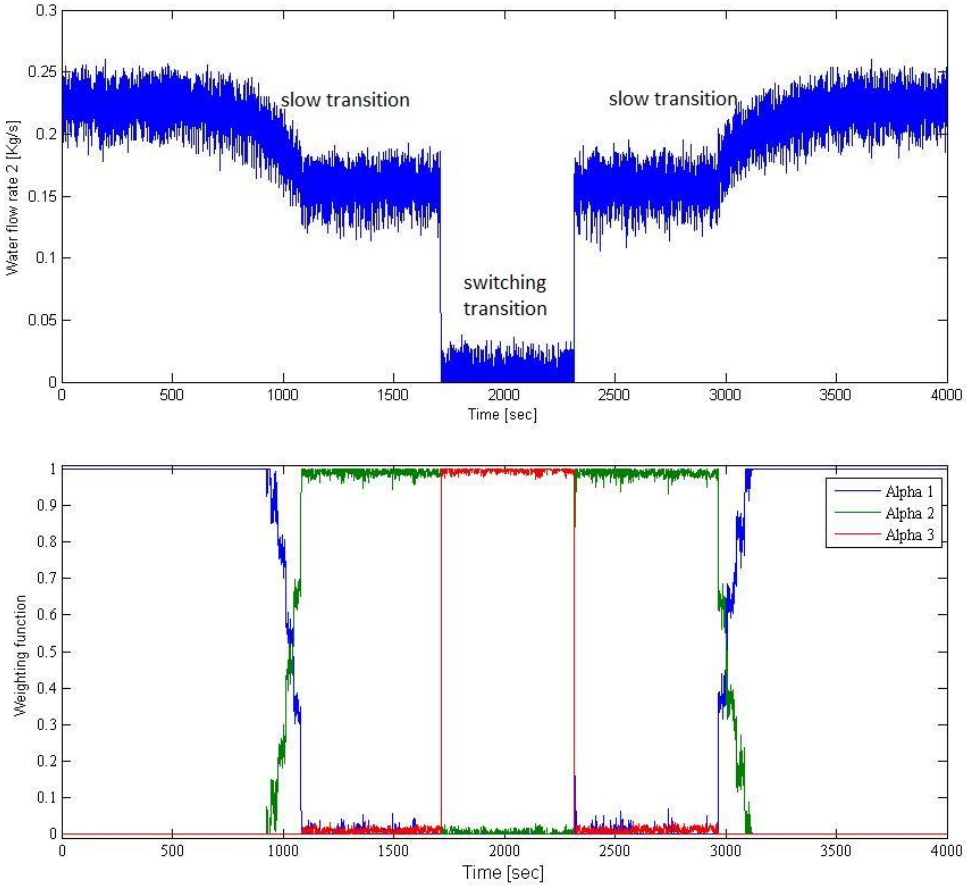

Fig. 5.16. Water flow rate and weighting functions.

Condenser pressure and compressor speed are presented in Figure 5.17. As discussed in Section 5.4.1, condensing pressure remains constant across the entire operating regime and compressor speed [rpm] is well regulated to achieve desired condensing pressure (1000 [kPa]).

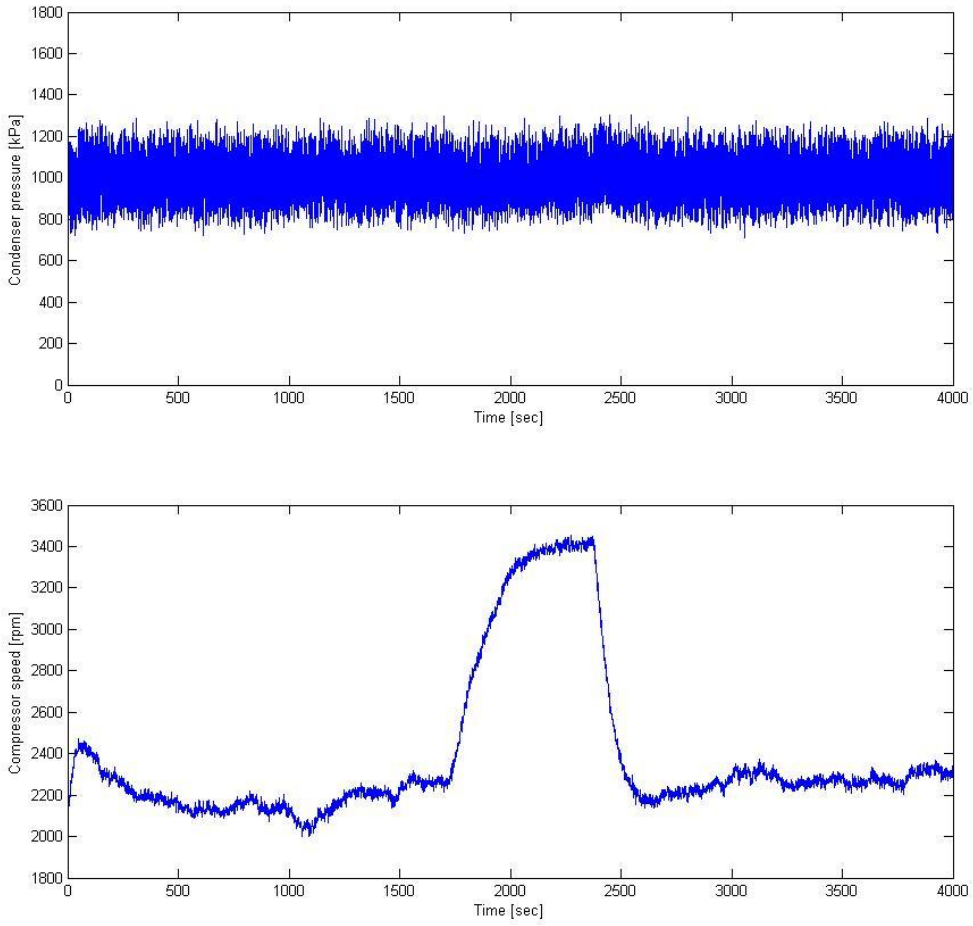

Fig. 5.17. Condensing pressure and compressor speed.

Figure 5.18 presents two evaporator cooling capacities supplied from two evaporators. Cooling capacities are relatively noisy, fluctuating in a wide range over the operating regime. However, cooling capacity of the second evaporator remains nearly zero at zero water flow condition while that of the first evaporator increases due to the large opening of EEV 1 that compensates the loss of cooling capacity of the second evaporator.

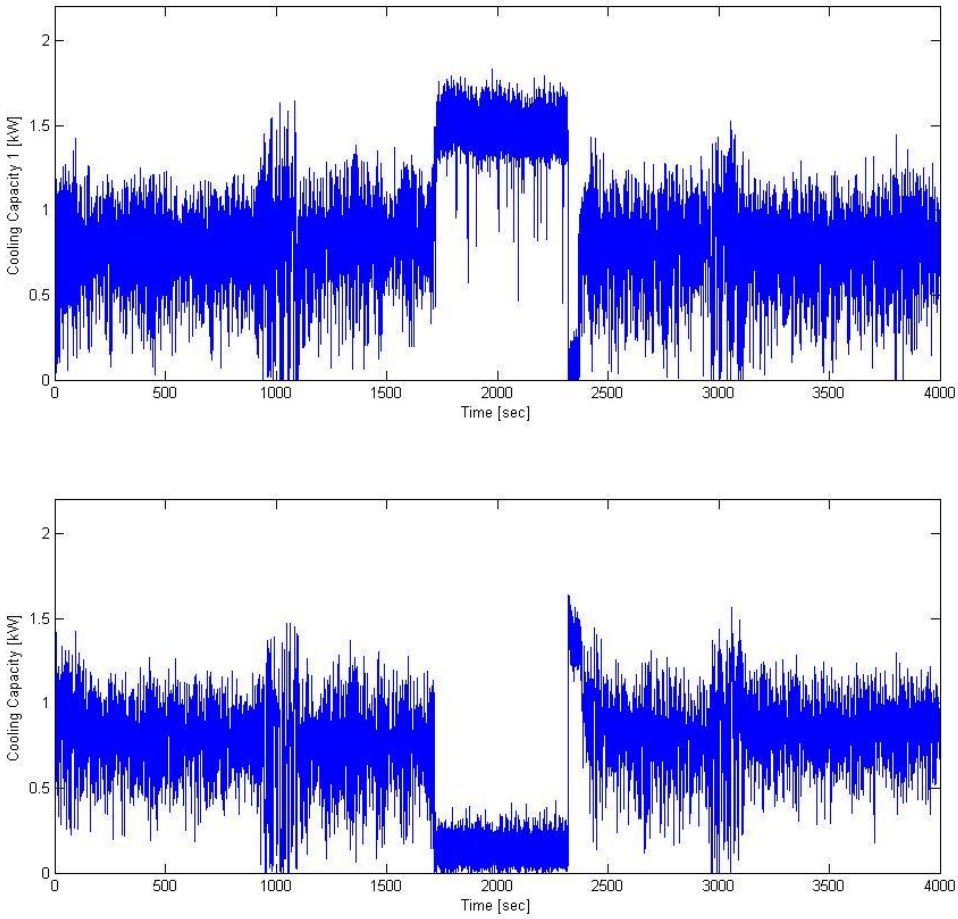

Fig. 5.18. Evaporator cooling capacities.

Figure 5.19 shows evaporator superheats and EEV openings of the system when gain-scheduled control is applied. When controller interpolation between high and medium water flow occurs, superheat of the first evaporator begins oscillating but recovers quickly since EEV 1 responds instantly to regulate superheat as a desired value, 10 [℃]. Furthermore, when the water flow valve is manually closed, EEV 2 is also closed instantly and EEV1 is opened sufficiently to compensate evaporator superheat 2. After the water flow valve is re-opened, EEV 2 also opens again and controller

interpolation is implemented properly. The reader recognizes that stability of the system can be guaranteed over the operating envelop. More important, the interpolated/switched controller can transition smoothly and stably from one design point to another.

Figure 5.20 presents superheat regulation where a single controller, LQR controller designed at high flow condition, is used over operating conditions. This single control case performs sufficiently well - even the second evaporator never loses superheat at zero water flow condition since second EEV never closes. However, the cascade control paradigm alleviates the strong effects of EEV on superheat in general control cases and results in an effective superheat regulation. This may not happen in practice since most physical systems are highly nonlinear and a single controller cannot achieve the desired control when cascade control may not reduce strong nonlinearities of the system.

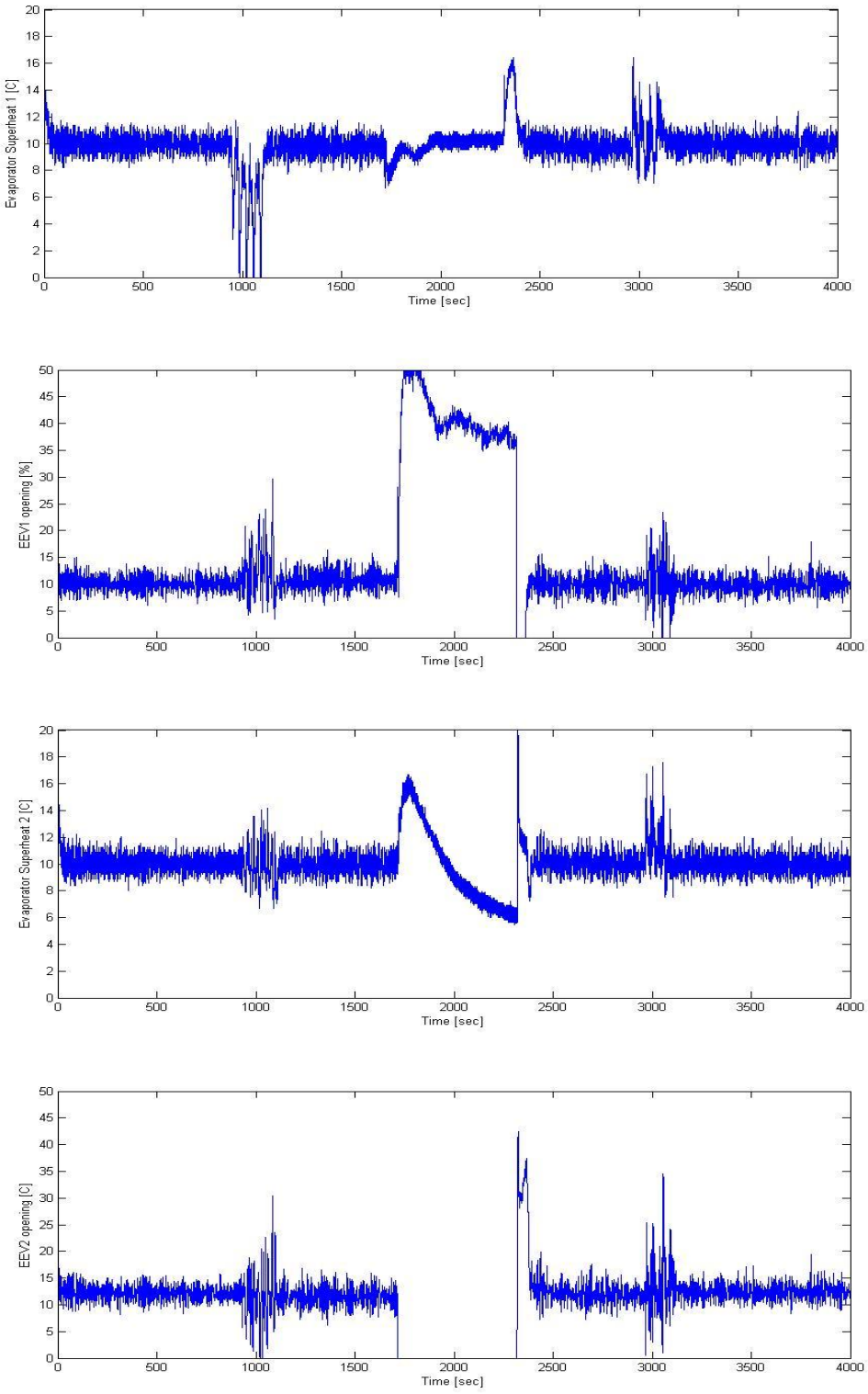

Fig. 5.19. Superheat regulation and EEV opening in gain-scheduled control system.

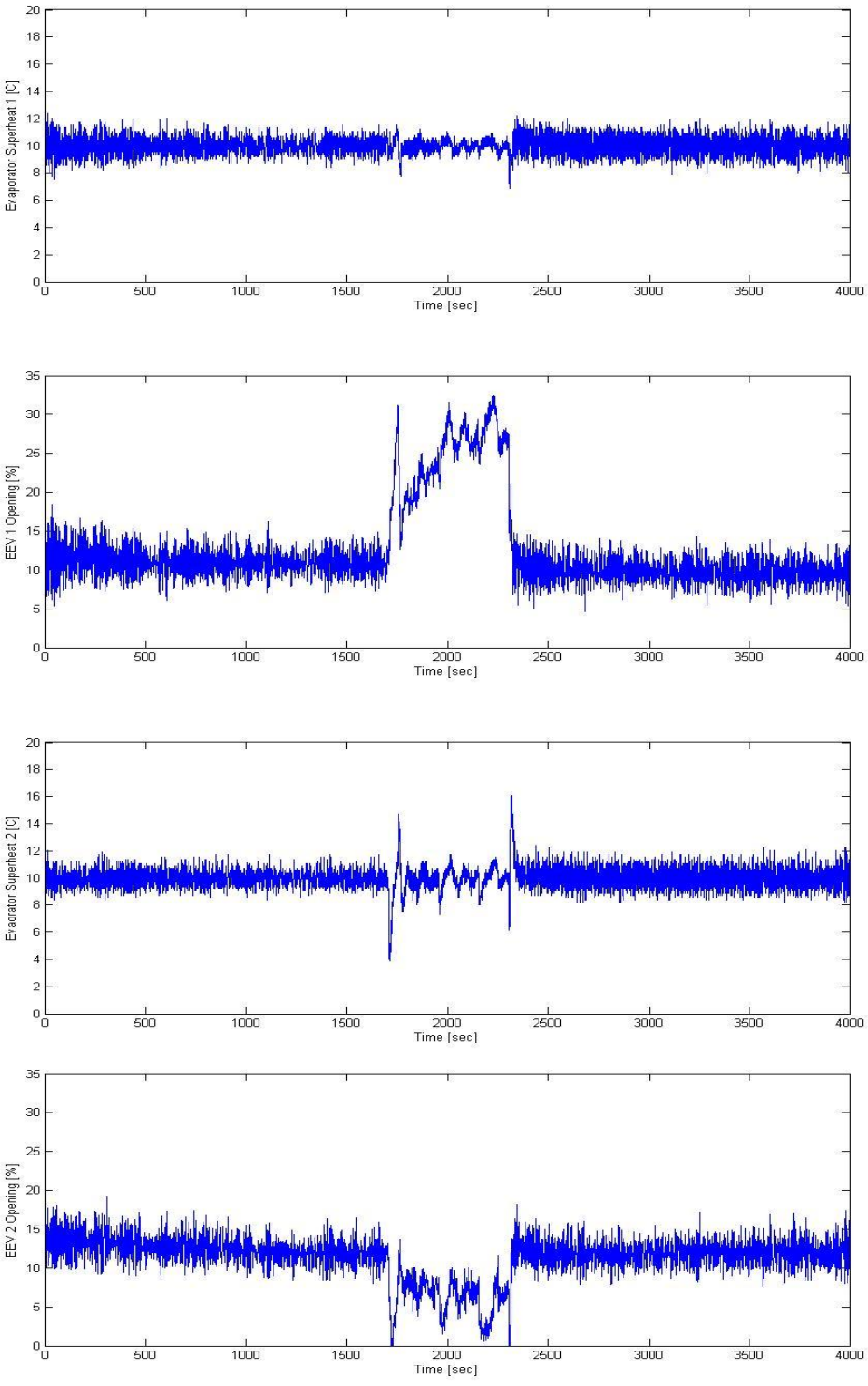

Fig. 5.20. Superheat regulation and EEV opening in LQR controlled system.

6. CONCLUSIONS AND FUTURE WORK

6.1 Summary of Research Achievement

This dissertation provides a method for stable controller interpolation for LPV systems using the Youla parameterization. The existence of a quadratic common Lyapunov function is given by construction, guaranteeing stability of the closed system despite arbitrarily fast transitions in the scheduling variables. A particular state transformation is used to allow the interpolated Q-system to share state variables, significantly reducing the number of the states required for controller interpolation. The approach has the advantage that controllers of different sizes and structures can be interpolated smoothly and stably with the performance of the local controllers recovered exactly at critical operating conditions.

A proposed stability analysis has been extended to the LPV closed loop system that includes robustness and performance considerations since the LPV plant model includes modeling that significantly affects the system dynamics. In this case, the plant model may not reflect the nonlinear system precisely and conventional stability analyses may not be sufficient to guarantee the stability of a nonlinear system. The proposed framework, utilizing L_2 gain of the modified LPV-Q system via optimizing feedback gains of a closed system, guarantees the global level of robust stability by minimizing the L_2 gain that remains within desired bounds over the operating envelop.

The efficacy of the proposed controller interpolation is demonstrated in experimentation using a multi-evaporator vapor compression system. The dynamics of vapor compression systems are highly nonlinear, thus the gain-scheduled control is the potential to achieve the desired stability and performance of the system. The proposed controller interpolation/switching method guarantees the nonlinear stability of the closed loop system during the arbitrarily fast transition and achieves the desired performance to subsequently improve thermal efficiency of the vapor compression system.

6.2 Future Work

This research mainly contributes nonlinear stability for gain-scheduled systems. The efficacy of the proposed method is demonstrated in simulation and experimentation. There exist a number of directions where attention for future work can be focused, including following.

Gain-scheduled Control:

In a proposed LPV-Q framework, stability of the nonlinear closed loop system is guaranteed by the existence of a quadratic common Lyapunov function but performance of the system is rather not to be considered in this dissertation. To improve the performance of the nonlinear system, a plant model should reflect the dynamics of the system more precisely since controllers are designed using a model that is constructed from system identification models. When an LPV model doesn't exist in practice, a data-driven or first principle model should represent real dynamics of the nonlinear

systems. Thus advanced methods in system identification-based plant modeling can become milestones in performance improvement.

Control of Vapor Compression System:

There are a plenty of choices in controllable inputs and outputs for vapor compression systems. We examined rather simple cases in experimental studies; other choices of controllable inputs and outputs may achieve high-level of thermal efficiency. Also, this dissertation has implemented control design at a steady state, not focusing on the start-up process; thus a comparatively large overshoot and sluggish settling time has appeared on start.-up. Control design with start-up and shut-down considerations will improve thermal efficiency via reducing the load applied to system.

REFERENCES

[1] D. J. Leith and W. E. Leithead, "Survey of Gain-Scheduling Analysis and Design," *International Journal of Control*, vol. 73, no. 11, pp. 1001-1025, 2000.

[2] J. S. Shamma and M. Athans, "Gain Scheduling: Potential Hazards and Possible Remedies," in *Proc. of the American Control Conference*, Boston, MA, Jun. 1991, pp. 516-521.

[3] S. Skogestad and I. Postlethwaite, *Multivariable Feedback Control: Analysis and Design*. Chichester, England: John Wiley & Sons, 1996.

[4] X. He, S. Liu, and H. H. Asada, "Modeling of Vapor Compression Cycles for Multivariable Feedback Control of HVAC Systems," *Journal of Dynamic Systems, Measurement, and Control*, vol. 119, pp. 183-191, 1997.

[5] B. P. Rasmussen, "Dynamic Modeling and Advanced Control of Air Conditioning and Refrigeration Systems," Ph.D diss., Department of Mechanical and Industrial Engineering, University of Illinois, Urbana, IL, Dec. 2005.

[6] K. J. Hunt, T. A. Johansen, J. Kalkkuhl, H. Fritz, and T. Gottsche, "Speed Control Design for An Experimental Vehicle using a Generalized Gain Scheduling Approach," *IEEE Transactions on Control Systems Technology*, vol. 8, pp. 381-395, 2000.

[7] R. A. Hyde and K. Glover, "Application of Scheduled H_∞ Controllers to a VSTOL Aircraft," *IEEE Transactions on Automatic Control*, vol. 38, pp. 1021-1039, 1993.

[8] R. T. Reichert, "Dynamic Scheduling of Modern-Robust-Control Autopilot

Designs for Missiles," *IEEE Control Systems Magazine*, vol. 12, pp. 35-42, Oct, 1992.

[9] D. J. Stilwell, "State-Space Interpolation for a Gain-Scheduled Autopilot," *Journal of Guidance, Control, and Dynamics*, vol. 24, pp. 460-465, 2001.

[10] T. A. Johansen, K. J. Hunt, and I. Petersen, "Gain-Scheduled Control of a Solar Power Plant," *Control Engineering Practice*, vol. 8, pp. 1011-1022, 2000.

[11] D. J. Leith and W. E. Leithead, "Appropriate Realization of Gain-Scheduled Controllers with Application to Wind Turbine Regulation," *International Journal of Control*, vol. 65, pp. 223-248, 1996.

[12] R. Zhang, A. Alleyne, and D. E. Carter, "Generalized Multivariable Gain Scheduling with Robust Stability Analysis," *ASME Journal of Dynamic Systems, Measurement, and Control*, vol. 27, pp. 668-687, Dec, 2005.

[13] W. J. Rugh and J. S. Shamma, "Research on Gain Scheduling," *Automatica*, vol. 36, no. 10, pp. 1401-1425, 2000.

[14] D. J. Stilwell, "J-Q interpolation for Gain Scheduled Controllers," in *Proc. of IEEE Conference on Decision and Control*, Pheonix, AZ, Dec. 1999, vol. 1, pp. 749-754.

[15] J. P. Hespanha and A. S. Morse, "Switching Between Stabilizing Controllers," *Automatica*, vol. 38, no. 11, pp. 1905-1917, 2002.

[16] D. J. Stilwell and W. J. Rugh, "Stability Preserving Interpolation Methods for the Synthesis of Gain Scheduled Controllers," *Automatica*, vol. 36, no. 5, pp. 665-671, 2000.

[17] H. Niemann and J. Stoustrup, "An Architecture for Implementation of Multivariable Controllers," in *Proc. of the American Control Conference*, San Diego, CA, Jun. 1999, pp. 4029-4033.

[18] K. J. Hunt and T. A. Johansen, "Design and Analysis of Gain-Scheduled Control using Local Controller Networks," *International Journal of Control*, vol. 66, no. 5, pp. 619-651, 1997.

[19] R. Murray-Smith and T. Johansen, *Multiple Model Approaches to Nonlinear Modelling and Control*. Bristol, PA: Taylor and Francis, 1997.

[20] A. Packard and M. Kantner, "Gain Scheduling the LPV Way," in *Proc. of the IEEE Conference on Decision and Control*, Atlanta, GA, Dec. 1996, vol. 4, pp. 3938-3941.

[21] F. Wu, "A Generalized LPV System Analysis and Control Synthesis Framework," *International Journal of Control*, vol. 74, no. 7, pp. 745-759, 2001.

[22] K. H. Tan and J. S. Shamma, "Nonlinear Gain-scheduled Control Design using Set-values Methods," in *Proc. of the American Control Conference*, Philadelphia, PA, Jun. 1998, pp. 1195-1199.

[23] F. Wu and K. M. Grigoriadis, "LPV-based Control of Systems with Amplitude and Rate Actuator Saturation Constraints," in *Proc. of the American Control Conference*, San Diego, CA, Jun. 1999, pp. 3191-3195.

[24] B. P. Rasmussen and A.G. Alleyne, "Gain Scheduled Control of an Air Conditioning System Using the Youla Parameterization," in *Proc. of the American Control Conference*, Minneapolis, MN, Jun. 2006, pp. 5336-5341.

[25] H. K. Khalil, *Nonlinear Systems*. Upper Saddle River, NJ: Prentice-Hall Inc., 1996.

[26] J. Stoustrup, P. Andersen, T. Pedersen, and M. Hangstrup, "Gain-scheduling Procedures for Unstable Controllers: A Behavioral Approach," in *Proc. of the American Control Conference*, San Diego, CA, Jun. 1999, pp. 4004-4008.

[27] G. Becker and A. Packard "Robust Performance of Linear Parametrically Varying Linear Feedback," *Systems & Control Letters*, vol. 23, pp. 205-215, 1994.

[28] J. S. Shamma and D. Xiong, "Set-valued Methods for Linear Parameter Varying Systems, *Automatica*, vol. 35, pp. 1081-1089, 1999.

[29] D. J Leith and W. E. Leithead, "Inpur-output Linearization of Velocity-based Gain-scheduling," *International Journal of Control*, vol. 72, pp. 229-246, 1999.

[30] D. J Leith and W. E. Leithead, "Analytic Framework for Blended Multiple Model Systems using Linear Local Models," *International Journal of Control*, vol. 72, pp. 605-619, 1999.

[31] D. J Leith and W. E. Leithead, "Gain-scheduled Controller Design: An Analytic Framework Directly Incorporating Non-equilibrium Plant Dynamics," *International Journal of Control*, vol. 70, pp. 249-269, 1999.

[32] W. Tan, K. Andrew, K. Packard, K. Stoustrup, and G. Balas, "Quasi-LPV Modeling and LPV Control of a Generic Missile," in *Proceedings of the American Control Conference*, Chicago, IL, Jun. 2000, pp. 3692-3696.

[33] Y. Huang and A. Jadbabaie, "Nonlinear H_∞ Control: An Enhanced Quasi-LPV Approach," in *Proc. of the IFAC World Congress*, Beijing, China, Jun. 1999, pp. 576-584.

[34] A. Jadbabaie and J. Hauser, "Control of a Thrust-vectored Flying Wing: A Receding Horizon – LPV Approach," *International Journal of Robust and Nonlinear Control*, vol. 12, no. 14, pp. 869-896, 2002.

[35] D. J Leith and W. E. Leithead, "Gain-scheduled Controller Design: An Analytic Framework Directly Incorporating Non-equilibrium Plant Dynamics," *International Journal of Control*, vol. 70, pp. 249-269, 1999.

[36] P. Apkarian and P. Gahinet, "Convex Characterization of Gain-scheduled H_∞ controllers," *IEEE Transactions on Automatic Control*, vol. 40, pp. 853-864, 1995.

[37] R. A. Nichols, R. T. Reichert, and W. J. Rugh, "Gain Scheduling for H-infinity Controllers: A Flight Control Example," *IEEE Transactions on Control Systems Technology*, vol. 1, pp 69-79, 1993.

[38] D. J. Stilwell and W. J. Rugh, "Interpolation of Observer State Feedback Controllers for Gain Scheduling," *IEEE Transactions on Automatic Control*, vol. 44, pp. 1225-1229, 1999.

[39] C. W. Scherer, P. Gahinet, and M. Chilali, "Multiobjective Output-feedback Control via LMI Optimization," *IEEE Transaction on Automatic Control*, vol. 42, pp. 896-911, 1997.

[40] L. Wang, *A Course in Fuzzy Systems and Control*. Upper Saddle River, NJ: Prentice Hall, 1996.

[41] D. Guo and W. J. Rugh, "An Approach to Gain Scheduling on Fast Variables," in *Proc. of the IEEE Conference on Decision and Control*, Tucson, AZ, Dec. 1992, vol. 1, pp. 759-763.

[42] P. Gahinet, P. Apkarian, and M. Chilali, "Affine Parameter-Dependent Lyapunov Functions and Real Parametric Uncertainty," *IEEE Transactions on Automatic Control*, vol. 41, pp. 436-442, 1996.

[43] C. W. Scherer, "LPV Control and Full Block Multiplier," *Automatica*, vol. 37, pp. 361-375, 2001.

[44] G. Becker, "Additional Results on Parameter-dependent Controllers for LPV Systems," in *Proceeding of the IFAC World Congress*, San Francisco, CA, Jul. 1996, pp. 351-356.

[45] J. Daafouz, P. Riedinger, and C. Iung, "Stability Analysis and Control Synthesis for Switched Systems: A Swithched Lyapunov Function Approach," *IEEE Transactions on Automatic Control*, vol. 47, no. 11, pp. 1883-1887, 2002.

[46] J. Yu and A. Sideris, "H_∞ Control with Parameter Lyapunov Functions: Induced L2-norm Control for LPV Systems with Bounded Paramoeter Variation Rates," *Systems & Control Letters*, vol. 30, pp. 57-69, 1997.

[47] E. Feron, P. Apkarian, and P. Gahinet, "Analysis and Synthesis of Robust Control Systems via Parameter-dependent Lyapunov Functions," *IEEE Transaction of Automatic Control*, vol. 41, pp. 1041-1046, 1996.

[48] F. Wu, H. Yang, A. Packard, and G. Becker, "Induced L_2-Norm for LPV System with Bounded Parameter Variation Rates," in *Proc. of the American Control Conference*, Seattle, WA, Jun. 1995, pp. 2379-2383.

[49] G. Zhai, H. Lin, and P. Antsaklis, "Quadratic Stabilizability of Switched Linear Systems with Polytopic Uncertainties," *International Journal of Control*, vol. 76, no. 7, pp. 747-753, 2003.

[50] M. Margaliot and D. Liberzon, "Lie-algebraic Stability Conditions for Nonlinear Switched Systems and Differential Inclusions," *Systems & Control Letters*, vol. 55, pp. 8-16, 2006.

[51] L. Vu and D. Liberzon, "Common Lyapunov Functions for Families of Commuting Nonlinear Systems," *Systems & Control Letters*, vol. 54, pp. 405-416, 2005.

[52] D. Liberzon, *Switching in Systems and Control*. Boston, MA: Birkhäuser, 2003.

[53] S. Boyd and Q. Yang, "Structured and Simultaneous Lyapunov Functions for System Stability Problems," *International Journal of Control*, vol. 49, pp. 2215-2240, 1989.

[54] T. Ooba and Y. Funahashi, "Two Conditions Concerning Common Quadratic Lyapunov Functions for Linear Systems," *IEEE Transactions on Automatic Control*, vol. 42, no. 5, pp. 719-721, 1997.

[55] R. Shorten, K. Narendra, and O. Mason, "A Result on Common Quadratic Lyapunov Functions," *IEEE Transactions on Automatic Control*, vol. 48, no. 1, pp. 110-113, 2003.

[56] V. Blondel, G. Campion, and M. Gevers, "A Sufficient Conditions for Simultaneous Stabilization," *IEEE Transactions on Automatic Control*, vol. 38, no. 8, pp. 1264-1266, 1993.

[57] V. Blondel, *Simultaneous Stabilization of Linear Systems*. New York: Springer-Verlag, 1994.

[58] H. Niemann, "Dual Youla Parameterisation," in *Proc. of IEE Control Theory and Applications*, vol. 150, no. 5, pp. 493-497, 2003.

[59] H. Niemann, J. Stoustrup, and R. Abrahamsen, "Switching between Multivariable Controllers," *Journal of Optimal Control Applications and Methods*, vol. 25, pp. 51-66, 2004.

[60] H. Niemann and J. Stoustrup, "An Architecture for Fault Tolerant Controllers," *International Journal of Control*, vol. 78, no. 14, pp. 1091-1113, 2005.

[61] B. P. Rasmussen and A. Alleyne, "Gain Scheduled Control of an Air Conditioning System Using the Youla Parameterization," *IEEE Transactions on Control Systems Technology*, in review.

[62] D. C. Youla, J. J. Jr. Bongiorno, and H. A. Jabr, "Modern Wiener-Hopf Design of Optimal Controllers Part I: The Single-Input-Output Case," *IEEE Transactions on Automatic Control*, vol. AC-21, no. 1, pp. 13-30, 1976.

[63] T. T. Tay, I. Mareels, and J. B. Moore, *High Performance Control*. Ann Arbor, MI: Birkhauser, 1998.

[64] P. Apkarian and R. J. Adams, "Advanced Gain-Scheduling Techniques for Uncertain Systems," *IEEE Transactions on Control Systems Technology*, vol. 6, pp. 21-32, 1998.

[65] P. Apkarian and R. J. Adams, "Advanced Gain-Scheduling Techniques for Uncertain Systems," *IEEE Transactions on Control Systems Technology*, vol. 6, pp. 21-32, 1998.

[66] J. S. Shamma, "Robust Stability with Time-varying Structured Uncertainty," *IEEE Transactions on Automatic Control*, vol. 39, pp. 714-724, 1994.

[67] K. Zhou, J. C. Doyle, and K. Glover, *Robust and Optimal Control*. Upper Saddle River, NJ: Prentice Hall, 1996.

[68] F. Wu, X. H. Yang, A. Packard, and G. Becker, "Induced L2-norm Control for LPV Systems with Bounded Parameter Variation Rates," *International Journal of Control*, vol. 9, pp. 983-998, 1996.

[69] M. Chilali and P. Gahinet, "H_∞ Design with Pole Placement Constraints: An LMI Approach," *IEEE Transaction of Automatic Control*, vol. 41, pp. 358-367, 1996.

[70] Anonymous, "Energy Information Administration: International Energy Outlook 2009," http://www.eia.doe.gov/oiaf/ieo/world.html, 2009

[71] M. S. Elliott, "Decentralized Model Predictive Control of A Multiple Evaporator HVAC System," M.S Thesis, Department of Mechanical Engineering, Texas A&M University, College Station, TX, Aug. 2008.

[72] M. Moran and H. Shapiro, *Fundamentals of Engineering Thermodynamics*. New York: John Wiley & Sons, 2007.

[73] J. S. Shamma and M. Athans, "Analysis of Nonlinear Gain Scheduled Control Systems," *IEEE Transaction of Automatic Control*, vol. 27, pp. 898-907, 1991.

[74] S. Boyd, E. Ghaoui, and M. Chilali, *Linear Matrix Inequalities in System and Control Theory*. Philadelphia, PA: SIAM, 1994.

[75] P. Gahinet, "Explicit Controller Formulas for LMI-based H_∞ Synthesis," *Automatica*, vol. 32, pp. 1007-1014, 1994.

[76] A. Packard, "Gain-scheduling via Linear Fractional Transformations," *International Journal of Control, Systems & Control Letters*, vol. 22, pp. 79-82, 1994.

[77] H. Niemann and J. Stoustrup, "Gain Scheduling Using the Youla Parameterization," in *Proceedings of the IEEE Conference on Decision and Control*, Pheonix, AZ, Dec. 1999, vol. 3, pp. 2306-2311.

[78] J. Stoustrup and H. Niemann, "Starting Up Unstable Multivariable Controllers Safely," in *Proceedings of the IEEE Conference on Decision and Control*, San Diego, CA, Dec. 1997, vol. 2, pp. 1437-1438.

[79] J. D. Bendtsen, J. Stoustrup, and K. Trangbaek, "Bumpless Transfer between Observer-based Gain Scheduled Controllers," *International Journal of Control*, vol. 78, no. 7, pp. 491-504, 2005.

[80] J. Bendtsen, J. Stoustrup, and K. Trangbaek, "Bumpless Transfer between Advanced Controllers with Applications to Power Plant Control," in *Proceedings of the IEEE Conference on Decision and Control*, Maui, Hawaii, Dec. 2003, vol. 3, pp. 2059-2064.

[81] J. Bendtsen, J. Stoustrup, and K. Trangbaek, "Multi-Dimensional Gain Scheduling with Application to Power Plant Control," in *Proc. of the IEEE Conference on Decision and Control*, Maui, Hawaii, Dec. 2003, vol. 6, pp. 6553-6558.

[82] H. Niemann and J. Stoustrup, "Reliable Control using Primary and Dual Youla Parameterization," in *Proc. of the IEEE Conference on Decision and Control*, Las Vegas, NV, Dec. 2002, vol. 4, pp. 4353-4358.

[83] D. J. Stilwell and W. J. Rugh, "Interpolation of Observer State Feedback Controllers for Gain Scheduling," in *Proc. of the American Control Conference*, Philadelphia, PA, Jun. 1998, pp. 1215-1219.

[84] D. J. Stilwell and W. J. Rugh, "Interpolation Methods for Gain Scheduling," in *Proc. of IEEE Conference on Decision and Control*, Tampa, FL, Dec. 1998, vol. 2, pp. 3003-3008.

[85] D. J. Stilwell, "State-Space Interpolation for a Gain-Scheduled Autopilot," *Journal of Guidance, Control, and Dynamics*, vol. 24, no. 3, pp. 460-465, 2001.

[86] B. P. Rasmussen and Y. J. Chang, "Stable Controller Interpolation/Controller Switching for LPV Systems," *Journal of Dynamic Systems, Measurement, and Control*, Accepted in publication, 2009.

[87] Y. J. Chang and B. P. Rasmussen, "Stable Controller Interpolation for LPV Systems," *in Proceedings of the American Control Conference*, Seattle, WA, Jun. 2008, pp. 3082-3087.

[88] W. Xie and T. Eisaka, "Design of LPV Control Systems Based on Youla Parameterization," *IEE Proceedings of Control Theory and Applications*, New York, NY, Dec. 2004, vol. 151, no. 4, pp. 465-472.

[89] K. H. Johansson, "Quadruple-Tank Process: A Multivariable Laboratory Process with an Adjustable Zero," *IEEE Transactions on Control Systems Technology*, vol. 8, no. 3, pp. 456-465, 2000.

[90] P. Apkarian, P. Gahinet, and G. Becker, "Self-scheduled H-infinity Control of Linear Parameter-varying Systems: A Design Example," *Automatica*, vol. 31, pp. 1251-1261, 1998.

[91] W. Xie, Y. Kamiya, and T. Eisaka, "Robust Control System Design for Polytopic Stable LPV Systems," *IMA Journal of Mathematical Control and Information*, vol. 20, pp. 201-216, 2003.

[92] W. Xie and T. Eisaka, "Robust State Feedback for Linear Parameter Varying Systems with Parameter Uncertainties," *SICE Annual Conference*, Kokkaido, Japan, Aug. 2004, pp. 2644-2647.

[93] G. E. Dullerud and F. Paganini, *A Corse in Robust Control Theory: A Convex Approach*. New York: Springer, 2000.

[94] X. He and H. H. Asada, "A New Feedback Linearization Approach to Advanced Control of Multi-Unit HVAC Systems," in *Proc. of the American Control Conference*, Denver, CO, Jun. 2003, pp. 2311-2316.

[95] X. He, S. Liu, and H. H. Asada, "A Moving-interface Model of Two-phase Flow Heat Exchanger Dynamics for Control of Vapor Compression Cycle," *Heat Pump and Refrigeration System Design, Analysis, and Application*, pp. 69-75, 1994.

[96] N. Hewitt, J. McMullan, and N. Murphy, "Comparison of Expansion Valve Performance," *International Journal of Energy Research*, vol. 5, pp. 43-54, 1995.

[97] J. M. Choi and Y. C. Kim, "Capacity Modulation of Iverter-driven Multi-air Conditioner using Electronic Expansion Valves," *Energy*, vol. 28, pp. 141-155, 2003.

[98] E. Bristol, "On A New Measure of Interaction for Multivariable Process Control," *IEEE Transaction on Automatic Control*, vol. 11, pp. 133-134, 1966.

[99] B. C. Moore, "Principle Component Analysis in Linear Systems: Controllability, Observability, and Model Reduction," *IEEE Transaction on Automatic Control*, vol. 26, pp. 17-31, 1981.

[100] Mathworks, "MATLAB System Identification Toolbox Documentation," http://www.mathworks.com/access/helpdesk/help/toolbox/ident/, 2009.

[101] G. F. Franklin, J. D. Powell, and A. Emami-Naeini, *Feedback Control of Dynamic Systems*. Upper Saddle River, NJ: Prentice Hall, 2002.

VITA

Name: Young Joon Chang

Address: 452-39 Daeheung-dong Jung-gu
Daejeon, South Korea, 301-803

Email Address: blueair93@gmail.com

Education: B.S., Mechanical Engineering, Inha University, 2000
M.S., Mechanical Engineering, Inha University, 2002
Ph.D., Mechanical Engineering, Texas A&M University, 2010

Experience: Graduate Assistant-Research, TAMU Dept. of Mech. Engr.
1/2006-8/2009, College Station, Texas

Researcher, Korea Institute of Energy Research
1/2003-12/2003, Daejeon, South Korea

Graduate Assistant-Research, Inha Univ. Dept. of Mech. Engr.
1/2001-8/2002, Inchon, South Korea

Graduate Assistant-Teaching, Inha Univ. Dept. of Mech. Engr.
3/2000-12/2000, Inchon, South Korea

Researcher, Korean National Science Foundation
1/2000-1/2002, Seoul, South Korea